# POLYMER AND CARBON NANOTUBE BOUND FOLIC ACID AND METHOTREXATE FOR CANCER THERAPY

**Jacob Masiala Ngoy**

A dissertation submitted to the Faculty of Engineering and the Built Environment, University of the Witwatersrand, Johannesburg, in fulfillment of the requirements for the degree of Master of Science

Johannesburg, 2010

**DECLARATION**

I declare that this dissertation is the fruit of my own work. It is being submitted for the degree of Master of Science of Engineering in the University of the Witwatersrand, Johannesburg, South Africa. It has not been submitted before for any degree or examination in any other University.

Signed……

……day of……2010

**ABSTRACT**

Folic acid (FA) is an amino acid that helps in the replication of normal cells and it deficiency may lead to oncogenic cells development. Methotrexate (MTX) on the other hand is a highly potent drug against leukemia and other neoplasias, which can induce toxic side effects and drug resistance to target cells. The principal objective was to develop a bioconjugate that will enhance therapeutic effectiveness of these agents (FA and MTX) using functionalized carbon nanotubes and polymer toward cancer cells. Furthermore, bioreversible binding to a water-soluble and biocompatible carrier polymer and carbon nanotubes are advanced technology designed to circumvent critical pharmacological and efficacious biological action.

The formation of biofissionable bond (CONH) for drug release was evaluated in this work by using nuclear magnetic resonance (NMR) spectra with $D_2O$ as solvent, and infrared (IR) spectra to identify the necessary peak shifts for the bioreversible conjugation of FA and MTX as anticancer drug. Polyaspartamide and carbon nanotubes (CNTs) were both functionalized and used as carriers for solubility behavior, steric accessibility and reactivity of anchoring sites, aiming to enhance therapeutic effectiveness of MTX.

In order to obtain the polymeric carrier, to polysuccinimide (PSI) synthesized via polycondensation of aspartic acid was attached 3-(N,N–dimethylamino)propylamine (DMP) and 1,3-propylenediamine (PDA) for solubility behavior and reactivity of anchoring of the drug respectively. This, through the use of an ester 2-(1H-benzotrial-1-yl)-1,1,3,3-tetramethylurium hexafluorophosphate (HBTU), as coupling agent led to the polymer drug conjugate after reacting with FA. The reaction was subjected to the polymer cleavage which caused the dropping of yield after chromatography and dialysis operations. After kinetic reaction investigation, the optimum reaction time was set within the range of 120-130 minutes for an optimum yield of coupling within the range of 80-85% where the incorporation of FA in the polymer was maximum though the polymer cleavage. In addition, CNTs obtained via chemical vapour deposition (VCD) was covalently functionalized at RT, 50ºC and 100ºC with a mixture of sulphuric and nitric acids to generate the phenol and carboxyl groups on the surface, and at 230 ºC with aspartic acid to generate only the carboxyl group. It resulted that

the mol ratio (OH/COOH) was increasing, the size of f-CNTs was decreasing from 80, 30 to 20nm and the water solubility was increasing with the increase in temperature from RT, 50ºC to 100ºC. The carboxyl on the surface of f-CNTs was attached to DMP and FA through HBTU to get f-CNTs-FA conjugate. This resulted to the prodrug with different sizes of 50nm and 170nm with 94% and 101.3% incorporation of folic acid respectively.

CNTs noncovalently coated with polysuccinimide (PSI) in DMF at 160ºC were attached to DMP and PDA. Thereafter, FA reacted with PDA via HBTU to give a prodrug of 60nm with 105.3% FA incorporation. The f-CNTs functionalized with polymer can be more beneficial due to the size for the cell penetration and average molecular weight for renal clearance. Therefore the biomedical evaluation is recommended for future work.

**DEDICATION**

To the Holy Ghost: The Spirit of the Lord

The Spirit of wisdom and of understanding

The Spirit of counsel and of power

The Spirit of knowledge and of the fear of the Lord

I dedicate this work.

**ACKNOWLEDGEMENT**

Particular thanks are due to Professor E. Sunny Iyuke, my supervisor, for the many hours spent offering advice, encouragement, suggestions and guidance. Without your involvement and expertise in research, the completion of this project would not have been possible.

Grateful acknowledgement is made to Professor E.W. Neuse my co-supervisor, for suggesting the research topic and for the provision of financial support and facilities which enabled this investigation to be undertaken.

Thanks to Bradlow Postgraduate Awards (2008-2009) for your financial assistance.

To Esther Masiala my wife, I say thanks for the attention that you have given to this research by preparing a refreshing framework for me.

To my daughters, Souviel Masiala and Gael Masiala, in your presence I could relax to discharge my mind.

**TABLE OF CONTENTS**

**LIST OF SCHEMES**

**LIST OF FIGURES**

**LIST OF TABLES**

## LIST OF ABREVIATIONS

AFM: Atomic force microscopy

ALL: Acute lymphocytic leukemia

CCVD: Chemical catalytic vapour deposition

CNTs: Carbon nanotubes

CVD: Chemical Vapor Deposition

DCC: Dicyclohexylcarbodiimide

DET: Diethylenetriamine

DHFR : dihydrofolate reductase

DMF: N,N-dimethylformamide

DMP: 3-dimethylamino-1-propylamide

DNA: Deoxyribonucleic acid

EDDA: 2-2- (ethylenedioxy)-diethylamine

EPR: Enhanced permeability and retention

$Et_2O$: diethyl ether

FA: Folic acid

f-CNTs : Functionalized Carbon Nanotubes

FMDV: Foot-and mouth disease virus

GI: gastrointestinal

HBTU: 2-(1H-benzotriazol-1-yl)-1,1,3,3-tetramethyluronium fluorophosphates

HiPco: High Pressure Carbon Monoxide Conversion

$^1H$ NMR: Hydrogen Nuclear Magnetic Resonance

HPMA: 2-hydroxypropyl-methacrylate polymers

IR: Infrared

MTX: Methotrexate

MWCNTs: Multiwalled Carbon Nanotubes

O/N: Over night

PAAs: Poly(amidoamines)

PABA: para-aminobenzoic acid

PDA: 1,3 diaminopropane acetylene

PEO: Poly (ethylene oxide)

Pgp: p-glycoprotein

pH: Potential of Hydrogen

pKa: Potential of constant of acid

PNA: Peptide nucleic acid

RFC: Reduced folate carrier

RNA: Ribonucleic acid

RT : Room temperature

SDBS: Sodium dodecyl-benzene sulfonate

SDS: Sodium dodecyl sulfate

SWCNTs: Single Walled Carbon Nanotubes

TEA: Triethylamine

TEM: Transmission Electron Microscopy

TMU: Tetramethylurea

WHO: The world health organization

# CHAPTER 1

# INTRODUCTION

## 1.1 Background and Motivation

### 1.1.1 Folic acid

Folic acid is needed for the de novo synthesis of the nucleoside thymidine required for DNA synthesis. The presence of folic acid causes the synthesis of DNA, RNA, thymidylates, and proteins by the affinity that it can develop with dihydrofolate reductase (DHFR), an enzyme that is part of the folate synthesis metabolic pathway. Dihydrofolate reductase catalyses the conversion of dihydrofolate to the active tetrahydrofolate. Folic acid is an important nutrient for the growth of cells via essentially purine and pyrimide synthesis. Adequate folate intake helps the replication of normal cells conducing to good health. Thereto adequate folate intake, causing rapid cell division and growth, is helpful for the pregnancy and the infancy.[(1)] Thus, the first four weeks of pregnancy (when most women do not even realize they are pregnant) require folic acid for proper development of the brain, skull, and spiral cord. While folate deficiency, affecting hematopoietic cells and neoplasms, hinders DNA synthesis and cell division. RNA transcription and subsequent protein synthesis are less affected by folate deficiency, as the mRNA can be recycled and used again (as opposed to DNA synthesis where a new genomic copy must be created). Both adults and children need folate to form normal red and white blood cells and prevent anemia [(2)], because some of those large cells, although immature (reticulocytes) are released early from the marrow in an attempt to compensate for the anemia [(3)].

In the event of random proliferation of cells, condition becomes harmful to the abnormal cells; enhanced chemotherapy will be requested to stop the cause of the growth of cells. The association between folate and cancer appears to be complex. It has been suggested that folate may help prevent cancer, as it is involved in the synthesis, repair, and

functioning of DNA, and a deficiency of folate may result in damage to DNA that may lead to cancer [4].

### 1.1.2 Methotrexate (MTX)

Methotrexate was originally used as part of combination chemotherapy regimens to treat many kinds of cancers. It is still the mainstay for treatment of many neoplastic disorders including acute lymphoblastic leukemia. The metabolism of 7,8-dihydrofolate to 5,6,7,8 tetrahydrofolate smashes rapidly into DNA synthesis which generates the multiplication of cells in disorder, results to cancer. The activity of this metabolism is accelerated with the presence of dihydrofolate reductase, an enzyme that is part of the folate synthesis metabolic pathway.

MTX competitively and reversibly inhibits dihydrofolate reductase (DHFR) due to its affinity for DHFR which is about one thousand-fold that of folate for DHFR. As a result, there is a reduction in purine and pyrimidine-nucleic acid metabolism. MTX acts especially during DNA and RNA synthesis, and thus it is cytotoxic during the S-phase of cell cycle. Note that MTX has a greater toxic effect on rapidly dividing cells, which replicate their DNA more frequently and thus inhibits the growth and proliferation of these non-cancerous cells, as well as side effects. MTX is absorbed completely from the intestine, and metabolized via the kidney. It enters the cell and is polyglutamated like folic acid, therefore retaining within the cell and providing its effectiveness.

MTX tends to work faster and more effectively compared to most disease modifying antirheumatic drug. It has a considerable interaction with many drugs. Caution should be applied when used together with trimethoprim, probenecid, and nonsteroidal anti-inflammatory drugs, especially in the face of renal impairment. Lower doses of MTX have been shown to be very effective for the management of rheumatoid arthritis and psoriasis. In these cases, inhibition of dihydrofolate reductase (DHFR) is not thought to be the main mechanism, rather the inhibition of enzymes involved in purine metabolism,

leading to accumulation of adenosine, or the inhibition of T cell activation and suppression of intercellular adhesion molecule expression by T cells [5].

### 1.1.3. Polymer-drug conjugation

Chemotherapy is a significant module among many emerging biomedical technologies used for cancer management and control. Among the requirements that must be fulfilled by the systemically acting antiproliferative medicinal agent in order to qualify as an efficacious carcinostatic drug, the following may be cited: (1) *Complete solubility in aqueous media,* ensuring rapid dissolution and dissipation in the (aqueous) vascular system. (2) *Low systemic toxicity,* allowing for continuing drug administration at high dose levels with resultant large therapeutic index. (3) *Non-polar, uncharged structure,* a precondition for efficacious membrane crossing and cell entry by the normal passive diffusion mechanism, with optimal intracellular bioavailability and minimal risk of capture in the interstitial fluid by the reticuloendothelial system. (4) *Cell-specific drug action,* leading to preferential accumulation in the cancerous tissue while leaving healthy tissue unaffected. This presupposes that a specific drug, or drug combination, must be available for each one of the different kinds of proliferative syndromes defined as cancers. (5) *Extended circulation half-life,* concomitant with grossly retarded elimination through catabolic processes, serum protein binding, or macrophage action. (6) *Continuous long-term effectiveness with* low probability of emerging drug resistance, thus permitting ongoing treatment at sustained dose level.

With the realization of pathological complexity of cancerous growths and the multitude of hurdles a therapeutic agent has to overcome in order to act incisively on site, to eradicate a neoplastic lesion, it has become clear that, at the current level of proficiency, long-lasting remissions can be achieved by chemotherapeutic means only for a very selected number of cancers. More often, remissions are temporary, requiring additional treatment modes. Success rates for modalities combating invasive growth are extremely low, and therapies increasingly lack effectiveness upon prolonged systemic drug administration. The reasons are obvious: most of the anticancer drugs in current clinical

administration lack the qualifying features listed in the foregoing, to a major or lesser extent. Specifically, the drugs generally reach unduly low levels of bioavailability as they possess polar or salt-like structures, lack cell specificity, or are rapidly eliminated from central circulation by a variety of depletion mechanisms. More crucially, they generally cause severe toxic side-effects in addition to showing a tendency to elicit single, or even multiple, drug resistance in the affected cells. As a consequence, the therapeutic effectiveness of present-generation anticancer agents has remained unsatisfactorily low, in spite of extensive research worldwide. A state of the art treatment of the topic is found in a reference book published by the American Chemical Society [(6)].

With recognition given to the therapeutic inadequacies associated with most currently administered antitumor drugs, a special trend in drug research has been observed in recent years which aims at the provision of pharmacokinetic assistance to a given drug system through attachment to macromolecular compounds, acting as protecting transport vehicles and drug delivery agents. This trend has resulted in the development of drug-containing liposomes, microencapsulations, and nanoparticles as variably successful delivery systems. One of the most promising macromolecular drug release strategies utilizes water-soluble, biodegradable polymers as carriers of the medical agents. This strategy has in recent years matured into a highly successful tool of chemotherapy, circumventing many of the problems associated with the direct administration of the original low-molecular-mass drugs. The polymer-drug conjugation concept, pioneered by Chu and Whiteley [(7)] and significantly refined by Rigsdorf [(8)], is based on a carrier model comprising a linear polymer chain composed of subunits bearing water-solubilizing groups, other subunits equipped with functional groups suitable for reversible drug binding (anchoring). Other subunits comprise a homing device, i.e. some molecular entity capable of directing the conjugate molecular selectively to the target tissue. The conjugate nearly always represents a prodrug from which the active agent is released in the predestined biological environment (generally the cytoplasmic lysosomes) by hydrolysis or through enzymatic action.

Several excellent reviews are available in which the fundamental structural requirements and performance criteria are discussed in detail [9, 10]. The most outstanding benefits to derive from drug conjugation include the following:

(i) Even if inherently hydrophobic and insoluble in water, the drug will be carried immediately into the aqueous phase of the central circulation system or the intraperitonal cavity. This will ensure rapid drug distribution in the fluid system.

(ii) While in transit in the central circulation system, the polymer-bound drug will experience temporary protection from enzymatic attack, serum protein binding and other scavenging processes. This will lead to reduced renal clearance and prolonged serum life-time with substantially enhanced drug bioavailability.

(iii) The polymer-drug conjugate will experience facilitated endocytotic cell entrance, thus circumventing potential problems caused by drug polarity or iconicity in the normal process of membrane crossing, by passive diffusion common to nonpolymeric solutes. The mechanism is pinocytotic in nature and thus not subject to the limitations imposed by the reticulo-endothelical system on phagocytotically captured particles. Ideally, adsorptive pinocytosis is utilized by the conjugate for increased efficiency of translocation, and cationic polymers are good examples of compounds so translocated. Endocytotic cell entrance may additionally assume unique importance where drug resistance, due to excessive P-glycoprotein-medicated efflux from the cytoplasm has become an issue.

(iv) Enhanced drug affinity for the transformed (i.e. cancerous) cell may be achieved by incorporation of a homing group, e.g. certain sugars or strongly cationic functionalities, as well as, in the ultimately perfect form, monoclonal antibodies.

(v) Drastically reduced toxic side effects will result from the “anchored” nature of the drug in the initial stage of administration, restricting it to the desired pharmacokinetic path and reducing the risk of accumulation in healthy tissue.

(vi) Polymer conjugates, in common with macromolecules in general, tend to accumulate in solid tumors because of enhanced intratumoral vascular permeability, allowing for substantial leakage of the polymeric molecules into the tumor tissue. Whereas, in normal tissues, macromolecules in intestinal space are efficiently recovered by the lymphatic system, this lymphatic clearance is grossly retarded in tumor tissue. And this represents a weighty factor contributing to the tumoritropic characteristics of polymers. This enhanced permeability and retention (EPR) effect associated with macromolecules, renders drug administration more efficacious while reducing systemic toxicity in other organs; see (v), above.

The water-soluble, intravenously administered conjugate will be constructed so as to: (i) rapidly enter and dissipate in the aqueous central circulation; while in transit, the drug will be protected against premature renal clearance (thus reducing nephrotoxicity), serum protein binding and capture by the reticuloendothelial system (thus avoiding irreversible inactivation); (ii) remain polymer-bond while in circulation (thus preventing drug serum levels from exceeding the toxic level); (iii) undergo facilitated (pinocytic) entry into the cancerous target cell (thus overcoming problems of charge, polarity, or excessive drug efflux, the last-named factor being a cause of drug resistance); and (vi) accumulate preferentially in tumor tissue because of vascular leakage and reduced lymphatic clearance. The cited factor will combine to achieve a reduction of toxicity and more effective drug utilization. For proper functioning in the biological environment, in accordance with this proposal, the carrier polymers will be designed so as to (i) provide and retain water solubility of the derived conjugate, (ii) feature biocompatibility and biodegradability, (iii) provide preferential attraction to the cancerous cell, and (iv) possess drug-binding functionality capable of drug release in the cytoplasmic environment. With the conjugation to a carrier polymer so characterized, the drug systems, even if inherently hydrophobic and insoluble in water, will smoothly and rapidly enter (and be distributed in) the aqueous fluid system and, while in transit, will benefit from temporary protection against catabolic elimination. In addition, they are expected to experience facilitated transcytotic epithelial barrier crossing and pinocytotic target cell

entry, thus overcoming problems in membrane penetration and risk of drug rejection by target tissues, having acquired drug resistance.

### 1.1.4. Drug delivery with carbon nanotubes

The search for new and effective drug delivery systems is a fundamental issue of continuous interest [(11)]. A drug delivery system is generally designed to improve the pharmacological and therapeutic profile of drug molecule [(12)]. A wide variety of delivery systems are currently available [(13)]. The ability of functionalized carbon nanotube (f-CNT) to penetrate into the cells, offers the potential of using f-CNT as vehicles for the delivery of small drug molecules [(14, 15)]. However, the use of f-CNT for the delivery systems of small drug molecules able to carry one or more therapeutic agents with recognition capacity, optical signal of imaging and/or specific targeting, is of fundamental advantage, for example in the treatment of cancer and different types of infectious diseases [(16)]. For this purpose a new strategy for the multiple functionalization of CNT with different types of molecules [(17)] has been developed. A florescent probe for tracking the cellular uptake of the material and an antibiotic moiety as the active molecule were covalently linked to CNT where multi wall carbon nanotubes (MWNT) were functionalized with amphotericin B and fluorescein.

The antibiotics linked to nanotubes was easily internalized into mammalian cells without toxic effects in comparison with the antibiotic incubated alone. In addition, amphotericin B bound to CNT preserved its high antifungal activity against a broad range of pathogens, including *Candida albicans*, *Cryptococcus neoformans* and *Candida parapsilosi*.

In view of these results, f-CNTs represent a new, emerging class of delivery systems for the transport and translocation of drug molecules into different types of mammalian cells. Although these CNT conjugates displayed no cytotoxicity in vitro, further development will be important to assess their metabolism, biodistribution and clearance from body.

## 1.2. Problem statement

Cancer presents one of the most formidable health problems worldwide. More than 10 million people are diagnosed with cancer every year. The world health organization (WHO) estimated that there will be 12 million new cases every year by 2030. Cancerous diseases cause 6 million deaths every year, almost 12% of worldwide mortality. The incidence and mortality rates of certain types of cancer have wide geographical differences, which are attributed to racial, cultural, and especially environmental influences [(18)].

In South Africa, cancer is the second most common cause of death in the white, coloured, and Asian population, and the third most common cause in the black population group[(19)]. On average, South Africa rates for certain malignancies such as cervical, oesophageal, and skin cancers rank among the highest world-wide. Cancers of the lung and prostate rate among the top six cancers with white and non-white, and melanoma represents one of top six cancers with white females. Other types of cancer, including the various forms of leukemia, although of lower incidence, are nonetheless a cause for serious concern.

The problem will be aggravated in the years to come as increasing urbanization is expected to create environmental and dietary conditions conducive to further initiation and spread of cancers. It will be further compounded by finding that cancerous afflictions occur in approximately one-third of all male and female adult breadwinners in the age bracket of 15-54 years. A novel factor now coming into play is the rapid spread of AIDS; immunodepressed patients will be at special risk to develop early cancerous lesions, and virus-related cancers may well find particularly suitable targets among such patients [(20)].

The available anticancer drugs have distinct mechanisms of action, which may vary in their effects on different types of normal and cancer cells. Chemotherapy constitutes an important cancers treatment modality, alone or in conjunction with other treatment regimens. However, despite much progress in drug research, complete cures by

chemotherapy are still the exception rather than the rule. In general, remissions remain incomplete or short-lived, especially whenever secondary cancers (metastases) have developed or resistance phenomena emerged. The inadequate effectiveness of present-day anticancer drugs can be traced to a combination of factors, including poor solubility in aqueous media, inefficacious membrane crossing and cell entry because of structural charge or polarity, lack of cell specificity, short serum half-life, and most critically, excessive toxicity and a propensity for induction of drug resistance. For this reason, cancer chemotherapy may consist of using several drugs in combination for varying lengths of time.

### 1.3. Research questions

There are many modalities for cancer treatment. They are highly variable and dependent on a number of factors such as the type, location and amount of disease and the health status of the patient. The treatments are designed to directly kill or remove the cancer cells or to lead to their eventual death by depriving them of signals needed for cell division, or to stimulate the host immune system after killing or removal of these cells. The four principal modalities utilized are surgery, radiation, chemotherapy, and immunotherapy. Many questions have been asked on chemotherapy, which is the impetus of this study and will create awareness of some new therapies still in their infancy. Chemotherapy, while representing a vital component of cancer treatment modalities, has not yet fulfilled basic expectations. Cure rates are unsatisfactory and relapses frequent for reasons of limited therapeutic drug efficacy, detrimental side effects, resistance problems and pharmacological deficiencies.

### 1.4. Research hypothesis

Within the framework of macromolecular and carbon nanotubes drug research in the Schools of Chemistry and Chemical Engineering of the University of the Witwatersrand, the present project represents a contribution to cancer drug development.

It is the project's primary objective, addressing the problem of inefficiency of drug, to provide a vehicle for improved pharmacokinetic utilization of anticancer agents. Various strategies will be used to set the active drug out of the critical pharmacological obstacles which render the clinical usefulness very inadequate. Among various strategies, the formation of bioreversible bond between a medicinal drug and water-soluble and biocompatible carriers (polymers and carbon nanotubes) represents an advanced technology that is designed to avoid the critical pharmacological obstacles which the drug must clear for efficacious biological action. The polymer-drug conjugate and carbon nanotubes-drug conjugate resulting from the carrier-drug anchoring step, act as free-form at the target site.

This will be accomplished through bioreversible conjugation of selected anticancer drug models with water-soluble macromolecular and functionalized carbon nanotube carriers, designed in accordance with specific biomedical requirements. Especially carbon nanotubes will be used as platforms for multiple derivatization by loading their surface with therapeutic agents (treatment), aiming to be rendered fluorescent, magnetic, or radionuclide probe (tracking), and active recognition segments (targeting). The conjugates will be constructed so as to act as prodrugs, comprising the chosen drug systems: folic acid and methotrexate (hereinafter abbreviated to MTX). Following facilitated pharmacokinetic pathways, the bioactive drug species will be released in the transformed target cell by hydrolytic or enzymatic mechanisms.

In the polymer Laboratory of school of chemistry in the University of Witwatersrand, the concept of polymer-drug conjugation has been utilized in numerous projects aiming at increasing the therapeutic effectiveness of experimental anticancer-active agents, and preliminary biomedical screening results reflect high to excellent activity of the conjugates tested. The experience gained in these preceding projects is being used to propel this project forward.

## 1.5. Research objectives

The principal objective is to develop a class of anticancer agents with enhanced therapeutic effectiveness. The proposed approach will be instrumental in fulfilling the project's specific aims, viz. (1) reduction of toxic side effects and emerging resistance problems; (2) widening of the agents' activity spectrum and therapeutic window; (3) increase in bioavailability through enhanced water solubility, serum residence time, accumulation in the tumor tissue, and pinocytotic cell entry; and, most importantly; (4) development of combination drug conjugates for ultimate co-administration with mainstream drug conjugates of MTX and folic acid.

## 1.6. Expected Contribution to Knowledge

1. In this project, a series of the novel drug systems with high carcinostatic activity will be synthetically and analytically developed as contribution to the national and worldwide cancer management programs.
2. This work will provide adequate information on the development of good vehicle for improved pharmacokinetic utilization of anticancer agents.
3. This work will provide useful information from biomedical testing results. In vitro screening tests will be performed in order to allow the synthesis work to be redirected as required for the attainment of optimal biological activity.
4. Using two different methods, the first is the conjugation of selected anticancer drug models with water-soluble macromolecular carriers; and the second is the functionalized carbon nanotubes. This work will assist in finding the best performing method.

## 1.7. Terminology and definition

### 1.7.1. Deoxyribonucleic acid (DNA)

DNA is a nuclei acid that contains the genetic instructions used in the development and functioning of all known living organisms. The main role of DNA molecules is the long-term storage of information and DNA is often compared to a set of blueprints, since it contains the instructions needed to construct other components of cells, such as proteins and RNA molecules. The DNA segments that carry this genetic information are called genes, but other DNA sequences have structural purposes, or are involved in regulating the use of this genetic information.

Chemically, DNA is a long polymer of simple units called nucleotides, with a backbone made of sugars and phosphate groups joined by ester bond. Attached to each sugar is one of four types of molecules called bases. It is the sequence of these four bases along the backbone that encodes information. This information is read using the genetic code, which specifies the sequence of the amino acids within proteins. The code is read by copying stretches of DNA into the related nucleic acid RNA, in a process called transcription. Most of these RNA molecules are used to synthesize proteins, but others are used directly in structures such as ribosomes and spliceosomes.
Within cells, DNA is organized into structures called chromosomes and the set of chromosomes within a cell make up a genome. These chromosomes are duplicated before cells divide, in a process called DNA replication. Eukaryotic organisms such as animals, plants, and fungi store their DNA inside the cell nucleus, while in prokaryotes such as bacteria it is found in the cell's cytoplasm. Within the chromosomes, chromatin proteins such as histones compact and organize DNA, which helps control its interactions with other proteins and thereby control which genes are transcribed.

Ribonucleic acid or RNA as a nucleic acid polymer consisting of nucleotide monomers, plays several important roles in the processes that translate genetic information from DNA into protein product. Thus, RNA acts as a messenger between DNA and the protein

synthesis complexes known as ribosomes, forms vital portions of ribosomes, and acts as an essential carrier molecule for amino acids to be used in protein synthesis.

### 1.7.2. Enzymes

Enzymes are proteins that catalyze (i.e. accelerate) chemical reaction [21].In enzymatic reactions, the molecules at the beginning of the process are called substrates, and the enzyme converts them into different molecules, the products. Almost all processes in a biological cell need enzymes in order to occur at significant rates. Since enzymes are extremely selective for their substrates and speed up only a few reactions from among many possibilities, the set of enzymes made in a cell determines which metabolic pathways occur in that cell.

Enzyme activity can be affected by other molecules. Inhibitors are molecules that decrease enzyme activity; activators are molecules that increase activity. Many drugs and poisons are enzyme inhibitors. Activity is also affected by temperature, chemical environment (e.g. pH), and the concentration of substrate. Some enzymes are used commercially, for example, in the synthesis of antibiotics. In addition, some household products use enzymes to speed up biomedical reactions (e.g. enzymes in biological washing powders break down protein or fat stains on clothes; enzymes in meat tenderizers break down proteins, making the meat easier to chew) [22].

### 1.7.3. Chemotherapy

Chemotherapy is given to eradicate and stop the progress of the expansion of secondary tumors resulting from outstanding and untraceable cancer cells that often reside in the body after surgery.

During chemotherapy many anticancer agents and other chemical entities aim to apply immune-stimulating effects on the cancer patient’s immune system. Chemical agents impressing toxic effects on the cancerous cell, for the most part cause interference with

the cell's replicative mechanism and therefore with intracellular nucleic acid synthesis and the ultimate role played by the nuclear DNA in mitosis. Whenever the target tissue consists of rapidly dividing cells, as is generally the case in a malignant system, the effectiveness of the anticancer drugs is generally, although not exclusively, at an optimal level. Nevertheless, the human body disposes a number of compartments in which normal, i.e. healthy cells are required to replicate at a high rate for the accomplishment of their physiological role, e.g. the bone marrow, the linings of the gut and the urinary tract. It is, indeed, in these compartments where most of the systemically acting anticancer drugs exert their most undesirable toxic side effects, as the rapidly proliferating cells do not provide sufficiently long-time intervals during which normal repair mechanism, mediated by selective repair enzymes, can remain operative [23, 24].

### 1.7.4. Antimetabolites

The antimetabolites, as structural analogs of naturally occurring compounds, interfere with the production of nucleic acids and work through a variety of mechanisms, including competition for binding sites on enzymes and incorporation into nucleic acids. Antimetabolites are divided into three categories: antifolates, purine analogs and pyrimidine antimetabolites. They then operate to inhibit the development of the most rapidly proliferating cells in the body (e.g. bone marrow, gastrointestinal tract, etc.). Antifolate antimetabolites: They produce both the first striking remissions in leukemia [25] and the first cure of solid tumor, choriocarcinoma.

#### 1.7.4.1. Methotrexate

*History of clinical use*: Metotrexate (Scheme 1.1), a folate antimetabolite synthesized five decades ago, has been in clinical use for more than 35 years. It has a long history of use in treatment of various immunologic diseases. MTX began as a drug for cancer treatment, particularly childhood leukemia, in the early 1940s [26]. In the 1960s it was used for the treatment of rheumatoid arthritis and psoriasis. In the mid-1980s [27] many rheumatologists reported their experiences with MTX use in studies of rheumatoid

arthritis. Guidelines for MTX use were developed to address dosing, liver biopsy and monitoring strategies, which were aimed at reducing the incidence of adverse effects [28]. Currently, methotrexate is indicated for the treatment of acute lymphocytic leukemia (ALL), as well as for rheumatoid arthritis and psoriasis. The drug has also been found efficacious in treatment of other diseases, including asthma, systemic lupus erythematosus, Crohn's disease, myositis, vasculitis and ectopic pregnancy [29, 30].

*Mode of action*: The passive diffusion of MTX through cell membrane is limited, due to its hydrophilic nature. Indeed, MTX is highly polar; and owing to this polarity, at the nearly neutral pH of biological fluids, it is present mainly in the doubly anionic species form. This leads to inhibition of cell penetration. As a consequence, only a small portion of MTX successfully enters the intracellular space by passive diffusion while the major portion enters by carrier-mediated mechanism. The main pharmacological target of action of MTX is the competitive inhibition of dihydrofolate-reductase (DHFR), an intracellular enzyme which reduces folic acid to tetrahydrofolate cofactors, which are in turn key intermediates in several important biochemical pathways. Among these are the *de novo* biosynthesis of purines and of thymidylate. Mathews et al. [31], using Raman spectra of the MTX-DHFR complex, showed that the inhibition occurs as result of ionic binding between the N-1 of the pterin portion and the enzyme. Lack of reduced folates, purines and thymine in actively proliferating cells, such as those of the tumors, leads to a blockage of DNA and RNA synthesis, and eventually to cell death.

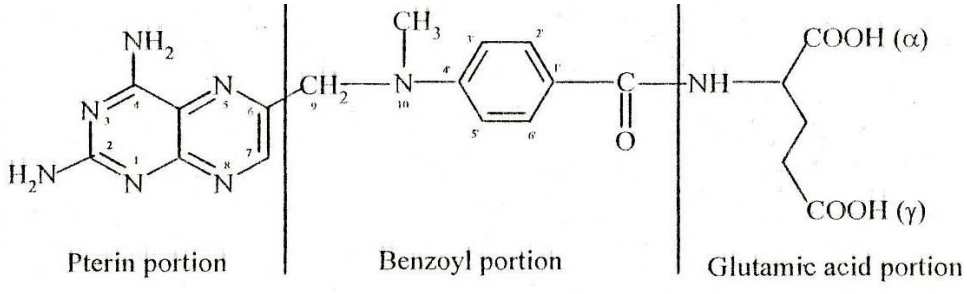


**Scheme 1.1: Structure of Methotrexate (MTX)**

### 1.7.4.2. Folic acid

Folic acid, or pteroylglutamic acid, consists of a pteridine that is linked to para-aminobenzoic acid (PABA) and glutamic acid (Scheme 1.2).

*Physiological role*: As a pharmaceutical product, folic acid (FA) is a vitamin, a nutritional supplement, and a diagnostic aid in folate deficiency [32]. Folic acid, referring to the folate form, is a well-known water-soluble vitamin of the B-complex. It is mainly evolved from natural sources, but as it is available in small quantities in biological material, worldwide efforts are focused on its development and synthesis. The pharmaceutical product is chemically synthesized, and the L-enantiomer is the biologically active form. Folic acid is involved in many metabolic mechanisms leading to the synthesis of DNA and normal erythropoiesis. In intestinal cell, FA is mostly reduced to tetrahydrofolate ($H_4$folate), the active form of this vitamin in a two-step reaction, which is catalyzed by the enzyme folate reductase. Inhibitors of this enzyme, like MTX, act as antifolate. Scheme 1.3 depicts the fate of folic acid in the biological environment.

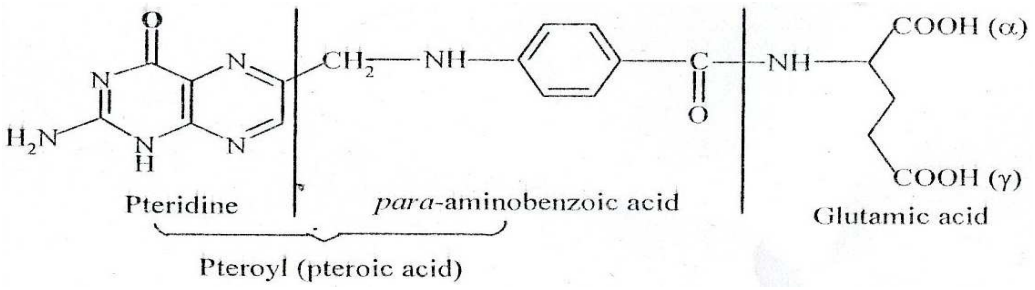


**Scheme 1.2: Structure of folic acid**

$H_4$folate functions as a coenzyme, a carrier of various activated one-carbon units in metabolic reactions. Folic acid and vitamin $B_{12}$ metabolic pathways intersect at the conversion of homocysteine to methionine. FA is also proven to be completely ineffective [33] against any type of cancerous disease. However, it is also known to impact deeply on cancer development. Indeed, folate deficiency appears to play a crucial role in early cervical carcinogenesis by facilitating genetic modification at a fragile

chromosomal site [34]. Folic acid plays a crucial role in DNA synthesis, where it enables cells to replicate normally.

*Mechanism of intracellular uptake*: Folic acid is transported into cells either through a receptor-mediated endocytosis [35] facilitated by the folate receptor, or with the help of carrier proteins, such as the reduced folate carrier (RFC). The membrane-associated folate receptor is known to be overexpressed on the surface of a variety of human tumor cells, including cancers of the ovary, colon, kidney, uterus, tests, brain, lung, breast, and myelocytic blood cells, while it is highly restricted in most normal tissues [36].

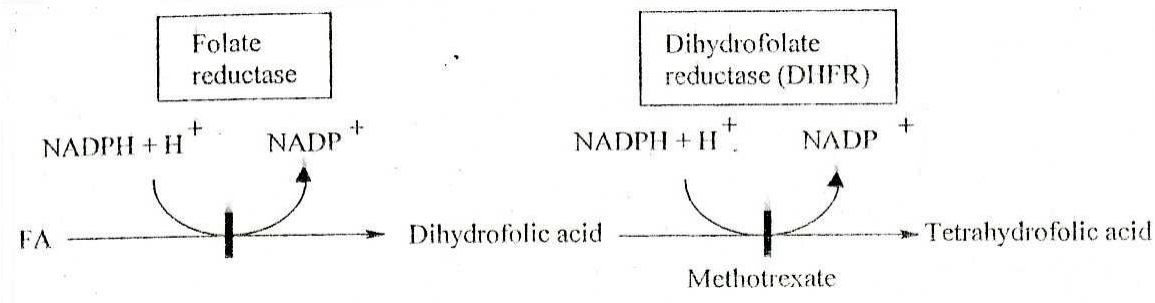


**Scheme 1.3: Two-step conversion of folic acid to the active tetrahydrofolate by the enzyme folate reductase and its inhibition by methotrexate**

### 1.7.5. Toxicity of Carbon nanotubes

Generally, the harmful effects of nanoparticles arise from the combination of various factors, two of which are particularly important: (a) the high surface area, and (b) the intrinsic toxicity of the surface [37]. In contrast with conventional particles of larger mean diameter, nanoparticles under 100 nm can potentially be more toxic to the lung (portal of entry), can redistribute from their site of deposition, can escape from the normal phagocytic defences and can modify the structure of proteins. Therefore, nanoparticles can activate inflammatory and immunological responses and may affect the normal tissue function [38]. CNTs, in the context of toxicology, can be classified as 'nanoparticles' due to their nanoscale dimensions, therefore unexpected toxicological effects upon contact with biological systems may be induced. The nanometer-scale dimensions of CNTs make

quantities of milligrams possess a large number of cylindrical, fibre-like particles, with a concurrent very high total surface area. This total surface area will also depend on their degree of bundling and aggregation of nanotubes in solution. Note that the intrinsic toxicity of CNTs does not depend on the degree of surface functionalization and the different toxicity of functional groups. Batches of pristine CNTs (non-purified and/or non-functionalized) readily after synthesis contain impurities such as amorphous carbon and metallic nanoparticles (catalysts: Co, Fe, Ni and Mo).

### 1.7.6. Biocompatibility of carbon nanotubes

Despite the evidence of CNTs cytotoxicity, there have also been a number of published studies into CNT-based biomaterials, which support the biocompatibility of CNTs and CNT-based materials. This section gives a detailed discussion of investigations into interactions between CNT-based materials, neutral cells, osteoblasts, fibroblasts, antibodies and the immune system, ion channels and cellular membranes.

Functionalization of CNTs has been used to address the problem of CNTs insolubility in aqueous media and, in many cases, has permitted linking of biologically active peptides and medicinal drugs to the CNTs side-wall [39, 40]. These properties have generated interest in using CNTs as drug or vaccine delivery vehicles and to this end there have been several studies conducted on CNTs functionalization with vaccine or drug molecules [41, 42].

# CHAPTER 2

# LITERATURE REVIEW

## 2.1. Polymers as Drug carriers

The control of drug release in cancer through therapeutic systems is more advanced in modern pharmaceutical technology [43, 44]. Rising interest in this ground sorts out, on the one hand from the often unsuccessful research for effective and non-toxic new drugs, and on the other hand from new knowledge of the biochemical events around and inside tumor tissues. In fact, the active agent is spread over the entire body and reaches not only the target cells or tissues but also interacts with healthy cells. This results in the peripheral toxicities and low therapeutic efficiency, and prompts the search for novel therapeutic strategies. The enhancement of drug delivery systems has been necessary, including drug-antibody conjugates (immunoconjugates), conjugates obtained by linking drugs to natural or synthetic polymers (macromolecular prodrugs) [45, 46], vesicular or particulate systems (liposomes [47], nanoparticles [48], microparticles for regional therapy [49]) and polymeric implants [50]. Unfortunately some of these systems have often disappointed early expectations. In the case of immunoconjugates, the inefficacy was mainly due to the limited access of these relatively big molecules into tumor mass, the heterogeneity of tumor cells and the different humeral response among patients [51]. Therefore, a strong interest was developed in the potentially promising systems, and water-soluble carriers covalently linked to the drug through a biodegradable spacer constitute one of them.

### 2.1.1. Requirements for polymeric drug carrier

There are two types of polymers to be used as drug carriers: the natural and the synthetic macromolecules. They must operate by aiming to maximize their potential as polymeric drug carriers by decreasing the toxicity, and (or) increasing the therapeutic index of the

anticancer drug. Therefore they must meet certain requirements including hydrosolubility, biodegradability, biocompatibility, and chemical composition.

#### 2.1.1.1. Hydrosolubility

Water solubility is an important requirement for any drug carrier, either polymer or carbon nanotubes intended to be used in the biomedical field. This will demand the polymer to be linear and highly flexible. Working with the polymer the entropy of the solution will increase, and therefore favour the dissolution process and the presence of intra-or extrachain hydrophilic entities such as hydroxyl- and amino-terminals. These hydrophilic entities are of excellent utility as they are capable of undergoing effective hydration. The ability to incorporate charged species into the polymer also leads to its hydrosolubility property. In addition, the application of poly(ethylene oxide) (PEO) in the polymer therapeutic field rose in interest, owing to its numerous properties such as the solubility in both aqueous and organic media, ease of chemical modification, and biocompatibility [52, 53], which are also imparted once PEO is incorporated into a polymer.

#### 2.1.1.2. Biodegradability

The candidate carrier must be sufficiently large, this will be important for the hindrance of rapid excretion by kidneys observed with low molecular weight. The biodegradation and resultant catabolic elimination following drug release, will be possible through the composition of the backbone comprising segments amenable to hydrolytic and enzymatic cleavage. Most biodegradable polymers are designed to degrade as a result of hydrolysis of the polymer chains into biologically acceptable, and progressively smaller, compounds. In some cases—as, for example, polylactides, polyglycolides, and their copolymers—the polymers will eventually break down to lactic acid and glycolic acid, enter the Kreb's cycle, and be further broken down into carbon dioxide and water and excreted through normal processes. Degradation may take place through bulk hydrolysis, in which the polymer degrades in a fairly uniform manner throughout the matrix. For some degradable polymers, most notably the polyanhydrides and polyorthoesters, the

degradation occurs only at the surface of the polymer, resulting in a release rate that is proportional to the surface area of the drug delivery system [54].
In order to increase the biodegradability of a polymeric carbon backbone, the equipment of the latter with peptide, saccharide or nucleotide sequences is required, as they are recognized and biodegraded by numerous enzymes present in the lysosomal compartment of the cell.

All of the previously described systems are based on polymers that do not change their chemical structure beyond what occurs during swelling. However, a great deal of attention and research effort are being concentrated on biodegradable polymers. These materials degrade within the body as a result of natural biological processes, eliminating the need to remove a drug delivery system after release of the active agent has been completed.

#### 2.1.1.3. Biocompatibility

The polymeric backbone must be non-toxic, non-immunogenic, and non-thrombogenic in order to avoid any carrier-generated toxic, immunogenic, and blood-clotting side effects. When these requirements are unsuccessful it will result in premature destruction of the carrier through attack by the host defense systems, which renders the drug delivery system ineffective. PEO is found to be a promoter of cell fusion and hydration [55] as well as a chemical entity for reducing or controlling the antigenicity of immunogenic proteins [56]. An earlier review article [57] stressed the conjugation of PEO to protein or liposome as an important tool for reducing the shortcomings encountered in using these therapeutic agents, namely the degradation by proteolytic enzymes, thermal instability, and immunogenicity. More recently it has been reported that the presence of PEO segments in polyelectrolyte causes complexation with plasmids, reducing the side effects and increases the lifetime of these complexes in vivo [58, 59] .

#### 2.1.1.4. Chemical composition

The carrier macromolecule must comprise reactive functional groups suitable for drug anchoring and release. The separation of these groups should be completed from the principal chain by short side chains or spacers. The presence of spacers will serve to diminish the steric inaccessibility due to the polymeric backbone. By their nature, the spacers should be stable in the bloodstream [(60)] but susceptible to either enzymatically catalyzed or pH-dependent hydrolysis in the lysosomal compartment [(61)]. Polymeric carrier should equally develop the aptitude to be intended for predetermined cell types. This will be achieved by the incorporation of targeting moieties such as cationic functions and antibodies [(62)]. The presence of cationic function, including tertiary amino groups, is required in the carrier backbone as this will facilitate adsorptive pinocytotic cell entry [(63)] and therefore prevent problems related to potential iconicity or polarity of the monomeric drug, and on the other hand, increase drug selectivity for the transformed cell, given that many types of cancer are characterized by negative surface charge. Also, the macromolecular carrier should incorporate an interposition between the spacer-bearing units, of subunits lacking drug-binding abilities along the principal chain. This will prevent multifunctional drug binding by reducing spacer density in the molecule.

### 2.1.2. Natural polymers as drug carriers

The preparation of natural polymers may be restricted by the need for several purification steps, and their use is limited by their high immunogenicity. Nevertheless they have the advantage of easy availability and biocompatibility. Many of them have been identified and have been used as possible drug or possess an intrinsic anticancer activity. It has been noticed that albumin, bovine serum albumin (BSA), chitins, and dextran have been successfully conjugated to doxorubicin [(64, 65)] and mitomycin [(66)], respectively. In general, these polymers being biodegradable owing to their natural origin, they will be excreted from the bloodstream by natural catabolic mechanism. Nevertheless, their use as drug carriers is often limited. Indeed, the substitution of natural macromolecules with covalently linked low-molecular-weight drug molecules generally results in the

hampering of the host's ability to enzymatically degrade the polymeric carrier effectively [67]. The loss of biodegradation ability into easily eliminated fragments causes the resistance of elimination from the body. The administration of natural macromolecules has been inefficacious due to the main problem such as short intravascular half-life, immunogenicity, and sometimes poor solubility [68]. In order to dramatically increase their therapeutic effectiveness, their modification with synthetic macromolecules is needed.

### 2.1.3. Synthetic polymers as drug carriers

The synthetic polymers operating as drug carriers must respond to the general requirement to be fulfilled by any polymer in an attempt to serve in biological environment (section 1.7.1.1), especially their entire molecular-weight distribution must be under the kidney threshold (30 000-50 000 KD) if they are not biodegradable. This will have the advantage of minimizing storage. Polymeric drug delivery systems are attractive as a means of effectively controlling drug concentration and targeting specific regions in the body. Until recently, most polymers investigated for drug-delivery applications were either linear (nonbranched) or crosslinked (highly branched in nature). Current advances in polymers with highly branched and defined architectures have opened new opportunities for developments within the drug-delivery field. These polymers are frequently referred to as being hyperbranched or dendritic to emphasize the role of branching in the polymer architecture. A variety of intriguing systems are being explored that exploit the potential of hyperbranched polymers for use as drug-delivery agents [69].

Controlled drug delivery occurs when a polymer, whether natural or synthetic, is judiciously combined with a drug or other active agent in such a way that the active agent is released from the material in a predesigned manner. The release of the active agent may be constant over a long period, it may be cyclic over a long period, or it may be triggered by the environment or other external events. In any case, the purpose behind controlling the drug delivery is to achieve more effective therapies while eliminating the potential for both under- and overdosing. Other advantages of using controlled-delivery

systems can include the maintenance of drug levels within a desired range, the need for fewer administrations, optimal use of the drug in question, and increased patient compliance. While these advantages can be significant, the potential disadvantages cannot be ignored: the possible toxicity or nonbiocompatibility of the materials used, undesirable by-products of degradation, any surgery required to implant or remove the system, the chance of patient discomfort from the delivery device, and the higher cost of controlled-release systems compared with traditional pharmaceutical formulations.

Note that the synthetic polymers are categorized according to the chemical nature (e.g. polysaccharides, vinylic, acrylic polymers, poly(amino acids), etc.), the stability of the backbone, and the molecular weight. More interest was developed in the use of the synthetic polymers as drug carriers since Rigsdorf [70] proposed his model of water-soluble macromolecule prodrugs in the mid-Seventies. In the following text it has been found out whether, and to what extent, these prerequisites are met in the structural compositions of the three selected carrier types (1) the α,β-DL-polyaspartamides, (2) the poly(amidoamines), and (3) the 2-hydroxypropyl-methacrylate polymers (HPMA). In addition, polyamides obtained by polycondensation processes will cursorily be discussed because of their sporadic use as carriers.

### 2.1.3.1. *α,β*-DL-polyaspartamides

This carrier type has been exalted into recognition of polymer research some three decades ago [71, 72]. It can be synthetically prepared by high-temperature condensation polymerization of DL-aspartic acid in orthophosphoric acid medium, leading to a polysuccinimide intermediate (Scheme 2.1).

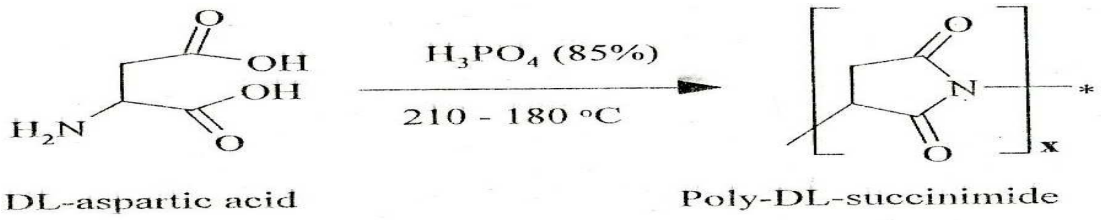


**Scheme 2.1: Synthesis of polysuccinimide (PSI)**

In the following polymer-homologous reactions suitably performed in a dipolar aprotic solvent such as N,N-dimethylformamide, the intermediary polysuccinimide is treated sequentially with amine nucleophiles ($NH_2$-$R_1$, $NH_2$-$R_2$); occasionally a third amine, $NH_2$-R3, may be employed in this operation, whereby amide ring opening gives rise to the generation of the ultimate polyaspartamides [73, 74]. These linear polyamides are composed of randomly distributed aspartamide repeat units bearing N-attached substituents ($R_1$, $R_2$, etc.) as introduced by the amine nucleophiles chosen. Scheme 2.2 depicts this sequence of ring opening steps [75].

Note that here and in subsequent polyaspartamide representations, only the α-peptidic forms are shown for convenience, although the isomeric β-forms, with two carbon atoms (rather than one only) separating –CO and NH-, are also present.

The structural arrangement in scheme 2.2 was made by substituting a solubilizing entity **S** for NH-$R_1$, a homing device **H** for NH-$R_2$, and a drug-binding functional group **F** for NH-$R_3$ (Scheme 2.3).

It should certainly result from the thorough discussion in the previous structure-function relationships that polyaspartamides complying with this schematic representation will be able to provide an excellent "workhorse" service in drug conjugation studies. Purposely, the following hold (Schema 2.3): (i) The vital prerequisite of water solubility will be afforded by the numerous freely rotating aliphatic main-chain bonds and, in particular, by the extrachain **S** units chosen so as to contain tert-amine, hydroxyl, or, perhaps, oligo(ethylene oxide) groups [76]. These functionalities will be prone to equation, that is, hydrogen bond formation with the aqueous solvent, and/or protonation with generation of cationic sites. (ii) Steric accessibility of the anchoring site **F** is optimized by insertion of a suitably long (say, 8-10 atomic constituents) aliphatic spacer link between F and backbone, thus reducing any steric hindrance potentially provided by the main chain proper. (iii) The chain construction has been rendered nontoxic through use of aspartic acid as the principal molecular backbone source. (iv) The chain is biodegradable hydrolytically at the CO-NH link for catabolic fragment elimination through the globular

system of the kidneys upon drug release. A vital detoxification process in light of the fact that, as mentioned before, large nondegradable macromolecules, such as vinyl-type polymers and other carbochain macromolecules strongly resist excretion and tend to induce toxicity. Such backbone degradation must be slow and controlled, however, so as to ensure stability during serum exposure, yet fragmentation in the endosomal compartment. In the polyaspartamide structure, these conditions are ideally met: in the serum environment (pH~7.5) only minimal hydrolytic CO-NH bond fission is observed, whereas in the endosomal space (pH~5) such fragmentation proceeds as expected, albeit slowly. The superimposition on hydrolytic bond fission is the process of enzymatic bond breaking effective both at main-chain NHCO sites and, to a variable extent, also at drug-binding links. Whereas natural polypeptides are prone to rapid degradation (unzipping) as a consequence of α-peptidase activity in the serum, such unzipping is grossly impeded by the presence of D-configured CH groups and β-peptide units in the chain that are inert to α-peptidase attack [77].

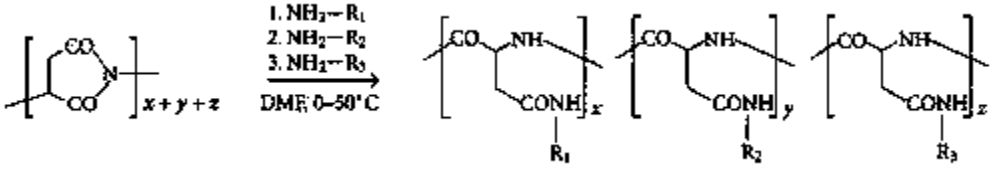


**Scheme 2.2: Amide ring opening process for polyaspartamide**

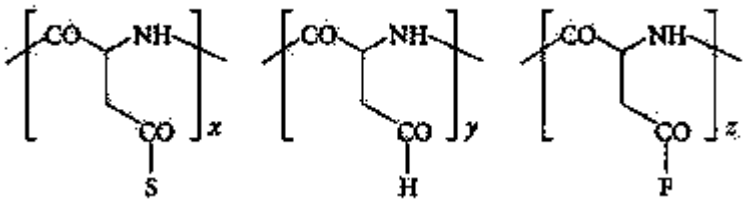


**Scheme 2.3: Substitution of a solubilizing entity S, a homing device H and a drug-binding functional group F to polyaspartamide**

### 2.1.3.2. Polyamidoamides

Poly(amidoamines) (PAAs) belong to the family of polymers characterized by the regular arrangement of amido groups and secondary (or/and tertiary) amines along the macromolecular chain. Pioneered by Ferruti [78], they are synthesized by polyaddition of

primary monoamines or bis(secondary amines) to bisacrylamides. Since they bind tightly to heparin, PAAs were introduced in biomedical application; initially as a heparin-adsorbing surface for medical devices (heparin renders the device non-thrombogenic) [79]. PAAs were later proposed as particularly promising drug and DNA [80] delivery carriers owing to their water solubility, biodegradability [81], conformation-changing ability with changing pH [82], and potentially low cytotoxicity compared with other synthetic polymers, e.g. poly-L-lysine. Furthermore, PAAs are also known to possess structure-cytotoxicity relatioships. They have both aminic and amidic sites in their backbones, and the polymers prepared are generally selected to incorporate several different variables to reinforce the aforementioned physicochemical properties. Using the pKa values different PAAs, Ferruti[83] demonstrated the basicity of aminic nitrogen atoms of each repeating unit to be independent of the degree of protonation of the whole macromolecule. Thus, the main influence on polymer basicity is governed by the aminic moiety; therefore several different monoamines were incorporated. The purpose of monoamine incorporation was to ensure firstly, higher basicity, as the mechanism of macromolecule cell entry, endocytosis, exposes the monoamine to pH changes, from pH 7.4 extracellular to pH 5.5-6.5 within the endosomal-lysosomal system [84], and secondly, increased water solubility. More recent review article from Ferruti's laboratory cover the synthesis of primary amine-functionalized PAAs [85], the biomedical applications [86] and the correlation between physicochemical and biological properties [87].

### 2.1.4. Polymer-drug conjugation

The drug systems investigated in this project have been the conjugation of copolyaspartamides as polymeric carriers by varying the molecule rate of solubilizing group and anchoring drug respectively. Thus, the conjugation is achieved by formation of either ester or amide biocleavage bond. Since Folic acid and methotrexate represent the same chemical property, the investigation made on polymers-bound folic acid can result to the conclusion of polymers-bound methotrexate.

### 2.1.4.1. Polymer-MTX conjugation

Aiming to improve its therapeutic index, including the site-specific targeting or proving controlled release, MTX has been conjugated to biopolymers like mono-and polyclonal antibodies [88, 89], serum albumins [90, 91], neoglycoproteins [92], chitosan [93]. The conjugation of MTX to synthetic polymers has been extensively reported [94, 95]. These reports include investigation from this laboratory. Indeed, following Ringsdorf's model of macromolecular prodrugs, MTX was conjugated with various polymeric carriers. In earlier project [96] polyaspartamides were conjugated with MTX through tethers containing an ester group as the biofissionable site, and in recent study [97] series of related conjugates were prepared with biocleavage carboxamide links in the connecting spacer.

### 2.1.4.2. Polymer-folic acid anchoring

The potential use of cellular nutrients for macromolecular and colloidal particle uptake is appealing, since receptor-mediated endocytosis is a cellular process designed for transporting critical molecules across the plasma membrane into the cytoplasm [98]. Rapidly-dividing cells express high affinities for folic acid because folate is an essential factor in purine, nucleotide, and DNA synthesis. Hence, the possibility of utilizing this pathway for promoting folate-linked molecules or colloidal particles to enter gastrointestinal (GI) epithelia. By virtue of its ability to be taken up by folate receptor overexpressed on certain tumor cells, folic acid has been widely investigated as a targeting molecule for active anticancer drug delivery. Proper synthesis procedures have been pointed out to link folic acid to drug carriers to produce targeting drug delivery systems. The folic acid molecule possesses two carboxyl groups, termed α-and γ-carboxyl group, which can act as handles for covalent attachment. However, according to literature, there is a stronger affinity of folate toward its receptor, when linked via the γ-carboxyl derivatives are not readily recognized [99].

Folate-induced receptor-mediated endocytosis has been extensively exploited to facilitate entry of anchoring drugs [100], antibodies [101], imaging agents [102], liposomes [103] or macromolecules [104], and proteins into cells. Folate-conjugated proteins present the advantages of conceivably contacting and binding to all cells in a culture medium simultaneously. This avoids a natural vitamin endocytosis pathway. Unlike hormone- or virus-mediated endocytosis, folate uptake occurs in all dividing cells, at reasonable rates, and folate is deposited into cytosolic rather than lysosmmal compartments [105].

## 2.2. Carbon nanotubes as Drug carriers

Nanotechnology is expected to influence all current industries including semiconductors, manufacturing and biotechnology, and it may also create several new ones. Major challenges remain, before to take these opportunities to the realization. Some of opportunities include the ability to assemble, characterize and manipulate materials at the nanoscale level. Nanomedicine is an area with particular promise and may inspire the construction of nanostructured carriers for the targeted delivery of small-molecule 'passengers' to a desired area. Nanosized delivery vehicles may also offer better or more efficient use of an active molecule (i.e. drugs, antigens, proteins, enzymes and nucleic acids) by controlling release rates, by protecting it from unwanted metabolic processes or through targeted delivery processes that can reduce side effects. A drug delivery system is usually designed to improve the pharmacological and therapeutic properties of conventional drugs and to overcome problems such as limited solubility, poor distribution, lack of selectivity and tissue damage. Cell membranes act as barriers and allow only certain structures with the right hydrophilicity to hydrophobicity ratio to pass. Among the currently available delivery systems, which include liposomes, emulsions, polymers and microparticles [106], carbon nanotubes (CNTs) have recently gained popularity as potential drug carriers of therapeutic agents and diagnostic tools [107]. They have nanoscale dimensions, and can be modified through covalent bonding of functional organic molecules. CNTs have been shown to penetrate easily through cell membranes, have been proposed as components for DNA and protein biosensors, ion channel blockers

and as bioseparators and biocatalysts [108]. CNTs have also been used as platforms to detect antibodies associated with human auto-immune diseases.

### 2.2.1. Carbon nanotubes

Carbon nanotubes (CNTs) are interesting new molecular forms of carbon in the fullerene family, discovered by Iijima [109]. Due to unique electronic and mechanical properties of CNTs [110] and also their resistance to acid/basic media [111] they have attracted a special attention.

CNTs can be imaginatively produced by rolling up a single layer of graphene sheet (single-walled CNTs; SWNTs) [112, 113], or by rolling up many layers to form concentric cylinders (multi-walled CNTs; MWNTs) [114]. As-produduced CNTs, both SWNTs and MWNTs, are commercially available, with different details and degrees of purity. Pristine CNTs are completely insoluble in all solvents, which has generated some health concerns; consequently, their biological properties are being studied in terms of toxicity [115]. The development of efficient methodologies for the chemical modification of CNTs has stimulated the preparation of soluble CNTs that can be employed in several biological applications, among which drug delivery appears to be particularly promising [116, 117, 118, 119].

However, the hydrophobic and inert nature of the surface of as-prepared nanotubes is unfavorable for these applications [120]. In order to improve the interaction of CNTs and foreign molecules it is necessary to modify the surface of the nanotubes. This manner of modifying the surface of nanotubes results in the functionalization of carbon nanotubes.

#### 2.2.1.1. Synthesis of Carbon nanotubes (CNTs) by Chemical Vapor deposition (CVD)

Chemical Vapor Deposition (CVD) is a versatile technique often used in the semiconductor industry for deposition of materials on various substrates. In the CVD

process, a gas or vapor precursor is transformed into solids, such as thin films, powders, or various structured materials, inside a reactor. Chemical vapor deposition has also been used for many years to produce carbon fibers, filaments, and tubular carbon materials. Recently, CVD has been used to synthesize a variety of nanostructured materials, including carbon nanotubes and nanowires composed of various materials, as well as graphene and thin films. It is an inherently scalable method, providing an important path from research to production.

The development of the Chemical Vapor Deposition (CVD) method used to produce carbon nanotubes, has enabled the synthesis of high quality carbon nanotubes that grow in specified locations and with greater purity. Carbon nanotubes can be grown by CVD directly onto substrates or onto bulk-supported catalysts. The process typically consists of flowing a carbon feedstock, over a catalyst-covered substrate at elevated temperature; the feedstock molecules decompose upon the catalyst, releasing their carbon to form nanotubes. Advantages of using the CVD process for nanostructure synthesis include:

#### 2.2.1.2. Comparison of CVD to Other Methods Used to Make Nanotubes

**A CVD**

Chemical vapor deposition (CVD) has been found to provide a number of benefits over other nanostructure synthesis methods. Nanotubes are obtained at relatively low temperatures with high quality and purity. The comparatively simple process can provide nanotubes of long length and controllable diameter. Catalyst deposition on substrates allows for formation of novel structures. In addition, the CVD method is scalable to industrial production levels [(121)].

**B Arc Discharge**

In the arc discharge method, nanotubes are found in soot produced in arc discharge with catalytic metals (e.g. Fe, Ni, Co). Two graphite rods, separated by a few millimeters, are connected to a power supply. At 100A, carbon vaporizes and forms hot plasma [(122)].

Unlike CVD, in arc discharge, it is generally difficult to control the location and alignment of nanotubes. The resultant nanotubes are produced in small quantities, often short with random sizes and orientations, and typically tangled, making some applications difficult. The method requires evaporation of carbon atoms from solid targets at very high temperatures and the products generally require purification [123].

**C. HiPco (High Pressure Carbon Monoxide Conversion)**

In the HiPco method, high pressure carbon monoxide (CO) is heated with a volatile catalyst precursor (e.g. $Fe(CO)_5$) at high temperature. The SWNT form in the gas phase and are removed by filter from flowing, recirculating CO [124].

Unlike CVD, the HiPco method requires pressurized carbon monoxide, very high process temperatures, and a metal catalyst that is difficult to remove at the end of a process [125].

**D. Laser Ablation or Vaporization**

In the laser ablation method, nanotubes are produced by pulsed YAG laser ablation of a graphite target in a furnace at temperatures near 1200°C. The target is hit with intense laser pulses, generating carbon gas from which the nanotubes are formed [126].

Unlike CVD, in the laser ablation method, it is difficult to control the location and alignment of the nanotubes produced. Small quantities of nanotubes result from this process and they are generally tangled, making some applications difficult. The method also requires evaporation of carbon atoms from solid targets at very high temperatures [127].

### 2.2.2. Functionalization of Carbon nanotubes for biological applications

As produced, raw carbon nanotubes have highly hydrophobic surfaces, and are not soluble in aqueous solutions. To overcome the problem of poor processabilty, the functionalization and solubilization of CNTs have received much recent attention. For biomedical applications, surface chemistry or functionalization is required to solubilize CNTs, and to render biocompatibility and low toxicity. The functionalization generates functional groups at the surfaces of CNTs. These functional groups could react with other

chemicals, prepolymers and polymers, and give rise to a homogeneous dispersion or solubilization of CNTs. Surface functionalization of carbon nanotubes may be covalent or noncovalent. Chemical reactions form bonds on nanotube sidewalls resulting into covalent functionalization, while noncovalent functionalization exploits favorable interactions between the hydrophobic domain of an amphiphilic molecule and the CNT surface, affording aqueous nanotubes wrapped by surfactant.

Thus chemical functionalization plays an essential role in tailoring the properties and application versatility of CNTs. The requirement is that the functionalized carbon nanotubes have to exhibit: - high propensity, - biocompatibility, -solubility, - excretion, - little toxicity.

#### 2.2.2.1. Covalent functionalization of carbon nanotubes

The covalent functionalization of CNTs is the alternative and extremely promising approach for applications in fields such as that of functional and composite materials and that of biology. According to the location of the functional groups, two main strategies are used to covalently functionalize CNTs with biomolecules: (i) defect functionalization, and (ii) sidewall functionalization [128, 129].

**A. Defect functionalization**

Various covalent reactions have been developed to functionalize carbon nanotubes, oxidation being one of the most common. CNT oxidation is carried out with oxidizing agents such as nitric acid [130, 131]. During the process, carboxyl groups are formed at the ends of tubes as well as at the defects on the sidewalls. Zeng et al. observed $sp^3$ carbon atoms on SWNTs after oxidation and further covalent conjugation with amino acids [132].

Permanganate is a well known oxidizer in organic chemistry [133]. Potassium permanganate has been used as the oxidant in the presence of sulfuric acid to functionalize CNTs [134]. It is also used along with a phase transfer catalyst [135]. Other oxidants used to functionalize CNTs are concentrated nitric acid [136, 137] and concentrated

sulfuric acid as the oxidant [138]. This procedure of functionalization of CNTs generates mainly the –OH and –COOH functional groups, more easily at the caps than at the walls. By utilization of such functional groups, it is possible to attach CNTs to various polymeric agents and then to make them soluble in organic solvents [139, 140].

Chemical treatments, such as strong oxidizing acid mixtures of $HNO_3/H_2SO_4$ under sonication, modify CNT surfaces with anchor groups, including carboxylic, carbonyl and hydroxyl functions, eventually used to covalently connect molecules to the tubes (Scheme 2.4). The carboxylic acid groups are often the most common choice to connect the CNTs with the amino-terminated sites present on the biomolecules. Before covalent modification, the carboxylic acids are often activated by thionyl or oxalyl chloride, carbodiimides or active esters, to get highly reactive intermediate groups, to link different types of biomolecules to CNTs via stable covalent bonds. The carboxyl groups of CNTs were activated, for example, in the presence of N-hydroxysuccinimide and carbodiimide. This can facilitate the conjugation of peptide nucleic acid (PNA, an uncharged DNA analogue) to the end of CNTs via a stable amide bond. PNAs were then hybridized with complementary DNA sequences, showing the possibility of recognition-based assembly and the potential use as biological sensors. Similar methods based on the amide linkage were used to immobilize DNA [141]. In this research the carboxyl groups of CNTs were activated in the presence of 2-(1H-benzotrial-1-yl)-1,1,3,3-tetramethylurium hexafluorophosphate (HBTU). They showed that aqueous solubility can be assured by a covalent attachment of hydrophilic moieties.

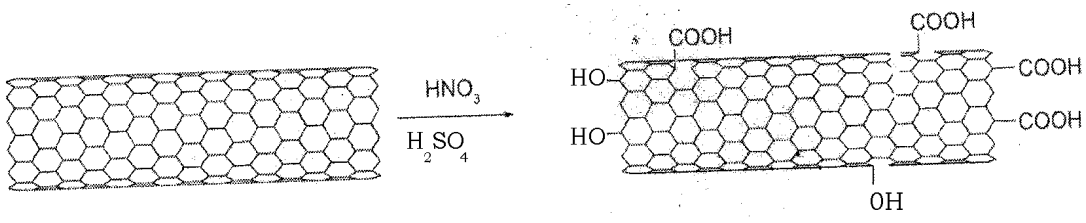


**Scheme 2.4: f-CNTs with Sulphuric acid and Nitric acid**

**B. Sidewall Functionalization**

This type of covalent functionalization is based on the addition reactions to CNTs. By exploiting the chemistry of fullerenes, 1,3-dipolar cycloaddition of azomethine ylides, aryl diazonium salt addition or reductive alkylation using lithium and alkyl halides have been successfully employed to CNTs [142, 143, 144, 145, 146]. Such direct sidewall modification of CNTs permits the incorporation of different functional groups on the nanotube which could be further derivatized [147]. The covalent bond presents the advantage of being more robust during manipulation and processing in comparison to the noncovalent dispersion. Nevertheless, both covalent and noncovalent functionalization of CNTs have been exploited for application of such materials in the field of drug delivery.

### 2.2.2.2. Noncovalent functionalization of carbon nanotubes

Compare to covalent functionalization, noncovalent functionalization of CNTs can be modified with amphiphilic surfactant molecules or polymers. The noncovalent dispersion of CNTs in a solution allows preservation of their aromatic structure and thus their electronic characteristics. The dispersion procedures usually involving ultrasonication, centrifugation and filtration are quick and easy. Since the chemical structure of the π-network of carbon nanotubes is not disrupted, except for shortening of length due to the sonication employed in the functionalization process, the physical properties of CNTs are essentially preserved by the noncovalent approach. Hydrophobic or π-π interactions often evoked as likely responsible for noncovalent stabilization. Consequently, aqueous solution of CNTs, especially SWNTs, engineered by noncovalent functionalization are promising for multiple biomedical applications, including imaging.

An ideal noncovalent functionalization coating on CNTs for biological applications should have the following characteristics. First, the coating molecules should be biocompatible and non-toxic. Second, the coating should be sufficiently stable to resist detachment from the nanotubes surface in biological solutions, especially in serum having high salt and protein contents. The amphiphilic coating molecules should have very low critical micelle concentrations (CMC) value so that the nanotubes coating is stable, after removal of most of the excess coating molecules from CNT suspension.

Lastly, the coating molecules should have functional groups which are available for bioconjugation with antibodies or other molecules to create various functional CNT conjugates for different biological applications. The polyaromatic graphitic surface of carbon nanotube is accessible to the binding of aromatic molecules via π-π stacking [148, 149] Chen et al. showed that proteins can be immobilized on SWNTs by an amine-reactive pyrene derivative [150] Wu et al. also used pyrene conjugated glycodendrimers to solubilize carbon nonotubes [151]

Nowadays, three classes of molecules are mainly used for CNTs dispersion. Surfactants are used because they are easily available and low-cost. Polymers and biopolymers (nucleic acids and peptides) are also very efficient in the dispersion process.

**A. Surfactants**

A series of anionic, cationic and nonionic surfactants have been proposed to disperse nanotubes. Sodium dodecyl sulfate (SDS) and Triton X-100 were used to obtain CNTs suspensions up to 0.1 and 0.5 mg/mL, respectively [152]. However, the stability of this suspension was not longer than one week. A better result was obtained by using sodium dodecyl-benzene sulfonate (SDBS), which was able to provide stability over one month reaching 10 mg/mL concentration of the suspension. The combination of π-π interactions of aromatic moieties between CNTs and SDBS and the long lipid chains of the SDBS increases the stability of the complex. Atomic force microscopy (AFM) and electronic transmission microscopy (TEM) studies of SDS/CNTs dispersions showed that CNT are mainly present as individual tubes uniformly covered by the surfactant [153].

Various amphiphiles have been used to suspend carbon nanotubes in aqueous solutions, with hydrophobic domains attached to the nanotube surface via van der Waals forces and hydrophobic effects, and polar heads for water solubility [154]. Carbon nanotube solubilized by those amphiphiles with relatively high critical micelle concentrations (CMC), are typically unstable without an excess of surfactant molecules in the solution. Large amounts of surfactants may lyse cell membranes and denature proteins, and are therefore not useful in biological environments.

**B. Polymers**

Polymers are widely used, for example as molecular carriers for drug delivery [155]. In the solubilization of CNTs they represent a good alternative to surfactants, although they do not have a better dispersion efficiency [156]. The mechanism of dispersion is based in this case on wrapping of the polymer around the tubes. The polymer wraps around ropes of nanotubes (Figure 2.1). The driving force of the phenomenon is likely to be the steric repulsion of the polymer. Once the polymer is attached to the surface of the nanotubes, it offers a sufficient repulsive potential stabilizing the dispersion [157]. In the case of nonionic polymers, based on poly(oxyethylene) copolymers, the efficiency of the dispersion is instead due to their hydrophilic counterpart. For particularly high molecular weight polymers, the suspendability is enhanced as the steric stabilization is increased by a wider coverage of the surface. In a similar approach, CNTs were dispersed by using cationic copolymers [158]. The nanotubes were covered by the hydrophobic backbone of the polymer while the positive tetraalkylammonim groups were exposed at the surface to display water solubility. These types of fluorescent polymers have also been employed to study the interaction with mammalian cells. Poly(vinylpyrrolidone) was conjugated with various fluorescent dyes. CNTs were suspended in 1% SDS and mixed with the florescent polymers to form supramolecular complexes, which were found to have potential applications as new molecular probes [159]. With respect to have a polymer which can easily present a peptide group after opening ring process by different amines, polysuccinimide has been chosen in this research as polymer coating of the carbon nanotubes for noncovalent functionalization.

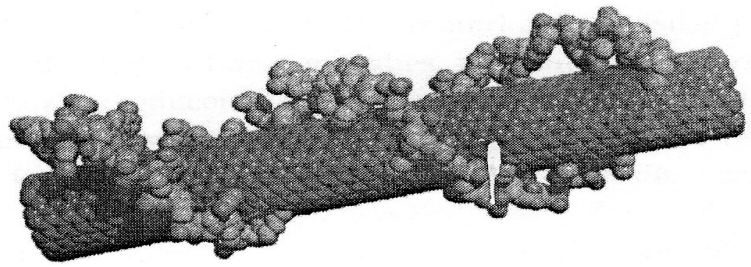

**Figure 2.1: Coating of CNTs with polymer**

**C. Biopolymers**

The solubilization of CNTs with biological components is certainly more appropriate towards integration of this new type of material with living systems. Self-assembly processes similar to π-π interactions typical of double-stranded DNA can be exploited, for example to disperse the nanotubes. Nucleic acids are certainly ideal candidates to form supramolecular complexes based on π-stacking between the aromatic bases and the CNTs surface. Indeed, Zeng et al. [160, 161] have described an easy way to solubilize carbon nanotubes by simple sonication in the presence of a single-strand DNA. A molecular modeling study was perfomed to explain the formation of the hybrids exerted by DNA wrapping and subsequent CNTs debundling. The DNA-nanotube complexes displayed solubility in the range of mg/ml, and their good stability permitted the purification using ion-exchange chromatography. Amphiphilic peptides belong to another class of biopolymers that efficiently disperse CNTs [162]. The presence of amino acids like tryptophan, phenylalanine, tyrosine and histidine into peptide sequence plays a key role on the solubilization process in water. These peptides could be selected from phase-display peptide libraries [163] or by design [164, 165]. The design of highly specific peptides to wrap around the nanotubes represent an interesting way to assure solubility and may even provide a useful tool for size-separation. More recently, cyclic peptides were also proven to have similar capabilities [166].

### 2.2.3. Application of CNTs in drug delivery

#### 2.2.3.1. Peptide delivery by CNTs

The application of CNTs has been investigated as template for presenting bioactive peptides to the immune system [167]. For this purpose, a B-cell epitope of foot-and mouth disease virus (FMDV) was covalently attached to the amine groups present on CNTs, using a bifunctonal linker. The peptides around the CNTs adopt the appropriate secondary structure for recognition by specific monoclonal and polyclonal antibodies. The immunogenic features of peptide-CNTs conjugates were subsequently assessed in vivo [168]. Immunization of mice with FMDV peptide-nanotube conjugates elicited high

antibody responses as compared with the free peptide. These antibodies were peptide-specific since antibodies against CNTs were not defected. In addition, the antibodies displayed virus-neutralizing ability. The use of CNTs as potential novel vaccine delivery tools was validated by interaction with the complement [169]. The complement is that part of the human immune system that is composed of a series of proteins responsible for recognizing, opsonising, clearing and killing pathogens, apoptotic or necrotic cells and foreign materials. Salvador-Morales et al. [170] showed that pristine CNTs activate the complement following both the classical and the alternative way by selective adsorption of some of its proteins. Because complement activation is also involved in immune response to antigens, this might support the enhancement of antibody response following immunization with peptide-CNTs conjugates.

#### 2.2.3.2. Methotrexate delivery by CNTs

To maximize the efficacy of a drug, the choice of the delivery system is of fundamental importance. Conventional drug administration often fails due to low drug solubility-instability in biological medium, poor distribution among the cells and lack of selectivity and damage of healthy tissues. Drug delivery systems are aimed to minimize the degradation, to increase its bioavailability, to target it to specific cells and to reduce the amount of drug need, deceasing toxicity and harmful side effects. CNTs possess an enormous aspect ratio (between length and the diameter) compared to classical drug delivery systems such as liposomes or polymer-based carriers, and are becoming a promising alternative in this field, since the first demonstration of their capacity to penetrate into cells. CNTs can be functionalized with antibiotics to deliver them into the cells.

Note that methotrexate (MTX) is a well-known and potent anti-cancer agent, used also to cure autoimmune disease [171]. However, MTX suffers low bioavailability and toxic side effects [172]. Therefore, an increased bioavailability and a targeted delivery are highly desirable. Being a drug widely used against cancer; high concentrations of drug are required due to its low cellular uptake [173, 174]. It has been found that MTX introduced

together with fluorescent probe around the CNTs sidewalls [175], can offer the possibility for improving bioavailability and, in the presence of a targeting unit, to address specifically cancer cells. Consequently MTX is rapidly internalized inside the cell by carbon nanotubes. Preliminary results have shown that MTX conjugated to carbon nanotubes is as active as MTX alone in a cell culture [176]. The stable amide bond between the MTX and the tubes could be the reason for lack of enhanced efficacy. Indeed, the drug is probably released too slowly from the tubes into the cytoplasm for an efficient interaction with its receptor. One solution to this problem could be to introduce a cleavage linker or a more enzymatically sensitive bond in the MTX conjugated CNTs, as demonstrated for conjugates based on dendrimers [177].

#### 2.2.3.3. Folic acid delivery by CNTs

Folic acid conjugated CNTs has been found necessary to operate as receptor for targeting moiety during the path uptake of drug delivery. Passive targeting approaches are limited in their scope and thus, tremendous effort has been directed towards the development of active approaches for drug targeting. Active targeting employs specific modification of drug/drug-carrier nanosystems with "active" agents having selected affinity for recognizing and interacting with a specific cell, tissue or organ in the body [178].Direct coupling of drug to targeting ligand, restricts the coupling capacity to a few drug molecules. In contrast, coupling of drug carrier nanosystems to ligands allows import of thousands of drug molecules by means of one receptor targeted ligand.

Drug targeting to specific cells has been explored utilizing the presence of various receptors, antigens/proteins on the plasma membrane of cells and also by virtue of the lipid components of the cell membranes. The presence of receptors on cell membranes potentiates active targeting by not only allowing specific interaction of drug carrier system with cells, but also facilitating its uptake via receptor mediated endocytosis.

Folic acid, a vitamin essential for de novo nucleotide synthesis is taken up by cells via receptor mediated endocytosis using membrane associated folate receptors. Folate

receptors are expressed only on certain epithelial cells in humans, but are differently over-expressed in cells of cancers with epithelial origin. It has been primarily used for tumor specific drug delivery in many cancers including breast, ovary, brain and lung malignancies. Significant over-expression of folate receptors on a variety of tumor cells allows targeting moety. Folate has been conjugated to radiolabelled dendrimers and to liposomes to affect preferential uptake and accumulation of therapeutic agents in tumor cells. Induction of folate receptors with retinoid compounds followed by folate conjugated liposomes, has been used successfully for therapy of acute myelogenous leukemia. This treatment modality was also found to bypass the p-glycoprotein (Pgp) mediated drug efflux mechanisms. The application of folic acid to MTX conjugated CNT as targeting moiety can render more efficacious the translocation of MTX to the cancerous cells.

# CHAPTER 3

# EXPERIMENTAL SECTION

## 3.1. General Procedures

$^1$H NMR spectra were obtained at 300MHZ and 400MHZ in $DO_2$ solution. The chemical shifts, δ in ppm, were referenced against sodium 3-(trimethylsily)-2, 2, 3, 3-$d_4$ propionate. The pH values of the sample in $DO_2$ solution were adjusted to 10-11 by adding sodium hydroxide in order to eliminate potential protonation effect. Solid-state Infrared (IR) spectra were recorded on KBr pellets over the region of 4000-600cm$^{-1}$. The attention was turned only on the significant bands.

Dialysis was performed using cellulose membrane spectra (Spectrum Industries, Los Angeles, CA), with a molecular mass cut-off limit of 12000-14000. Distilled water was used for the dialysis phase. Freeze-drying of aqueous polymer and conjugate solutions were performed in a VIRTIS bench-Top 3 Freeze-drier operating at -30˚C and 10-15Pa. The freeze-dried polymers were routinely post-dried in a SARTORIUS Thermo Control Infrared drying apparatus and kept in desiccators. Samples for analysis were dried using the Abderhalden apparatus, and calcium chloride was done on a HITACHI 2000 spectrometer, at a scan speed of 400nm/min; both analytical methods were performed in the school of chemistry of the University of Witwatersrand. Flash chromatography was performed using basic alumina as a solid support. The aprotic solvent, N,N-dimethylformamide (DMF), was redistilled and kept over molecular sieves. Using the gel permeation chromatography (GPC) with 2.5X60cm column packed with Sepharose 6 gel by the principle of weight average molecular weight (Mw), the polymer-drug conjugates were separated from other products.

The carbon nanotubes (CNTs) were synthesized by chemical catalytic vapour deposition (CCVD), and the following apparatus were used: vertical silica plug, reactor, furnace, temperature regulator, system of rotameters, pressure controllers, valves to control the

flow of gases into the reactor, condenser, two delivery cyclones. The transmission electronic microscope (TEM) was used to characterise CNTs samples.

## 3.2 Reagents and Solvents

The hydroxyamines and diamines were used as received (Adrich Chemie, Fluka AG). These included: D,L aspartic acid, phosphoric acid, 3-dimethylamino-1-propylamide (DMP), diethylenetriamine (DET), 2-2- (ethylenedioxy)-diethylamine (EDDA), 1,3 diaminopropane (PDA), dicyclohexylcarbodiimide (DCC), 2-(1H-benzotriazol-1-yl)-1,1,3,3-tetramethyluronium fluorophosphates (HBTU), triethylamine (TEA), ferrocene, folic acid, methotrexate, sodium hygroxide, chloridric acid, glacial acetic acid, ammonium hydroxide, sulphuric acid and nitric acid.
Acetylene, hydrogen, nitrogen and argon were high purity and used as received (AFROX, South Africa).

Distilled water was used for preparative work. The reaction solvent, N,N-dimethylformamide (DMF), was distilled under reduced pressure, with a fore-runs of around 10% being discarded, and was dried over molecular sieves 4Å. Tetramethylurea (TMU) was received as high purity (Fluka Chemie). All other solvents, Diethyl ether ($Et_2O$), hexane, acetone and toluene, were laboratory grade, received from commercial sources.

.

## 3.3 Experimental Procedures

### 3.3.1. Macromolecular carrier

#### 3.3.1.1. Preparation of poly-αß-DL-succinimide

A mixture of D.L. aspartic acid (25g) and $H_3PO_4$ (12.5g) was homogenized in a 2L round- bottom flask. Then the flask was placed on an oil bath at 250˚C. During the polymerization, the expansion of the mixture was controlled by nitrogen. The reaction

was allowed to proceed at 250˚C until the end of expansion. Thereafter, the temperature was reduced to 190˚C for another 2 hours. This product was washed with water until the pH was around 6. The product was then left in an oven for 72 hours. The yield was 14.82 g which was dissolved in 60 ml of DMF and stirred for overnight (O/N). The brownish solution obtained was stirred again for 1 hour in ice bath, and 1.73 g of DCC added while the solution was stirred for another 4 hours in ice bath. The solution was allowed to continue at room temperature (RT) for overnight (O/N). The solution was centrifuged off to give a clear solution which was precipitated with distilled water. The precipitate was filtered off and was kept in an oven for 48 hours to give a brittle solid which resulted to the yield of 12.75g. Several experiments were done that the values are shown in Table 4.1.

### 3.3.1.2. Synthesis of homopolymers

**A. PSI-DMP (X) EDDA (Y)**

* PSI-DMP (80) EDDA (20)

To a solution of PSI (2.95g; 30mmol) in DMF (37ml) was added DMP (2.40g; 24mmol) in DMF (7.5ml). The solution was flushed with Nitrogen gas and stirred for 24 hours at room temperature (RT). With stirring, the resultant solution was added dropwise to EDDA (2.67 g; 18mmol) in DMF (8ml) cooled in an ice bath. The solution was flushed with Nitrogen gas and stirring continued for 20 hours in the ice bath and for another 5 hours at room temperature. The solution was then concentrated on the roti-evaporator at 60˚C to reduce the volume to half. Polymer was precipitated out with a mixture of diethyl ether-hexane (2:1). Precipitate was washed with hot toluene followed by hot acetone several times. The precipitate was dissolved in distilled water. The pH solution was adjusted to 7-8 and the solution was dialyzed using 12000 membranes for 96 hours. For the last 6 hours of dialyses, the pH of the solution was adjusted to pH 4 for 5 minutes then re-adjusted to 9 with aqueous ammonia to eliminate N protonation. The product was freeze-dried to obtain the homopolymers of 4.1g as yield. The same procedure was observed for the preparation of all PSI-DMP (X) EDDA (Y) where the quantity of reagent was changing with the variation of mol ratio (X/Y) as illustrated in the table 4.2.

**B. PSI-DMP(X) PDA (Y)**

* PSI-DMP (80) PDA (20)

To a solution of PSI (2.95g; 30mmol) in DMF (37ml) was added DMP (2.40g; 24mmol) in DMF (7.5ml). The solution was flushed with Nitrogen gas and stirred for 24 hours at room temperature (RT). With stirring, the resultant solution was added dropwise to PDA (1.33g; 18mmol) in DMF (8ml) cooled in an ice bath. The solution was flushed with Nitrogen gas and stirring continued for 20 hours in the ice bath and for another 5 hours at room temperature. The solution was then concentrated on the roti-evaporator at 60˚C to reduce the volume to half. Polymer was precipitated out with a mixture of diethyl ether-hexane (2:1). Precipitate was washed with hot toluene followed by hot acetone several times. The precipitate was dissolved in distilled water. The pH solution was adjusted to 7-8 and the solution was dialyzed using 12000 membranes for 96 hours. For the last 6 hours of dialyses, the pH of the solution was adjusted to pH 4 for 5 minutes then re-adjusted to 9 with aqueous ammonia to eliminate N protonation. The product was freeze-dried to obtain the homopolymers of 5.58g as yield. The same procedure was observed for the preparation of all PSI-DMP (X) PDA (Y) where the quantity of reagent was changing with the variation of mol ratio (X/Y) as illustrated in Table 4.2.

### 3.3.2. Polymer-Folic acid conjugates

The conjugation of folic acid to amine-functionalized polymeric carriers was achieved by using 2-(1H-benzotriazol-1-yl)-1,1,3,3-tetramethyluronium fluorophosphates (HBTU) coupling agent. In addition, the experiment details followed the standard procedure adopted for the preparation of all polymer-folic acid conjugates herein investigated.

#### 3.3.2.1. General procedure for Polyaspartamide-Folic acid conjugates

**A. PSI-DMP(X)-PDA(Y)-FA.**

Polymer carrier PSI-DMP(X)-PDA(Y) was dissolved in DMF. Folic acid was dissolved in DMF at 50˚C which was added to the polymer solution and stirred. As stirring continued, HBTU predissolved in DMF, was then added dropwise over 20 minutes,

followed by the addition of triethylamine (TEA). The resulting yellow solution was saturated with $N_2$ and stirred at ambient temperature for 2 hours. The polymeric conjugate was precipitated with $Et_2$O-hexane (2:1), isolated upon centrifugation and dissolved in $H_2O$. The pH was adjusted to 10 using NaOH and followed by size exclusion chromatography on a 2.5×25cm column packed with Sephadex G25 and eluted with distilled $H_2O$. The pH of the solution was readjusted to 7 (glacial acetic acid) to prevent hydrolysis, and the solution was dialyzed for 48 hours in Spectre/Por 6 tubing. The pH of the retentate was adjusted to 4 (HCl) to regenerate the unconjugated carboxyl group of FA from its salt. The aqueous solution was stirred at ambient temperature for 5 minutes, then the pH re-adjusted to 6 ($NH_4OH$), and the dialysis in the same tubing was continued for another 8 hours with numerous changes of the aqueous outer phase for complete removal of inorganic salts. The retentate with pH ~8, was freeze-dried to afford z mg of yellow, water-soluble conjugate of Polyaspartamide-Folic acid.

**B. PSI-DMP (95)-PDA (5)-FA**

Quantity of compound and solvent needed.

Polymer (200 mg, 0.1 mmol) in DMF (7mL).

Folic acid (20.6 mg, 0.05 mmol) in DMF (3mL).

HBTU (15.93 mg, 0.04 mmol) in DMF (1mL)

TEA (10 mg, 0.1 mmol).

The results for $^1$H NMR spectra (7) evaluation are reported in Table 4.9.

### 3.3.2.2. Chemical kinetics of conjugates

**A. PSI-DMP (85)-PDA (15)-FA**

Quantity of compound and solvent needed.

Polymer (200mg, 0.1 mmol) in DMF (7mL); Folic acid (50mg, 0.11 mmol) in DMF (6mL); HBTU (40mg, 0.10mmol) in DMF (3mL); TEA (18.5mg, 0.18 mmol).

To establish the chemical kinetics, the reaction was stopped after an interval of time.

The data after $^1$H NMR spectra evaluation for reaction kinetic are illustrated in Table 4.5.

**B. PSI-DMP (80)-PDA (20)-FA**

Quantity of compound and solvent needed.

Polymer (200mg, 0.1 mmol) in DMF (7mL)

Folic acid (108mg, 0.22 mmol) in DMF (6mL)

HBTU (86mg, 0.20 mmol) in DMF (3mL)

TEA (25mg, 0.24 mmol)

To establish the chemical kinetics, the reaction was stopped after an interval of time.

The data after $^{1}H$ NMR spectra evaluation for reaction kinetic are illustrated in Table 4.7.

### 3.3.3. Carbon nanotubes (CNTs) carrier

#### 3.3.3.1 Preparation of CNTs

**A. Experimental Procedure**

a) Precautions taken during the experiment

- Caution should be taken when working with the furnace since it operates under higher temperature viz. 850-11500$^{0}$C.
- Always put on the dusk when handling nanotubes since they can easily be dispersed and can damage the eyes and lungs.
- Always put on the lab coat and hand gloves for safety measures.
- Exit door should always be opened in case of explosions within the system.
- Fire arresters are installed on the hydrogen and acetylene flow lines.

b) Production Procedures

The furnace reactor and the furnace vessel are initially heated to the desired temperatures in the presence of nitrogen flow within pipelines. When the temperature is still rising, all the leaks are checked within the system and get rectified. The leaks are usually noticed by the presence of bubbles when spraying small amounts of gas leak detector at the pipe joints. Since nitrogen is flammable and dangerous at higher temperatures, it is only allowed to flow when the furnace temperature is still lower than 500$^{o}$C. Above this temperature, nitrogen flow is stopped by closing the nitrogen gas cylinder (main valve), followed by the pressure gauge on the cylinder. Nitrogen is then allowed to drain from

the pipelines and when it is drained the valve on the nitrogen flow meter is closed. While nitrogen drains, argon is allowed to flow within the pipelines by opening the argon gas cylinder and controlling the flow using the valve on the flow meter. When the desired furnace and ferrocene vessel temperatures are attained, a specific mass of ferrocene in its powder form is added into the vessel ($150^oC$) while slowly opening the valves for hydrogen at $900^oC$ and acetylene at $1050^oC$ to the desired specifications, thereby allowing the flow of these gases together with argon and the catalyst within the pipelines. The system is then given enough time until the reaction commences. The product formed remains in the reaction tube and is collected when cleaning the equipment. During production, the gas sample is collected from the pipeline exit of the gas mixture. The system is stopped and allowed to cool for about 2 hours when there is no production of nanotubes anymore in the system or when blockage is encountered within the system.

In order to eliminate the amorphous carbon, treat with 30% $HNO_3$ the products collected in the cyclones, and stir the solution for 2 hours at room temperature. Then filter the solid products and wash the solid products to achieve pH 7. Finally, dry the solid products at $120^oC$ in hot air for 24 hours, and analyze the purified products with TEM, TGA, EDX, and Raman spectroscopy.

Guidelines used when stopping the system at the end of production

* Switch off the power source for all the temperature devices
* Close the main valves from cylinders for acetylene and hydrogen gas
* Allow all the gases to drain from the pipelines
* Finally close all the valves on the flow meters.

**B. TEM Procedures**

The Samples collected will be analyzed through the Transmission Electron Microscope (TEM) by checking for the presence of long carbon chains.

1) Before operating TEM machines, mix each representative sample with methanol and small droplet of each sample was dropped on the carbon grid.

2) Feed a carbon grid covered with the sample to the TEM for analysis.

3) Search the good spot of high purity nanotubes, thus longer length, by using the knobs indicated on TEM machine as depicted below.

4) Vary the magnification using magnification knob so to achieve a clear picture.

5) After photographing the desired picture, discharge the carbon grid from the machine and analyze the next sample by following the same procedure.

6) Collect the micrographs as result.

7) Scan and print to get microscopic images.

The total yield of multiwalled carbon nanotubes (MWCNTs) prepared was 8.56g. After TEM analysis, the microscopic image was captured with magnification 100000. This has led to evaluate the outer diameter ($d_o$) of 20nm and the inner diameter ($d_i$) of 10nm (Figure 4.16).

### 3.3.3.2. Functionalization of CNTs

#### A MWCNTs with sulphuric acid and nitric acid

a) Procedures:

Treatment 1: The pristine MWCNTs were treated with hydrochloric acid, to remove impurities. One gram of MWCNTs was placed in a 500ml round-bottom flask and 200ml of HCl (32%) was added. The mixture was stirred using magnetic stirrer for 2 hours, then diluted in water, filtered, washed with deionised water and then dried overnight in a vacuum at 40ºC.

Treatment 2: 0.1g of the purified MWCNTs were dispersed in 200ml of acid (mixture of sulphuric acid 95% and nitric acid 55% (3:1)) in a 500ml round bottom flask equipped with a condenser. The dispersion was kept differently for:

1) 4 hours working with 100ºC

2) 24 hours working with 50ºC

3) 96 hours working at room temperature

After that, the resulting dispersion was diluted in water and filtered. Then the resulting solid was washed up to neutral pH and the sample was dried in a vacuum at 40ºC overnight.

The modified CNTs material was quantitatively analyzed by titration to determine the COOH concentrations on the surface of treated CNTs. In a typical experiment, the carboxylated CNTs were added into a 25ml 0.04 M NaOH solution and stirred for 48h to

allow the solid CNT material to equilibrate with the NaOH solution. The mixture was titrated with a 0.04M HCl solution to determine the excess NaOH in the solution and the concentration of the carboxylates on CNTs.

b) TEM analysis:

1) f-CNTs: MWCNTs + $H_2SO_4$ + $HNO_3$ at 100ºC: $d_0$=20nm & $d_i$=12nm (Figure 4.17).

2) f-CNTs: MWCNTs + $H_2SO_4$ + $HNO_3$ at 50ºC $d_o$=30nm (Figure 4.18).

3) f-CNTs: MWCNTs + $H_2SO_4$ + $HNO_3$ at RT $d_o$=80nm & $d_i$=40nm (Figure 4.19).

c) $^1$H NMR evaluation

1) $^1$H NMR SPECTRA (26): f-CNTs: MWCNTs + $H_2SO_4$ + $HNO_3$ at 100ºC

A: -**$CH_2$**-COOH & B: -**$CH_2$**-OH. For 1Mol of COOH adsorbed on the surface of MWCNTs, correspond to 7.54 Moles of OH.

2) $^1$H NMR SPECTRA (27): f-CNTs: MWCNTs+$H_2SO_4$+$HNO_3$ at 50ºC

A: -**$CH_2$**-COOH & B: -**$CH_2$**-OH. For 1 Mol of COOH adsorbed on the surface of MWCNTs, correspond to 2.27 Moles of OH.

3) $^1$H NMR SPECTRA (28): f-CNTs: MWCNTs+$H_2SO_4$+$HNO_3$ at RT

A: -**$CH_2$**-COOH & B: -**$CH_2$**-OH. For 1Mol of COOH adsorbed on the surface of MWCNTs, correspond to 0.08 Mol of OH.

d) The results obtained from the $^1$H NMR spectra (26, 27 and 28) were used to evaluate the mol ratio incorporation of COOH and OH on the surface of CNTs by using the titration formula Y= 1 - 0.04X with Y: mmol of COOH on the surface of CNTs and X the volume of HCl in ml. The table 4.10 shows the incorporation of COOH and OH at variable temperatures.

**B. Aspartic acid**

a) Procedures:

0.15g of MWCNTs were dispersed in a mixture of 3g of Aspartic acid and 15ml of DMF in a round-bottom flask of 250ml equipped with a condenser, and the reaction was

controlled to 220ºC for 6 hours. After filtration, the solid was washed with water until neutral pH. The yield was 183mg.

Using titration formula Y= 1 - 0.04X with Y: mmol of COOH on the surface of CNTs and X the volume of HCl in ml, see section 4.3.2.1 (B. 4) for results.

b) $^{1}$H NMR (29) Analysis with $D_2O$ +NaOH has shown **$CH_2$**-COOH pick at the chemical shift (3-2.3) expected.

c) TEM Analysis according to microscopic image obtained in Figure 4.24 has shown the nanotubes structure with $d_0$ = 60nm.

**C. Poysuccinimide (PSI)**

a) Procedures

PSI (1g) was dissolved in 15ml of DMF in a round-bottom flask of 250ml occupied with the condenser, and 150mg of CNTs were dispersed in the same flask where the reaction was controlled to 160ºC after 48 hours, the pH was kept to 7. The solid was collected after filtering, dried and then washed with DMF in low temperature using the ice bath to remove free PSI and with acetone to remove DMF. Solid was collected, dried and kept in desiccators. The yield was 216mg

b) The $^{1}$H NMR spectra (30) analysis with $D_2O$+NaOH has shown the expected picks (see Appendix) –CO-**$CH_2$** (3.030-2.650), **CH**-N (4.5-4.45), **H** aromatic (7.940)

c) The TEM analysis

The micrograph image in figure 4.26 was evaluated: $d_o$ = 60nm and $d_i$ = 40nm.

### 3.3.4. Functionalized carbon nanotubes (f-CNTs)-folic acid conjugates

#### 3.3.4.1. f-CNTs ($H_2SO_4$+$HNO_3$ at 100˚C) bound folic acid

**A. Procedures**

100mg of f-CNTs (prepared at 100˚C) representing 0.38 mmol COOH was dispersed in 5ml of DMF, and 11.6mg (0.114 mmol) of 3-dimethylamino-1-propylamine (DMP) representing 30% of molecular rate, was dissolved in 4ml of DMF. After Nitrogen flashing, the dispersion and the solution were mixed together in a round bottom flask, stirred at 50˚C. While solution was still stirring, 75mg (0.32 mmol) of 2-(1H-benzotriazol-1-yl)-1,1,3,3-tetramethyluronium fluorophosphates (HBTU was added, and the pH was controlled to 7 using the triethylamine (TEA) dropwise. After 24 hours of reaction, a solution of 141mg (0.32mmol) 20% excess of folic acid in 10ml of DMF was prepared for 1 hour and was added in the main solution. Stirring continued during 6 hours while the pH was kept to 7 with TEA. The solid was collected by filtration and washed several times with tetramethylurea (TMU) to remove the excess of folic acid and acetone to remove the TMU. The solid was dried and kept in the desiccators.
The yield was 163mg.

**B. $^1$HNMR spectra (31)** analysis shows the expected picks as evaluated in Table 4.11.

**C. TEM analysis** according to the microscopic image was evaluated in Figure 4.28 to $d_0$ = 50nm & $d_i$ = 20nm as nanotubes structure size.

#### 3.3.4.2. f-CNTs (Aspartic acid) bound folic acid (f-CNTs-DMP (40)-FA (60))

**A. Procedures**

100mg of f-CNTs representing 40mg (0.88 mmol) of COOH was dispersed in 5ml of DMF, and 36mg (0.352 mmol) of 3-dimethylamino-1-propylamine (DMP) (40%) was dissolved in 4ml of DMF. After Nitrogen flashing, the dispersion and the solution were mixed together in a round-bottom flask, stirred at 50˚C. During stirring, 206mg (0.88

mmol) of 2-(1H-benzotriazol-1-yl)-1,1,3,3-tetramethyluronium fluorophosphates (HBTU) predissolved in 3ml DMF was added dropwise, and the pH was controlled at 7 using the triethylamine (TEA). After 24 hours of reaction, a solution of 303mg (0.7mmol) of folic acid in 15ml of DMF was prepared for 1 hour and was added into the main solution. Stirring continued for 6 hours while the pH was kept at 7 with TEA. The solid was collected by filtration and washed several time with tetramethylurea (TMU) to remove the excess of folic acid and acetone to remove the TMU. The solid was dried and kept in the desiccators.

The yield was 231mg.

**B.$^{1}$H NMR (32)** shows different expected picks: A, B, C, D, E, F, and G represented in the Table 4.12

In order to evaluate the incorporation of folic acid, A pick has been taken as reference pick where nH expected was 4H, and the aromatic picks (E, F, G) was calculated to 15.2H over 15H expected. This resulted to the folic acid incorporation of 101.3%.

**C. TEM Analysis** according to microscopic image (Figure 4 29) has shown the nanotubes structure with $d_0$ = 170nm.

### 3.3.4.3. f-CNTs (PSI) bound folic acid (f-CNTs-DMP (40)-PDA (60)-FA)

#### A. Procedures

The solid f-CNTs (200mg) were dispersed in 10ml of DMF in a round flask of 250ml. 23mg of DMP dissolved in 5ml of DMF, was added to solution. Solution was stirred for 24 hours at room temperature. Then 50mg PDA dissolved in 5ml of DMF was added dropwise in an ice bath for 24 hours. Filtered solid was collected and washed several times with hot toluene and acetone and filtered again, dried and dispersed in DMF. Folic acid 230mg dissolved in DMF was added to the solution. HBTU 134mg pre-dissolved in DMF was added dropwise while the solution was allowed to stay at pH of 7 using TEA. After 2 hours, the solid was collected, filtered and washed using TMU with the acetone. The yield: 356mg.

**B**. **The $^{1}$H NM spectra (33)** analysis with $D_2O$+NaOH has shown the expected picks (see Appendix) with A: -$CH_2$-$CH_2$-$CH_2$, B: $CH_2$-N($CH_2$)$_3$, C: $CH_2$-COONH, D: $COCH_2NH$, (E, F, G, H): H aromatic.

**C. The TEM analysis** was done (Figure 4.30)

The micrograph image in the Figure 4.30 was evaluated: $d_o$ = 80nm and $d_i$ = 40nm.

## CHAPTER 4

## RESULTS AND DISCUSSION

### 4.1. Polymeric Drug Carriers

With the objective to accommodate the anticancer drug models only to the cancerous cells, an attempt was made to afford tailor-made drug carriers through the design and derivation of several synthetic polymeric structures. This possibly will prevent the destruction of normal cells and provide an adequate liberation of the drug without any deposition to the kidney which could raise certain side effects due to the toxicity of the agents. Note that the synthesis by bioreversible conjugation of selected anticancer drug models with water-soluble macromolecule carriers, and the biological activity evaluation of the resulting conjugates, is two objectives to be fulfilled in respect of necessary prerequisites for any macromolecule intended to serve in the biomedical field. The polymeric carriers used for the anchoring of the selected drug models fell into the wide aliphatic polyamide type (schematized below) with subunits randomly distributed along the chain.

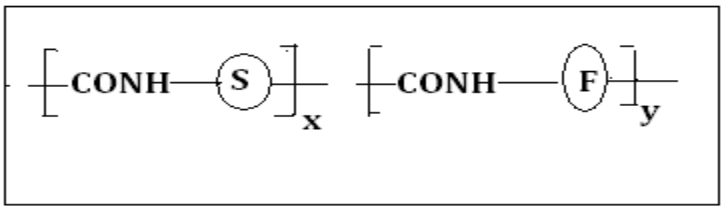


**Scheme 4.1: Structure of polyamide-type carrier**

In this scheme, **S** represents an extra-or intra-chain hydrosolubilizing group required to impart water–solubility to the ultimate polymer-drug conjugate. **S** is a tertiary amine, hydroxyl or methoxy functionality. **F** stands for extra-or intra-chain functional group capable of reversible-drug anchoring. In this study, to provide access to the polymer-drug binding via amide bond formation, the choice was made on a primary amino group. The most important point is that the amide bond performs the ability to develop biofission,

which results in the enzymatic activity in the intracellular lysosomal compartment, and causes the drug release from the cytoplasmic space. The incorporation of additional subunits of the preset structures, if necessary, will be granted to afford tailor-made polymers that are equipped with all required functions. This allows efficacious administration and enhanced pharmacokinetics of the anticancer drug.

The drug used being hydrophobic, the polymeric carriers were designed to provide a balance between the load of these inherently hydrophobic drugs and the solubilizing moieties on the polymer, because hydrophobic polymer-drug conjugates are required at varying concentrations. The side chains were tertiary amine. The choice of the structures was based on the following considerations:

(a) The weight-average molecular weight, generally in the range of 20 000-30 000, is sufficiently low to suppress (chain length-dependent) inherent polymer toxicity, but still high enough to retard renal clearance. The conjugates, therefore, enter cells easily owing to the enhanced permeability retention (EPR) effect.

(b) The intrachain amide groups assist in gradual backbone cleavage for ease of catabolic elimination of the polymer in the "spent" state. The stereoisomeric "scrambling" of any peptide units in the backbone chain impedes unduly rapid α-peptidase-mediated "unzipping", ensuring this fragmentation to be an appropriately retarded process.

(c) Property selected polyamides are essentially non-toxic, and immunogenicity of these synthetic polymers is expected to be appreciably lower in comparison with that commonly occurring with high-molecular-weight proteinaceous biopolymers.

(d) The **S**-modified subunits can easily be introduced as majority components (x>y), thus ensuring effective insulation of the **F**-modified subunits from each other. This will reduce the risk of intramolecular interaction of adjacent conjugated drug species.

(e) Tertiary amine functions can be introduced as side groups to provide the special functions of adsorptive pinocytotic cell entry and target cell affinity.

(f) While inherently water-soluble, with **S** comprising selected amine or hydroxyl functions, the polyamides can be made to acquire additional solubility in methanolic medium. This can be achieved by incorporation of poly(ethylene oxide) (PEO) side chains as additional solubilizing groups. This added solubility feature will be advantageous in follow-up reactions in alcoholic media.

(g) When synthesized from amino acid monomers, the polyamide carrier will provide vitally required nutrients for the rapidly growing cell tissue, and hence may be preferentially taken up by the cancerous cell.

The polyamide conforming to the basic carrier model (Scheme 2.2), namely Polyaspartamide (PAsA) was used for drug conjugation by amide bond formation between the carriers and the carboxylic acid-functionalized drugs. The primary amine functional groups of these polymers were introduced as terminals in component **F**. The subunits incorporating this binding site form 5 to 20 mol-% of the tert-amine for 80mol-% of **S**-labeled subunits of the tert-amine for hydrosolubilization. With recognition of the incorporation of drug from **F**-labeled subunits of the primary-amine, the carrier containing larger mole percentages of **F**-labeled subunits will be needed for utilization of an unduly large excess of drug to provide complete drug incorporation. In addition, the coupling products so obtained had displayed a predisposition for branching and crosslinking with concurrently decreasing solubility once they had been isolated in the solid state. The purification of polymeric carriers was completed by dialysis to remove constituents with molecular weight substantially below 12 000.

### 4.1.1. Polyaspartamide carriers (PAsA)

The Polyaspartamides containing the backbone bound to the solubilizing group at one side and anchoring drug at the other side were prepared from polysuccinimide.

#### 4.1.1.1. Synthesis of polysuccinimide (PSI)

Two different methods for the synthesis of polysuccinimide (PSI) have been set in the literature, including the polymerization of N-carboxyanhydride of α-amino acid in general (NCA method) [(179)] and the thermal phosphoric acid-catalyzed polycondensation

of aspartic acid (Neri method) [180]. The NCA method was found to be disadvantageous both in cost and production as the pendent reactive groups carried by the amino acid had to be protected before polymerization, and disclosed under harsh considerations to give poly (amino acid). Specially to organize the large amounts of phosgene, diphosgene or triphosgene, a reagent widely used for the synthesis of N-carboxyanhydride, raised complex safety problems in a large-scale plant. On the contrary, the Neri method is reported to deliver high molecular weight PSI in one step [181]. Because of this advantage, this approach was adopted for the synthesis of poly-DL-succinimide (PSI) from DL-aspartic acid as shown in Scheme 4.2. The crude polymer was treated with dicyclohexylcarbodiimide (DCC) coupling agent for further chain extension purposes. A representative polymer had a relative viscosity of 36 mL $g^{-1}$ in DMF at 30ºC, which corresponds to a weight-average molecular weight of 32000.

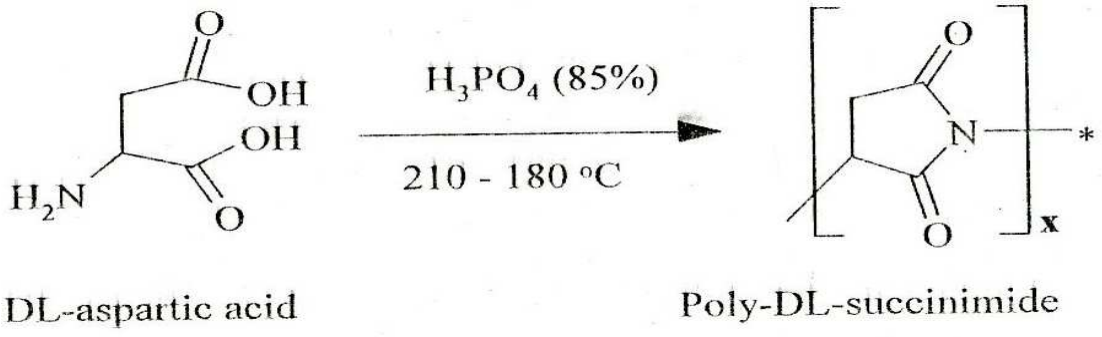


**Scheme 4.2: Synthesis of polysuccinimide (PSI)**

**A. Results of Synthesis of polysuccinimide (PSI)**

The $^1H$ NMR spectrum of PSI in DMSO-$d_6$ showed a large resonance at 5.2 ppm corresponding to the methine proton (NCO-CH). The methylene protons ($CH_2CH$) are seen as two peaks of the roughly equal intensity at 3.3 and 2.6 ppm.

In addition, several experiments were performed to prepare the poly-DL-succinimide (PSI-DCC) as shown in Table 4.1.

**Table 4.1: Quantitative values of PSI synthesis**

| EXP. NO | Aspartic. Acid (g) | Phosphoric Acid (g) | PSI*[a] Yield g (%) | DMF (ml) | DCC (g) | PSI Yield g (%) |
|---|---|---|---|---|---|---|
| 1 | 25 | 12.5 | 14.82 (59.28) | 60 | 1.73 | 12.75 (86.03) |
| 2 | 75 | 32.5 | 45.51 (60.68) | 130 | 5.31 | 41.23 (90.59) |
| 3 | 80 | 40 | 52.18 (65.23) | 64 | 6.10 | 43.98 (84.28) |
| 4 | 100 | 50 | 58.5 (58.50) | 150 | 6.83 | 49.91 (85.32) |
| 5 | 50 | 25 | 31.43 (62.86) | 126 | 3.67 | 27.95 (88.93) |
| 6 | 80 | 40 | 50.07 (62.26) | 150. | 5.84 | 41.64 (83.17) |
| 7 | 80 | 40 | 53.08 (66.35) | 150 | 6.20 | 47.16 (88.84) |
| 8 | 70 | 35 | 41.20 (58.86) | 150 | 4.78 | 36.70 (89.08) |

[a] PSI*: Before treatment with DCC coupling agent.

**B. Discussion of Results of Synthesis of polysuccinimide (PSI)**

The yield for the synthesis of polysuccinimide was varying in the range of (58-67%) before treatment with DCC coupling agent and (83-91%) after treatment with DCC (Table 4.1). This shows that the loss was more performed in the first stage of treatment ($PSI^{*}$) than in the second stage (PSI after DCC treatment). After investigation, the following options can be the cause of dropping of yield in the first stage of treatment:

1. A big quantity of free aspartic acid did not react during the polycondensation and was liberated when the product was washed to adjust the pH to 7.

2. During the operation of adjusting the pH to 7 by washing the product several times with the distilled water, the loss of polymer is inevitable. This, because some product can be hydraulically involved by the water and other being fractionated by hydrolysis.

The yield of PSI was in the range of (83-91%) after treatment with DCC coupling agent while the expected yield should be 100%.

**4.1.1.2. Preparation of homopoly (α, β-DL-aspartamides)**

Referring to Scheme 4.2 which reveals the structure of the X repeat units giving poly-DL-succinimide, the opening of the ring will be required to provide a long chain with subunits partly displaying in one hand the solubility, on the other hand the anchoring drug. Note that polyaspartamides are readily prepared from poly DL-succinimide by an aminolytic ring-opening process in anhydrous, dipolar aprotic medium, such as N,N dimethylformamide (DMF) at 0-25°C. The product is racemic and possesses both α-and β-peptidic repeat units. Scheme 4.3 shows the preparation of homopoly(α, β-DL-aspartamides) by the poly-DL-succinimide aminolytic ring-opening process using one type of amine reactant.

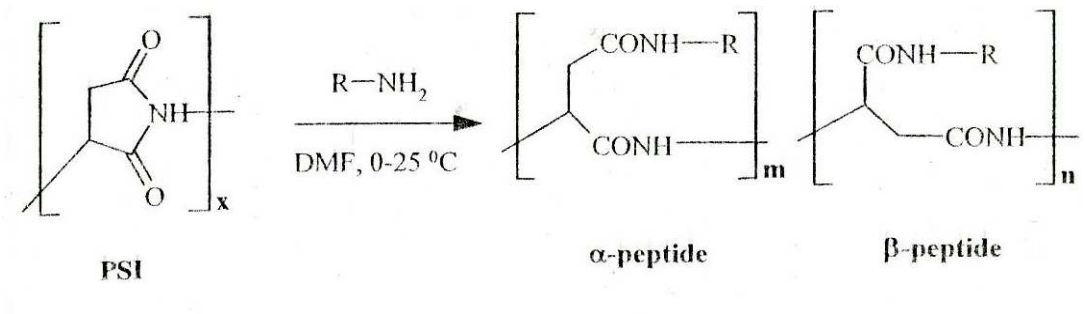


**Scheme 4.3: Preparation of homopoly(α, β-DL-aspartamides)**

While D-type polymers are resistant to enzymatic cleavage, L-type polymers are more prone to rapid enzymatic degradation. Therefore, a backbone structure of the DL-racemic mixture will ensure retarded enzymatic cleavage and ultimate backbone degradation as a result of hydrolytic cleavage.

### 4.1.1.3 Preparation of copolyaspartamides (PAsA)

Respecting a stepwise process which involves the utilization of two or more different amine reactants in a given stoichiometric feed ratio, aminolytic ring-opening can lead to the generation of copolyaspartamides. By using sequentially $H_2N$-R and $H_2N$-R'-$NH_2$ to form polyaspartamides, in which subunits featured R and R'-$NH_2$ in predetermined ratios along the chain. Varying R and R', a series of random copolyaspartamides were prepared as drug carriers.

When working with 3-(N, N-dimethylamino)propylamine (DMP) which R: -$(CH_2)_3$-N-$(CH_3)_2$, and 1,3-propylenediamine (PDA) which R': -$(CH_2)_3$- reaction parameters should be considered to lead the reaction to the expected products. DMP, being tertiary amine group, acts as both hydrosolubilizing and cell-selecting group. Many considerations supporting the choice of this group from all those investigated in this laboratory [(182)].

Note that the DMP is a strong base which means that the protonation will be evident even under weak basic conditions. The protonation, carrying more cationic, will cause the amino group to be positively charged, this will preferentially approach surfaces of certain types of cancer cells that are negatively charged. This will promote the adsorptive pinocytotic cellular uptake of the macromolecules as reported by Shen [(183)].

The challenge was to solve the problem of competition between $NH_2$-R (DMP), and $NH_2$-R'-$NH_2$ (PDA) which could take place during the reaction. The first reactant to be used was found to be less reactive than the second, and was used as major reactant (X > Y) in the two-step preparative process of these polymers. In accordance with chemical reactivity, $NH_2$-R'-$NH_2$ (PDA) due to both two extremes -$NH_2$, is more reactive than $NH_2$-R (DMP) presenting –$NH_2$ in one extreme only. Then, the first step is the reaction in anhydrous conditions between a given amount of polysuccinimide and its corresponding R-$NH_2$ counterpart. This reaction, based on the desired X/Y feed ratio, is performed at room temperature. With respect to achieve the desired percentage incorporation with complete ring opening and substitution of the remaining succinimide units of the substrate polymer without causing crosslinking through involvement of the terminal amino group, the following conditions were respected during the reaction:

1. Considering that –NH-R'-$NH_2$ (after reaction) is less reactive than $NH_2$-R'-$NH_2$, excess of PDA was needed to prevent –NH-R'-$NH_2$ to continue to react in another step. For the activity of –NH-R'-$NH_2$ in reaction is conditioned by the absence of $NH_2$-R'-$NH_2$ in the same reaction.

2. The diminution of the temperature to minimize the activity of PDA, thus the use of an ice bath was required to bring the temperature down.

3. The polymer solution was released dropwise in the PDA solution.

4. In addition, DMP and PDA steps were performed under strictly anhydrous conditions in order to avoid unwanted hydrolytic ring opening, resulting in the generation of free carboxylic side group.

The polymeric products were isolated as completely water-soluble solids by a series of operations which involved precipitation with adequate non-solvents, aqueous dialysis (in tubing with 12000 molecular weight cut-off-limit), and freeze-drying. As the consequence of the crude fractionation achieved by this dialysis step, yields did not exceed 85%, generally ranging from 85% to 70%. The inherent viscosities ($\eta_{inh}$) ranged from 11 to 22$mLg^{-1}$. The $^1$HNMR spectra of polymers (P1) measured in $D_2O$, and recorded at pH 10-11 for elimination of protonation effects, showed characteristic band

groups, some containing overlapping signals. Thus, the CH (methine) signal of aspartic appeared in the region of 4.75-4.5 ppm; $CH_2$-O (methylene) and CH-OH (methine) signals were grouped in the region of 3.7-3.6 ppm. The methylene protons of CONH-$CH_2$ were found in the region of 3.5-3.0 ppm. Proton signals of CO-$CH_2$, $CH_2$-$N(CH_3)_2$, $CH_2$-NH, and $CH_2$-$NH_2$ were found in the region of 2.9-2.0 ppm. Methylene protons of $CH_2CH_2CH_2$ were found in the 1.8-1.5 ppm region.

**A. PSI-DMP(X)-EDDA(Y)**

a) PSI-DMP (90)-EDDA (10)

Using 2.95g (30mmol) of PSI as reference, 2.76g (27mmol) of DMP and 1.33g (9mmol) of EDDA were required to prepare the polymeric carrier PSI-DMP (90)-EDDA (10). The results are presented in Tables 4.2, 4.3 and 4.4.

The evaluation of $^1$H NMR Spectra 1 (Appendix) calculated in Table 4.4 gave 98% incorporation of EDDA in the Homopolymer.

b) PSI-DMP (80)-EDDA (20)

Using 2.95g (30mmol) of PSI as reference, 2.45g (24mmol) of DMP and 2.67g (18mmol) of EDDA were required to prepare the polymeric carrier PSI-DMP (80)-EDDA (20). The results are presented in Tables 4.2, 4.3 and 4.4.

The evaluation of $^1$H NMR Spectra 2 (Appendix) calculated in Table 4.4 gave 95% incorporation of EDDA in the Homopolymer.

**B. PSI-DMP (X) PDA (Y)**

a) PSI-DMP (95)-PDA (5)

Using 2.95g (30mmol) of PSI as reference, 2.91g (28.5mmol) of DMP and 0.33g (4.5mmol) of PDA were required to prepare the polymeric carrier PSI-DMP (95)-PDA (5). The results are presented in Tables 4.2, 4.3 and 4.4.

The evaluation of $^1$H NMR Spectra 3 (Appendix) calculated in Table 4.4 gave 94% incorporation of PDA in the Homopolymer.

b) PSI-DMP (90)-PDA (10)

Using 2.95g (30mmol) of PSI as reference, 2.76g (27mmol) of DMP and 0.67g (9mmol) of PDA were required to prepare the polymeric carrier PSI-DMP (90)-PDA (10). The results are presented in Tables 4.2, 4.3 and 4.4.

The evaluation $^{1}$H NMR Spectra 4 (Appendix) calculated in Table 4.4 gave 98% incorporation of PDA in the Homopolymer.

c) PSI-DMP (85)-PDA (15)

Using 2.95g (30mmol) of PSI as reference, 2.60g (25.5mmol) of DMP and 0.63g (8.5mmol) of PDA were required to prepare the polymeric carrier PSI-DMP (85)-PDA (15). The results are presented in Tables 4.2, 4.3 and 4.4.

The evaluation of $^{1}$H NMR Spectra 5 (Appendix) calculated in the Table 4.4 gave 102% incorporation of PDA in the Homopolymer.

d) PSI-DMP (80)-PDA (20)

Using 2.95g (30mmol) of PSI as reference, 2.45g (24mmol) of DMP and 1.33 (18mmol) of PDA were required to prepare the polymeric carrier PSI-DMP (80)-PDA (20). The results are presented in Tables 4.2, 4.3,4.4.

The evaluation of $^{1}$HNMR SPECTRA 6 (Appendix) calculated in the Table 4.4 gave 101% incorporation of PDA in the Homopolymer.

**C. Results of Preparation of copolyaspartamides (PAsA)**

The results related to the preparation of different copolyaspartamides achieved by varying the solubilising groups and the mol ratio X/Y, are presented in Tables 4.2, 4.3 and 4.4. The corresponding inherent viscosity ($\eta_{inh}$) versus mol ratio (X/Y) plot is shown in Figure 4.1.

**Table 4.2: Quantitative values of PSI-DMP (X) –PDA (Y) /EDDA (Y) synthesis**

| Chemical compound | X | Y | X/Y | Mass (g) (mol) PSI | DMP | PDA / EDDA | Yield (g) |
|---|---|---|---|---|---|---|---|
| PSI-DMP (X) -PDA (Y) | 80 | 20 | 4/1 | 2.95 (30) | 2.40 (24) | 1.33 (18) | 5.58 |
| | 85 | 15 | 17/3 | 2.95 (30) | 2.55 (25.5) | 0.63 (13.5) | 4.02 |
| | 90 | 10 | 9/1 | 2.95 (30) | 2.70 (27) | 0.67 (9) | 3.86 |
| | 95 | 5 | 19/1 | 2.95 (30) | 2.91 (28.5) | 0.33 (4.5) | 3.86 |
| PSI-DMP (X)-EDDA (Y) | 80 | 20 | 4/1 | 2.95 (30) | 2.40 (24) | 2.67 (18) | 4.1 |
| | 90 | 10 | 9/1 | 2.95 (30) | 2.70 (27) | 1.33 (9) | 3.87 |

**Table 4.3: Inherent Viscosity, base molecular weight and yield for PSI-DMP (X)-PDA / EDDA(Y).**

| Chemical compound | X | Y | X/Y[b] | BMw[c] | $\eta_{inh}$[d] ($mLg^{-1}$) | Yield (g) |
|---|---|---|---|---|---|---|
| PSI-DMP (X)- PDA (Y) | 80 | 20 | 4/1 | 968.21 | 18.38 | 3.39 |
| | 85 | 15 | 17/3 | 3900.89 | 16.62 | 3.42 |
| | 90 | 10 | 10/1 | 1964.47 | 12.23 | 3.86 |
| | 95 | 5 | 19/1 | 3956.99 | 10.13 | 3.68 |
| PSI-DMP (X)-EDDA (Y) | 80 | 20 | 4/1 | 1042.29 | 18.7 | 4.13 |
| | 90 | 10 | 9/1 | 2038.55 | 11.31 | 4.52 |

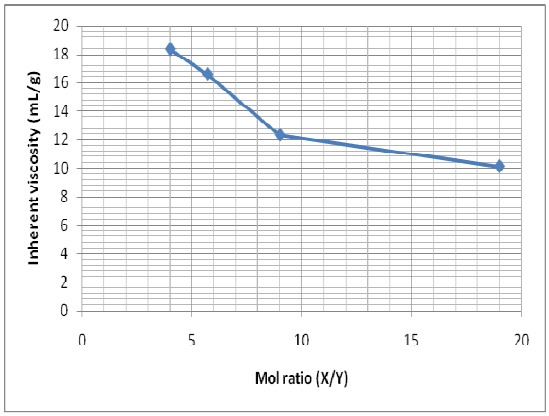


**Figure 4.1: Inherent viscosity of PSI-DMP (X)-PDA (Y) versus Mol Ratio (X/Y).**

[b] X/Y: Mole ratio of hydrosolubilizing to drug-anchoring groups
[c] BMw: Base molecular weight of simple recur
[d] $\eta_{inh}$: Inherent viscosity

**Table 4.4: $^{1}$H NMR spectra analysis of PSI-DMP (X)-PDA /EDDA (Y)**

| Chemical Compound | X | Y | X/Y | HNMR spectra | Chemical shift (δ/ppm) Calculated (expected) | | | | | % PDA / % EDDA | Yield (g) |
|---|---|---|---|---|---|---|---|---|---|---|---|
| | | | | | **CH** Asp 4.75-4.5 | CONH-**$CH_2$** 3.7-3.5 | -CO-**$CH_2$**, **$CH_2$**$NH_2$ 3.5-3.0 | CO-**$CH_2$**, $CH_2N$**$(CH_3)_2$**, 2.8-2.0 | $CH_2$**$CH_2$**$CH_2$ 1.8-1.5 | | |
| PSI-DMP(X)-PDA (Y) | 80 | 20 | 4/1 | 6 | 5 (5) | 10.1 (10) | 11.1 (12) | 33.3 (32) | 10 (10) | 104 | 3.39 |
| | 85 | 15 | 19/1 | 5 | 20 (20) | 40.8 (40) | 45.6 (46) | 140.8 (136) | 20 (20) | 104 | 3.42 |
| | 90 | 10 | 9/1 | 4 | 10.2(10) | 20 (20) | 23.2 (22) | 70.4 (72) | 20 (20) | 98 | 3.86 |
| | 95 | 5 | 19/1 | 3 | 20.4(20) | 40.8 (40) | 44.4 (42) | 144 (154) | 40 (40) | 94 | 3.68 |
| PSI-DMP(X)-EDDA(Y) | 80 | 20 | 4/1 | 2 | 5 (5) | 7.3 (8) | 10.3 (10) | 41.7 (44) | 8 (8) | 95 | 4.52 |
| | 90 | 10 | 9/1 | 1 | 10.3(10) | 9 (8) | 20.7 (21) | 92 (94) | 18 (18) | 98 | 4.13 |

**D. Discussion of Results of Preparation of copolyaspartamides (PAsA)**

The minimum molecular weight of carriers was equal or above 12000 due to the application of cellulose tubing with weight-average molecular weight cut-off limits of 12000. Since the weight-average molecular weight is one of biomedical requirements to determine the quality of the polymeric carrier, with the estimated minimum value of 12000, though this value is not comprised in 20000-30000 range as stipulated in section 2.1, it is possible to have most of the average molecular weight in the range aforementioned; this should be sufficiently low to suppress inherent polymer toxicity, unless the maximum molecular weight gives acceptable range. However, it will be high enough to retard renal clearance.

The inherent viscosity revealed large differences in the stiffness of these copolyapastamides. The relation between inherent viscosity and the mole ratio of hydrosolubilizing to a drug-anchoring group as data in Table 4.3, showed in figure 4.1 the decreasing of $\eta_{inh}$ when the mol ratio (X/Y) increased. The inherent viscosity ($\eta_{inh}$) of copolyaspartamide as water soluble found in the range of 10 to 19mL $g^{-1}$(Table 4.3) was less than the inherent viscosity (36mL $g^{-1}$) of the polysuccinimide which is water insoluble (Section 4.1.1.1). This shows how much the presence of solubilizing group as one of two subunits in the backbone displayed on the inherent viscosity. Since the inherent viscosity of the polysuccinimide without subunits is higher than the one for water soluble polymeric carrier, this confirms that the increasing of the quantity of solubilizing in the polymeric carrier relative to mol ratio X/Y (Fig. 4.1), involves the decreasing of inherent viscosity. When the quantity of amine used to solubilize the polymer decreases, the solubility of the carrier can be affected. Thus the solubility of macromolelar carriers is linked to the mol ratio which conditions the viscosity as shown in Figure 4.1.

**4.2. Polymer Drug Conjugation**

Varying the type of Polyaspartamide carrier, many polymer drug conjugations were prepared. The most important in this research is to prove the existence of the covalent

reversible attachment of the carrier through amide bond formation with the drug. Note that methotrexate and folic acid with both two carboxyl groups from their structures can be attached to the polymeric carrier through the amine group of the anchoring drug unit to form an amide group able to develop biofission. The investigation of folic acid will lead to the same conclusion when investigating methotrexate as agent. The rate incorporation of drug in the polymeric carrier calculated from $^{1}$H NMR integration, even in an acceptable range, could not confirm at all the covalent reversible attachment of the carrier with the drug. Nevertheless the chemical kinetics investigation through the change of fraction incorporation of the drug with the reaction time can assert the reversible attachment when the purification methods such as centrifugation, chromatography and dialysis are reliable.

### 4.2.1. Polymer-folic acid conjugates

The coupling was prepared in anhydrous medium (DMF) in the presence of HBTU coupling agent. HBTU was added to activate the reaction between the amine group of carrier and the carboxylic acid group of folic acid. The presence of bi-functionally active drug molecule can cause gradual crosslinking of ultimate conjugate especially when the coupling agent (HBTU) is used in higher mol ratio. There the use of HBTU in solution was done dropwise with an acceptable rate. To maintain the reaction pH between 6 and 7, an organic base triethylamine (TEA) was added dropwise to the solution.

#### 4.2.1.1. Results of Polymer-folic acid conjugates

In order to achieve the chemical kinetics investigation, all reactions performed with mol ratio 17/3 and 4/1 for PSI-DMP (X)-PDA (Y)-FA were running in the same condition while the time was varying in the range of 10 to 130 minutes. Different data of fraction of incorporation of folic acid in the polymeric carrier were calculated through the evaluation of different $^{1}$H NMR Spectra integration from $^{1}$H NMR Spectra 8 to 25 as shown in the appendix. Both the fraction of incorporation of folic acid and the coupling yield in terms of reaction time have made possible through the base molecular weight (BMw) the

calculation of fractions of the retained polymer, removed polymer and folic acid in the coupling as shown in Tables 4.5, 4.6, 4.7 and 4.8. From these Tables, the different graphs were plotted in terms of the reaction time leading to the following figures:

- Figure 4.2 and 4.9 related to fraction incorporation of folic acid versus the reaction time in the polymeric carrier (PSI-DMP (X)-PDA (Y)) for mol ratio (X/Y) 17/3 and 4/1 respectively.
- Figure 4.3 and 4.10 related to the fraction of coupling yield of PSI-DMP (X)-PDA (Y)-FA with mol ratio (X/Y) 17/3 and 4/1 respectively, versus the reaction time.
- Figure 4.4 and 4.11 related to the fraction of retained polymer with mol ratio (X/Y) 17/3 and 4/1 respectively, versus the time of reaction.
- Figure 4.5 and 4.12 related to the fraction of removed polymer with mol ratio (X/Y) 17/3 and 4/1 respectively, versus the time of reaction.
- Figure 4.6 and 4.13 related to the fraction of folic acid in the coupling with mol ratio (X/Y) 17/3 and 4/1 respectively, versus the time of reaction.
- Figure 4.7 and 4.14 related to the combining of all fractions versus the time with mol ratio (X/Y) 17/3 and 4/1 respectively, versus the time of reaction.
- Figure 4.8 and 4.15 related to the inherent viscosity of PSI-DMP (X)-PDA (Y)-FA with mol ratio (X/Y) 17/3 and 4/1 respectively, versus the reaction time.

**Table 4.5: Incorporation FA data in terms of time for PSI-DMP (85)-PDA (15)-FA conjugate reaction.**

| Reaction time (minutes) | $^{1}$HNMR SPECTRA (X) | Chemical shift δ/ppm nH counted (nH expected) | | % FA incorporation |
|---|---|---|---|---|
| | | 8.7-6.75 | 1.7-1.6 | |
| 10 | 8 | 1.2 (15) | 40 (40) | 8 |
| 20 | 9 | 3.2 (15) | 40 (40) | 21.3 |
| 30 | 10 | 4 (15) | 40 (40) | 26.7 |
| 40 | 11 | 4.4 (15) | 40 (40) | 29.3 |
| 50 | 12 | 4.8 (15) | 40 (40) | 32 |
| 60 | 13 | 5.2 (15) | 40 (40) | 34.7 |
| 70 | 14 | 7.2 (15) | 40 (40) | 48 |
| 80 | 15 | 8 (15) | 40 (40) | 53.3 |
| 90 | 16 | 9.2 (15) | 40 (40) | 61.3 |
| 100 | 17 | 12.4 (15) | 40 (40) | 82.7 |
| 110 | 18 | 12.8 (15) | 40 (40) | 85.3 |
| 120 | 19 | 13.6 (15) | 40 (40) | 90.6 |
| 130 | 20 | 14.4 (15) | 40 (40) | 96 |

**Table 4.6: Coupling Yield, FA incorporation and viscosity data in terms of time for PSI-DMP (85)-PDA (15)-FA conjugates reaction.**

| Reaction time (minutes) | % FA incorpor. ($^1$HNMR) | Yield Coupling | | Carrier in coupling | | Removed carrier | | FA in coupling | | $\eta_{inh}$ ($mLg^{-1}$) |
|---|---|---|---|---|---|---|---|---|---|---|
| | | mg | % | mg | % | mg | % | mg | % | |
| 0 | 0 | 200 | 75.44 | 200 | 100 | 0 | 0 | 0 | 0 | 16.62 |
| 10 | 8 | 203 | 76.57 | 198 | 99 | 2 | 1 | 5.4 | 2.7 | 17.02 |
| 20 | 21.3 | 204 | 76.98 | 190 | 95 | 10 | 5 | 13.8 | 6.8 | 17.95 |
| 30 | 26.7 | 206 | 77.70 | 189 | 94.5 | 11 | 5.5 | 17.1 | 8.3 | 18.83 |
| 40 | 29.3 | 207 | 78.08 | 188 | 94 | 12 | 6 | 18.7 | 9 | 18.34 |
| 50 | 32 | 209 | 78.83 | 188 | 94 | 12 | 6 | 20.5 | 9.8 | 19.06 |
| 60 | 34.7 | 209 | 78.83 | 187 | 93.5 | 13 | 6.5 | 22.1 | 10.6 | 19.27 |
| 70 | 48 | 215 | 81.10. | 185 | 92.5 | 15 | 7.5 | 30.2 | 14 | 19.58 |
| 80 | 53.3 | 219 | 82.60 | 185 | 92.5 | 15 | 7.5 | 33.5 | 15.3 | 19.93 |
| 90 | 61.3 | 223 | 82.60 | 184 | 92 | 16 | 8 | 38.3 | 17.2 | 20.49 |
| 100 | 82.7 | 225 | 84.87 | 176 | 88 | 24 | 12 | 49.5 | 22 | 20.65 |
| 110 | 85.3 | 225 | 84.87 | 174 | 87 | 26 | 13 | 50.5 | 22.4 | 21.58 |
| 120 | 90.6 | 223 | 84.11 | 170. | 85 | 30 | 15 | 52.4 | 23.5 | 21.78 |
| 130 | 96 | 220 | 83.98 | 166 | 83 | 34 | 17 | 54.1 | 24.6 | 22.07 |

**Table 4.7: Incorporation FA data in terms of time for PSI-DMP (80)-PDA (20)-FA conjugates reaction.**

| Reaction time (minutes) | $^1$HNMR SPECTRA (X) | Chemical shift δ/ppm nH counted (nH expected) | |
|---|---|---|---|
| | | 8.7-6.75 | 1.7-1.6 |
| 10 | 21 | 0.6 (5) | 10 (10) |
| 25 | 22 | 1.2 (5) | 10 (10) |
| 50 | 23 | 2.4 (5) | 10 (10) |
| 60 | 24 | 2.7 (5) | 10 (10) |
| 120 | 25 | 5 (5) | 10 (10) |

**Table 4.8: Coupling Yield, FA incorporation and viscosity data with the reaction time.**

| Reaction time (minutes) | % FA incorpor. ($^1$H NMR) | Yield Coupling | | Carrier in coupling | | Removed carrier | | FA in coupling | | $\eta_{inh}$ ($mLg^{-1}$) |
|---|---|---|---|---|---|---|---|---|---|---|
| | | mg | % | mg | % | mg | % | mg | % | |
| 0 | 0 | 200 | 69.6 | 200 | 100 | 0 | 0 | 0 | 0 | 18.38 |
| 10 | 12 | 205 | 71.3 | 194 | 97 | 6 | 3 | 10.6 | 5.2 | 18.86 |
| 25 | 24 | 215 | 74.8 | 194 | 97 | 6 | 3 | 21.2 | 9.9 | 19.47 |
| 50 | 48 | 226 | 78.6 | 185 | 92.5 | 15 | 7.5 | 40.6 | 18 | 20.08 |
| 60 | 54 | 231 | 80 | 185 | 92.5 | 15 | 7.5 | 45.6 | 19.8 | 20.74 |
| 120 | 100 | 238 | 82.8 | 163 | 81.5 | 37 | 18.5 | 74.5 | 31.3 | 23.02 |

#### 4.2.1.2. Discussion of Results of Polymer-folic acid conjugates

In a chemical reaction, the concentration of reactants decreases with reaction time, while the concentration of products increases when the reaction is irreversible. Figure 4.2 shows that the fraction of incorporation of folic acid in the polymer was increasing with reaction time and the rate of the reaction was also time dependent. Thus, working with the minutes as time, the rate with incorporation range of 21.3-34.7% within the time range of 20-60 minutes is 0.335% $min^{-1}$. The approximated rate of 0.443% $min^{-1}$was found with FA incorporation range of 82.7-96% within the time range 100-130 minutes. With FA incorporation range of 0-21.3% within the time range of 0-20 minutes, the rate was 1.065%$min^{-1}$ and the same rate was approximately 1.2 %$min^{-1}$ with FA incorporation range of 34.7-82.7% within the time range of 60-100 minutes. Hence, the rate was low within the time range of 0-20 minutes and 100-130 minutes, and high within the time range of 0-20 minutes and 60-100 minutes. The growth of rate incorporation of folic acid (drug) in the polymer involves the growth of the covalent reversible attachment of the carrier through amide bond formation with the folic acid (drug). Thus, the covalent reversible attachment of carrier will keep increasing until to reach, if possible, the maximum rate incorporation of folic acid in the polymeric carrier. Consequently, the coupling yield will always increase when the covalent reversible attachment is occurring as fast as the cleavage of polymer occurs. Dealing with irreversible reaction, the reaction between folic acid and the polymeric carrier should result to the growth of the coupling yield in terms of time as the rate of incorporation of folic acid in the polymeric carrier is increasing. However the consideration of the Figure 4.3 shows that the fraction of yield was moderately increasing in the time range of 0-60 minutes and became accentuated until to reach the maximum in the time range of 60-100 minutes, unlikely decreasing in the range of 100-130 minutes. The contrast is that the fraction of yield was not increasing all the time of reaction with the fraction of incorporation of folic acid as intended. To investigate the cause of the contrasting behaviour of the fraction of yield, it was found that the polymer with high molecular weight could be subject to cleavage during the reaction. Water-soluble polymers, mostly cationic polyelectrolytes, are widely used as flocculants. Mineral processing, water clarification, and paper manufacture are some

areas where these polymeric flocculants are extensively used [184, 185]. The cleavage of the intramolecular bonds may be classified in three cases; a) the scission can occur in any bonds, b) the cleavage of the main chain occurs in any bonds, after pendant groups break first, c) the main chain carbons with the pendant group break in any bonds of the main chain. The hydrolytic cleavage, however can occur during the dialysis, can not affect the change of yield while both the processes of chromatography and dialysis were observed in the same condition of work for every reaction time.

The use of 2-(1H-benzotrial-1-yl)-1,1,3,3-tetramethylurium hexafluorophosphate (HBTU) as coupling agent could dispose the polymer to the cleavage of the main chain in any bond. This reduces the length of certain long chains, as well as the molecular weight respectively. Therefore, during a chromatography process, all chains with molecular weight under 5000 can be removed from the solution and further, fewer than 12000 during the dialysis process. It resulted in both the decrease of fraction of polymeric carrier (Fig. 4.4) and the growth of the fraction of removed polymeric carrier (Fig. 4.5) during the reaction time.

Figure 4.7 (series 1 and 2) as combination of Figure 4.2 and Figure 4.3, shows that in the same range time of 60-100 minutes the growth of the fraction incorporation of folic (34.7 82.7%) was more pronounced and the fraction of coupling yield (78.83-84.87%) was accentually increasing. Hence, the incorporation of folic acid in the polymeric carrier was a decisive factor to involve the yield of occurred coupling. Though the fraction of remaining polymers due to the cleavage was decreasing (Fig. 4.4), this did not involve more the yield of coupling as long as the incorporation of folic acid was growing so fast than the polymer available for the coupling was decreasing. It is intending that the sites available for the covalent reversible attachment of the carrier through amide bond formation with the folic acid (drug) are limited to 100% of folic acid incorporation. Since the goal is to reach 100% of folic acid incorporation in the polymer, the coupling yield will be the result of the optimum reaction time required to reach the maximum incorporation. Accordingly, in order to reach the maximum incorporation of folic acid in the polymeric carrier, the reaction was kept running over 100 minutes, time related to

85% as maximum coupling yield (Fig 4.3). Then, taking the reaction to 96% incorporation of folic acid needed 30 minutes more (100-130) within which the yield was decreasing. As the incorporation of folic acid was progressing fast than the cleavage of polymer until 100 minutes, this caused a rapid reduction of available site capable to receive the folic acid into the polymer. Consequently, in the range of time of 100-130 minutes the fraction of retained polymer decreased more (Fig. 4.4 and Fig. 4.7) and relatively the fraction of removed polymers increased in the same way (Fig. 4.5 and Fig. 4.7). In the time range of 0-60 minutes the fraction of incorporation moderately increased because the activity of the coupling agent in the solution increases with the reaction time. The activity of HBTU in the reaction was more effective after 60 minutes of reaction due to the fact that the incorporation of folic acid was rapidly increasing within the range reaction time of 60-100 minutes where the sites available for reversible covalent attachment were reduced. Because HBTU as coupling agent has to assure the reaction between polymer and drug, the reduction of sites available for the binding after 100 minutes of reaction has limited the action of coupling agent. Therefore, the incorporation of folic acid was moderately increasing. In order to avoid more dropping coupling yield due to the polymer cleavage through the over action of HBTU as coupling agent, the reaction was asserted to be stopped within the range minutes (120-130) where the rate incorporation of folic acid was in the range (90-96%).

The inherent viscosity was increasing with the reaction time (Fig. 4.8 and 4.15) because of the incorporation of folic acid (drug) while challenging the solubility of the carrier, could make the compound more viscous (Fig. 4.1).

The variation of mol ratio (X/Y) from 17/3 to 4/1 as illustrated in Table 4.9 has led to the settlement of different figures. Figure 4.9 confirmed the increase of fraction incorporation with the reaction time. The fraction of coupling yield has kept increasing even while changing the ratio, and did not decrease anywhere because the range time (60-120) was so large, and could not show exactly the reaction time when the coupling yield was decreasing (Fig. 4.10). In Figure 4.11, the fraction of remaining polymers was decreasing while the fraction of lost polymers was relatively increasing with the reaction time (Fig.

4.11). When compare Figure 4.2 to Figure 4.9, the investigation showed that the carrier with mol ratio (4/1) has reached the maximum of the fraction of incorporation of folic acid at the record time than the carrier with mol ratio (17/3). The less the mol ratio (X/Y) is, the more anchoring drug quantity equivalent to the drug quantity is needed to complete the available site. As the reaction kinetics is generally dependent on concentration, temperature and catalyses; the excess of the drug, increasing the concentration, can have more effect on the reaction kinetics.

The comparison of Figure 4.15 to Figure 4.8 shows that the viscosity when working with PSI-DMP (80)-PDA (20)-FA (mol ratio 4/1) is higher than when working with PSI-DMP (85)-PDA (15)-FA (mol ratio 17/3). This, because the less mol ratio (X/Y) will need more folic acid which being water insoluble, increases the viscosity of the coupling. When the mol ratio X/Y decreases, the mol of anchoring drug unit increases, and more site for drug incorporation will be available for covalent reversible attachment. Thus, the more the compound is insoluble the more its viscosity is higher.

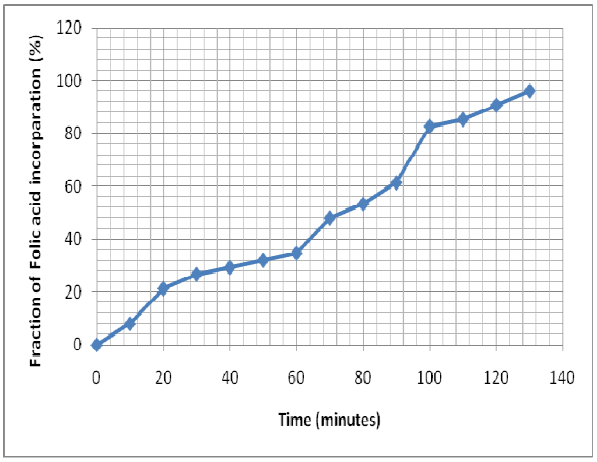


**Figure 4.2: Fraction FA incorporation versus reaction time (Mol ratio 17/3)**

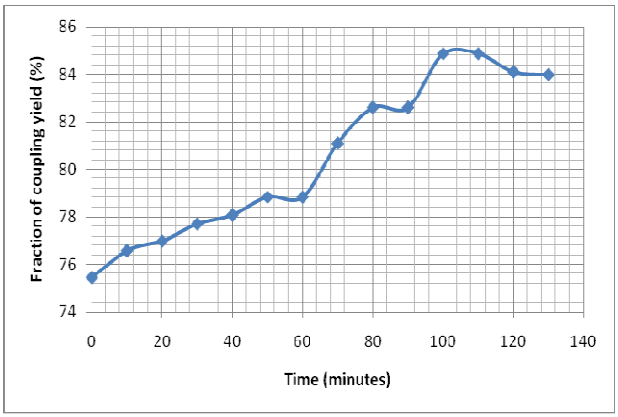


**Figure 4.3: Fraction of coupling yield versus reaction time (Mol ratio 17/3)**

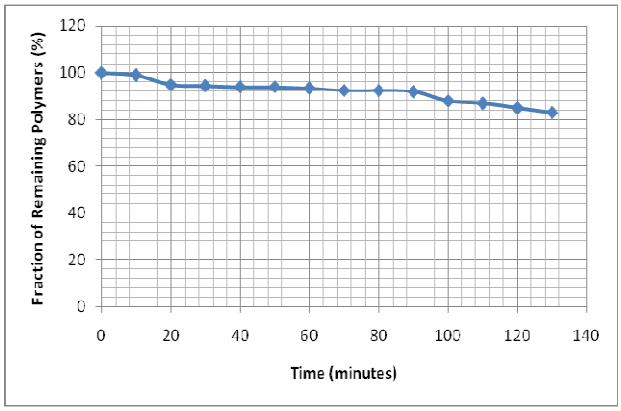


**Figure 4.4: Fraction of Retained Polymers versus reaction time (Mol ratio 17/3)**

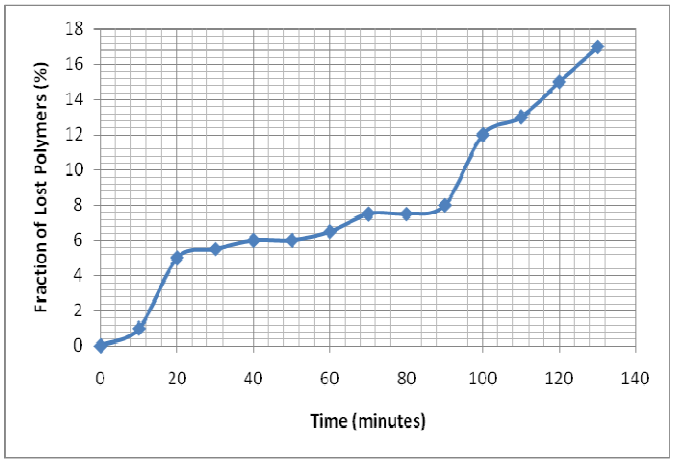


**Figure 4.5: Fraction of Removed polymers versus reaction time (Mol ratio 17/3)**

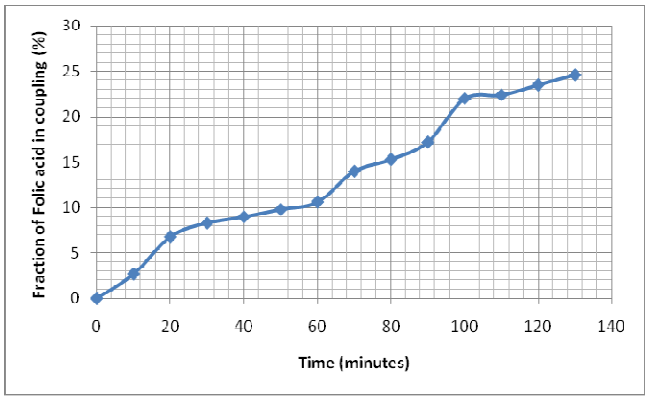


**Figure 4.6: Fraction of FA in coupling versus reaction time (Mol ratio 17/3)**

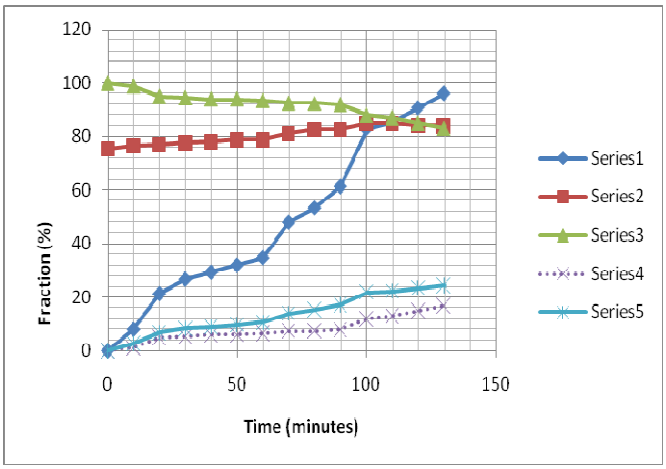


**Figure 4.7: Combining Fractions versus reaction time (Mol ratio 17/3)**

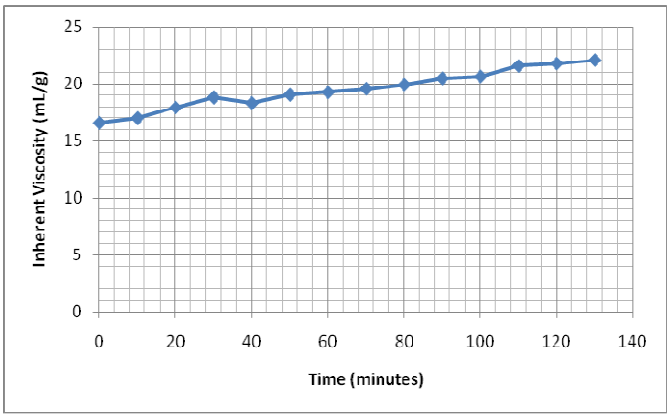


**Figure 4.8: Inherent viscosity versus reaction time (Mol ratio 17/3)**

Series 1: Fraction of FA incorporation in Polymers, series 2: Fraction of coupling yield, series 3: Fraction of retained Polymers, series 4: Fraction of removed Polymers, series 5: Fraction of FA in coupling

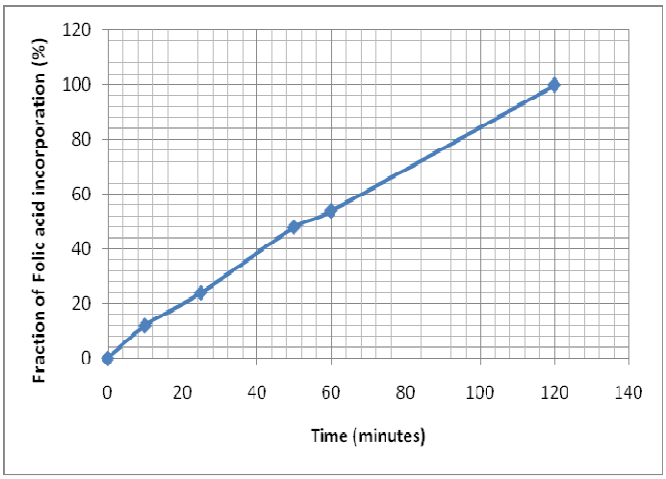


**Figure 4.9: Fraction FA incorporation versus reaction time (Mol ratio 4/1)**

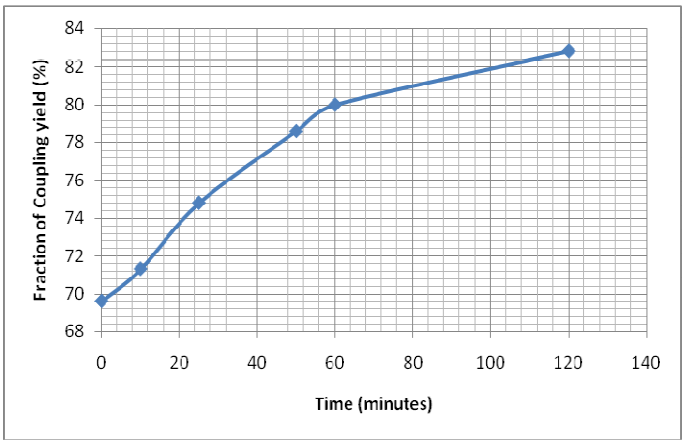


**Figure 4.10: Fraction Coupling versus reaction time (Mol ratio 4/1)**

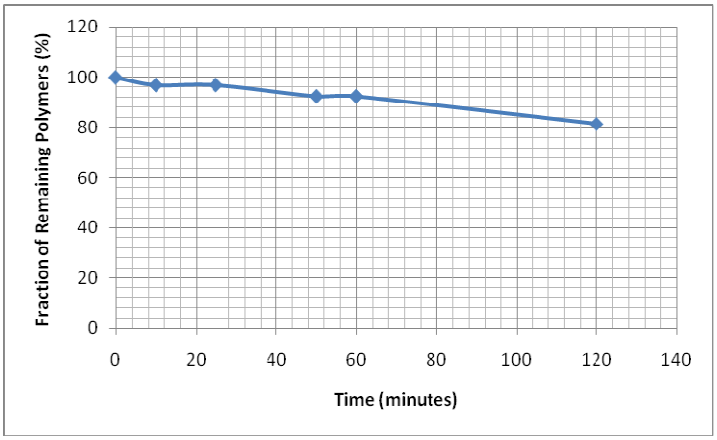


**Figure 4.11: Fraction of Retained Polymers versus reaction time (Mol ratio 4/1)**

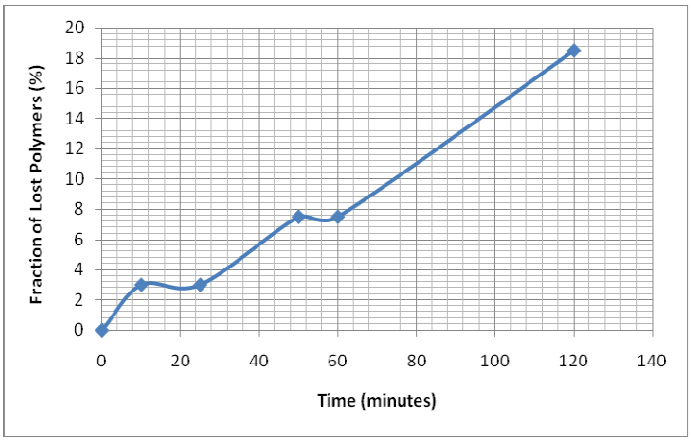


**Figure 4.12: Fraction of Removed Polymers versus reaction time (Mol ratio 4/1)**

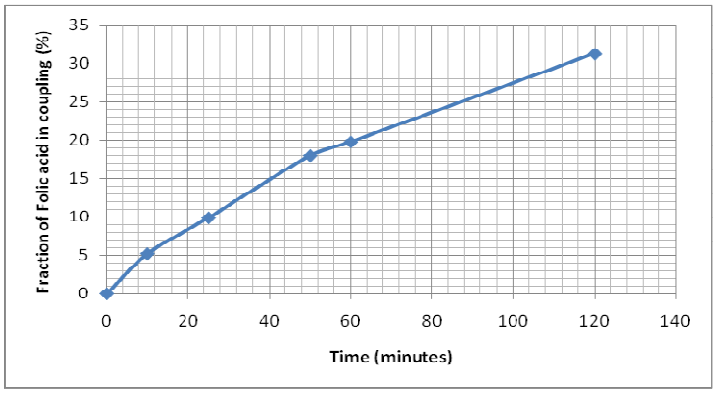


**Figure 4.13: Fraction of FA in coupling versus reaction time (Mol ratio 4/1)**

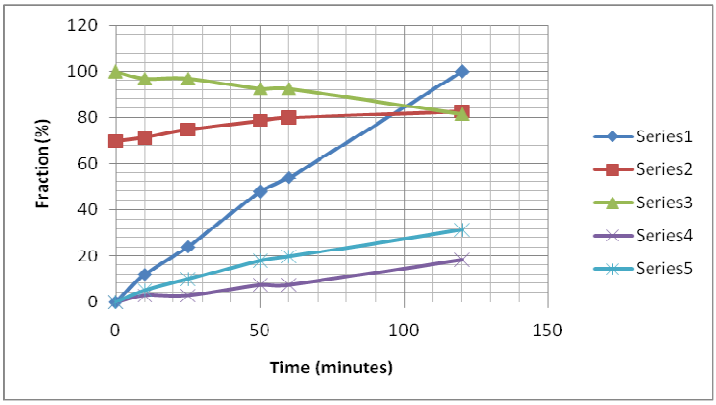


**Figure 4.14: Combining Fraction versus reaction time (Mol ratio 4/1)**

Series 1: Fraction of FA incorp. in Polymers, series 2: Fraction of coupling yield, series 3: Fraction of retained Polymers, series 4: Fraction of lremoved Polymers, series 5: Fraction of FA in coupling

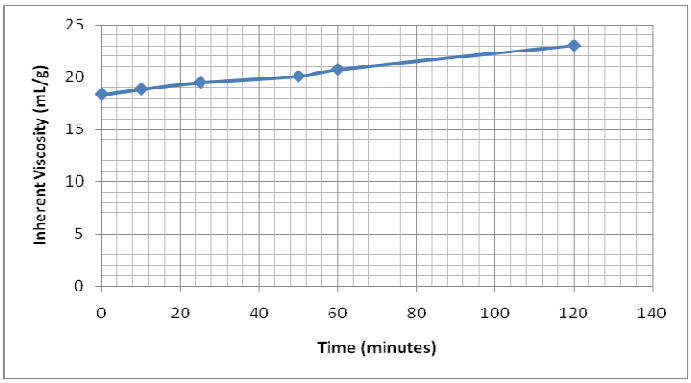


**Figure 4.15: Inherent Viscosity versus reaction time (Mol ratio 4/1)**

### 4.2.1.3. Comparative study of PSI-DMP(X)-PDA(Y)-FA conjugates

After the optimization of the reaction time at 120 and 130 minutes, the coupling obtained by varying the mol ratio at 19/1, 17/3 and 4/1, shows the decreasing of yield respectively (Table 4.9). The more the mol ratio is big, the more the anchoring drug need for folic acid is less. Since the mol of HBTU coupling agent is anchoring drug dependent, the small quantity of HBTU need for a big mol ratio (X/Y) will lead to the minimization of the polymer cleavage. This corroborates the option that the coupling agent in the reaction of polymeric carrier drug conjugate is one of factors capable to promote the polymer cleavage.

**Table 4.9: HNMR spectra data for PSI-DMP (X)-PDA (Y)-FA conjugates**

| Chemical compound | X | Y | X/Y | HNMR Spectra | Chemical shift δ/ppm Calculated (expected) 8.7-6.75 Aromatic & heteroaromatic **CH** | 1.7-1.6 $CH_2\mathbf{CH_2}CH_2$ | % FA Incorp. | BMw | $\eta_{inh}$ ($mLg^{-1}$) | Yield % |
|---|---|---|---|---|---|---|---|---|---|---|
| | 95 | 5 | 19/1 | 7 | 5.2 (5) | 40 (40) | 104 | 4380.4 | 15.81 | 88.53 |
| PSI-DMP (X)-PDA (Y)-FA | 85 | 15 | 17/3 | 20 | 14.4 (15) | 40 (40) | 96 | 5171.1 | 22.07 | 83.98 |
| | 80 | 20 | 4/1 | 25 | 5 (5) | 10 (10) | 100 | 1391.6 | 23.02 | 82.80 |

### 4.3. Carbon nanotubes drug carriers

#### 4.3.1. Synthesis of Carbon nanotubes

The CNTs used in this study are multiwall carbon nanotubes (MWNTs) which are prepared by chemical vapour deposition (CVD). In this method, source of Fe catalyst was ferrocene which is dissolved in acetylene as a gas carbon source and this gas was carried to a synthetic reactor by argon. During synthesis process, amorphous carbon is also produced and was removed through the oxidation in the presence of the air. The CNTs obtained were refluxed in $HNO_3$ to eliminate the metal catalysis. The results obtained after TEM analysis, are illustrated in Figure 4.16.

##### 4.3.1.1. Results of Synthesis of Carbon nanotubes

The total yield of multiwall carbon nanotubes (MWCNTs) prepared after 25 experiments was 8.56g with the mean yield of 345mg per experiment. The microscopic image from the TEM analysis as shown in Figure 4.16, captured with magnification 100000, shows tubes with average outer diameter ($d_o$) of 20nm and inner diameter ($d_i$) of 10nm.

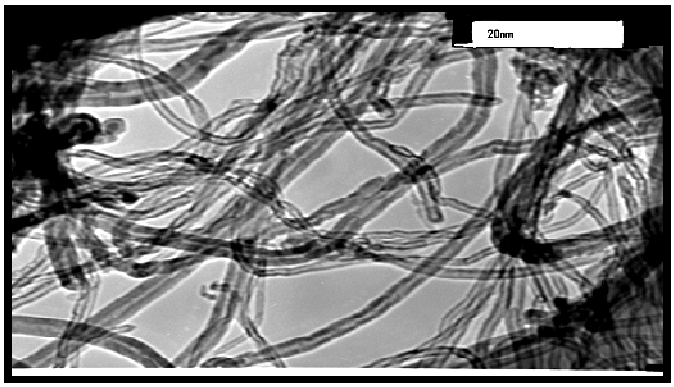


**Figure 4.16: MWCNTS microscopic image (TEM)**

##### 4.3.1.2. Discussion of Results of Synthesis of Carbon nanotubes

The CNTs found could have a variety of applications because of their novel structure, especially the small size and remarkable mechanical, thermal and electrical properties. Small-diameter MWCNTs have ability to display enhanced reactivity relative to larger-

diameter nanotubes, due to increased curvature strain. However, because of their novel structure of elemental carbon, CNTs are insoluble in all organic solvents. In addition, the CNTs found got a very high surface energy with a tendency to aggregate together. This makes them difficult to be dispersed.

Thus, the carbon nanotubes found could be used for many applications. Their compatibility with aqueous environments was made possible by chemical functionalization of their surface. The functionalized carbon nanotubes, in respect of certain requirements such as pH and peptide availability bond, can easily interact with biological components including mammalian cells.

### 4.3.2. Functionalization of carbon nanotubes

#### 4.3.2.1. Covalent functionalization of carbon nanotubes

**A. Functionalizationof CNTs with concentrated nitric acid and sulfuric acid**

a). Results of Functionalization of CNTs with concentrated nitric acid and sulfuric acid

In this study, CNTs were functionalized with $H_2SO_4/HNO_3$ in mol ratio 3:1 differently at 100°C, 50°C and room temperature respectively (RT). After TEM analysis the following results were recorded:

With the variation of temperature, at 100ºC the outer diameter ($d_0$) =20nm and the inner diameter ($d_{in}$) = 12nm (Fig. 4.17) while at 50ºC $d_o$= 30nm (Fig. 4.18) and at room temperature (RT) $d_0$= 80nm and $d_{in}$= 40 (Fig.4.19). In order to evaluate the variation of the size of f-CNTs in terms of temperature, a graph of diameter versus temperature was plotted as shown in Figure 4.20.

The water solubility of f-CNTs was decreasing from 100°C to RT especially from pH = 9 and above.

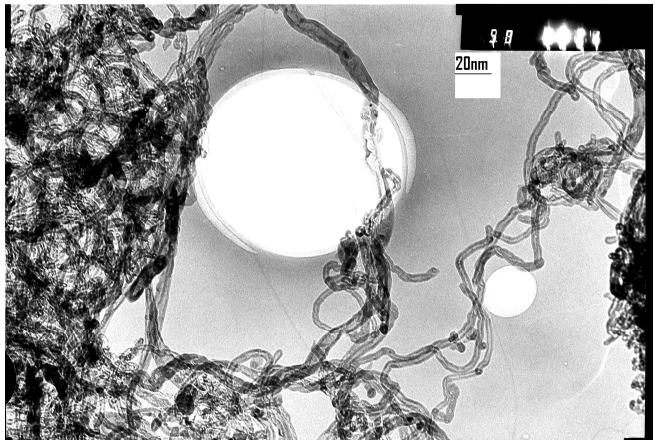


**Figure 4.17: f-CNTs ( $H_2SO_4/HNO_3$ at 100°C) microscopic image**

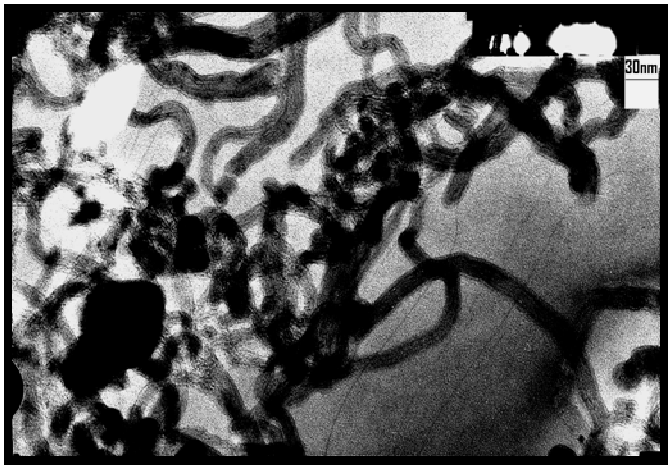


**Figure 4.18: f-CNTs ($H_2SO_4/HNO_3$ at 50°C) microscopic image**

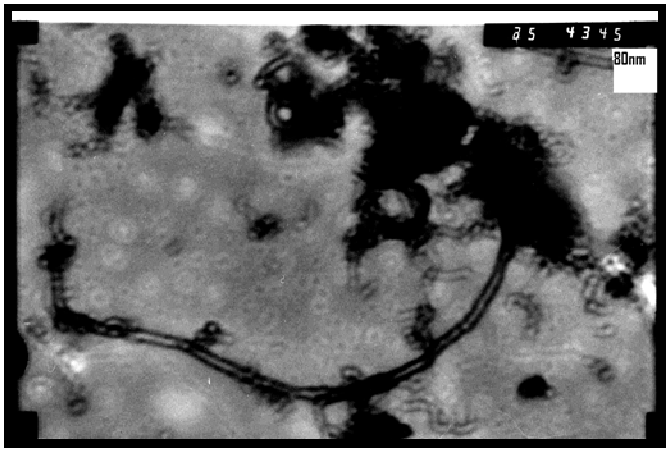


**Figure 4.19: f-CNTs ($H_2SO_4/HNO_3$ at RT) microscopic image**

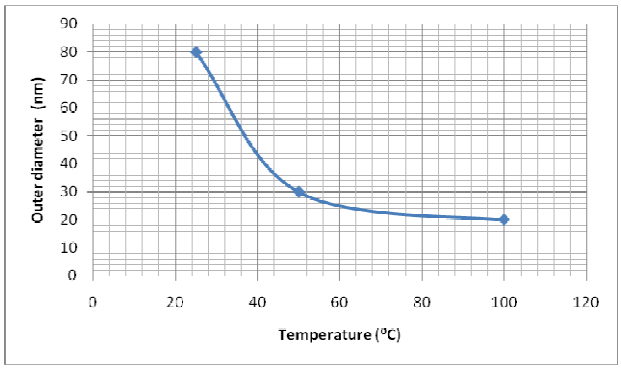


**Figure 4.20: Size of CNTs versus temperature**

The analysis of $^{1}$H NMR Spectra 26, 27, 28 (in appendix) done for f-CNTs obtained at different temperatures including 100°C, 50°C, RT respectively shows peaks A and B in chemical shift δ/ppm (1.5-2.5) for –**CH$_2$**COOH and (2.7-3.7) for –**CH$_2$**OH. In order to calculate the quantity of COOH and OH, the integration of peak A (–**CH$_2$**COOH) corresponding to 1 mol was used as reference to evaluate the peak B (–**CH$_2$**OH). After calculation, the following results were obtained:

1) The integration of peaks A and B in $^{1}$H NMR Spectra (26) for f-CNTs (100ºC) shows after evaluation that 1 mol of COOH adsorbed on the surface of MWCNTs, corresponded to 7.54 moles of OH.
2) The integration of peaks A and B in $^{1}$H NMR Spectra (27) for f-CNTs (50ºC) shows after evaluation that 1mol of COOH absorbed on the surface of MWCNTs, corresponded to 2.27 mol of OH.
3) The integration of peaks A and B in $^{1}$H NMR Spectra (28) for f-CNTs (RT) shows after evaluation that 1 mol of COOH absorbed on the surface of MWCNTs, corresponded to 0.08 mol of OH.

A sample of 200mg of f-CNTs was used for titration to evaluate the quantity of COOH in mmol incorporated on the surface of f-CNTs which through the mol ratio COOH/OH calculated from different $^{1}$H NMR spectra integration was used to calculate the quantity of OH in mmol incorporated on the surface of f-CNTs. The experimental data from

titration was used through the formula Y= 1-0.04X[e] to complete the Table 4.10 shown below. The graphs include the data from the Table 3.10 were plotted to show the evolution of both the fraction of incorporation of COOH and OH versus the temperature as shown in Figure 4.22 and the mol ratio COOH/OH versus the temperature as shown in the figure 4.23.

Different peaks including A, B, C, D and E were shown in the infrared (IR) investigation as presented in Figure 4.21(a) and (b).

A: O-H stretch, (3331.44 cm & 3334.86 cm) intermolecular hydrogen bonded

B: C-H stretch; (2892.90cm & 2902.20 cm)

C: C=O, stretch; (1693.04 cm & 1716.56 cm)

D: C-O (1158.92 $cm^{-1}$- 1028.01 $cm^{-1}$) & (1156.39 $cm^{-1}$-1030.67 $cm^{-1}$), stretch

E: Ring C=C, bend, (663.67 $cm^{-1}$-574.56 $cm^{-1}$), this confirm the CNTs the graphene structure with $sp^2$ -bond carbon.

[e] Y is the quantity of COOH in mmol incorporated on the surface of f-CNTs and X is the volume of HCl in ml

**Table 4.10: Fraction incorporation of COOH and OH on the surface of CNTs with variable temperature**

| TºC | 25ºC (RT) | 50ºC | 100ºC |
|---|---|---|---|
| Mass of f-CNTs | 200mg | 200mg | 200mg |
| nH: COOH | 1 | 1 | 1 |
| nH: OH | 0.08 | 2.27 | 7.54 |
| X ml | 16ml | 13ml | 6ml |
| Y mmol | 0.36mmol | 0.48mmol | 0.76mmol |
| % COOH incorp. | 8.1% | 10.8.% | 17.1% |
| % OH incorp. | 0.25% | 9.9% | 48.7% |

nH: number of Hydrogen atom,
X: the volume of HCl in ml
Y: the quantity of COOH in mmol incorporated on the surface of f-CNTs

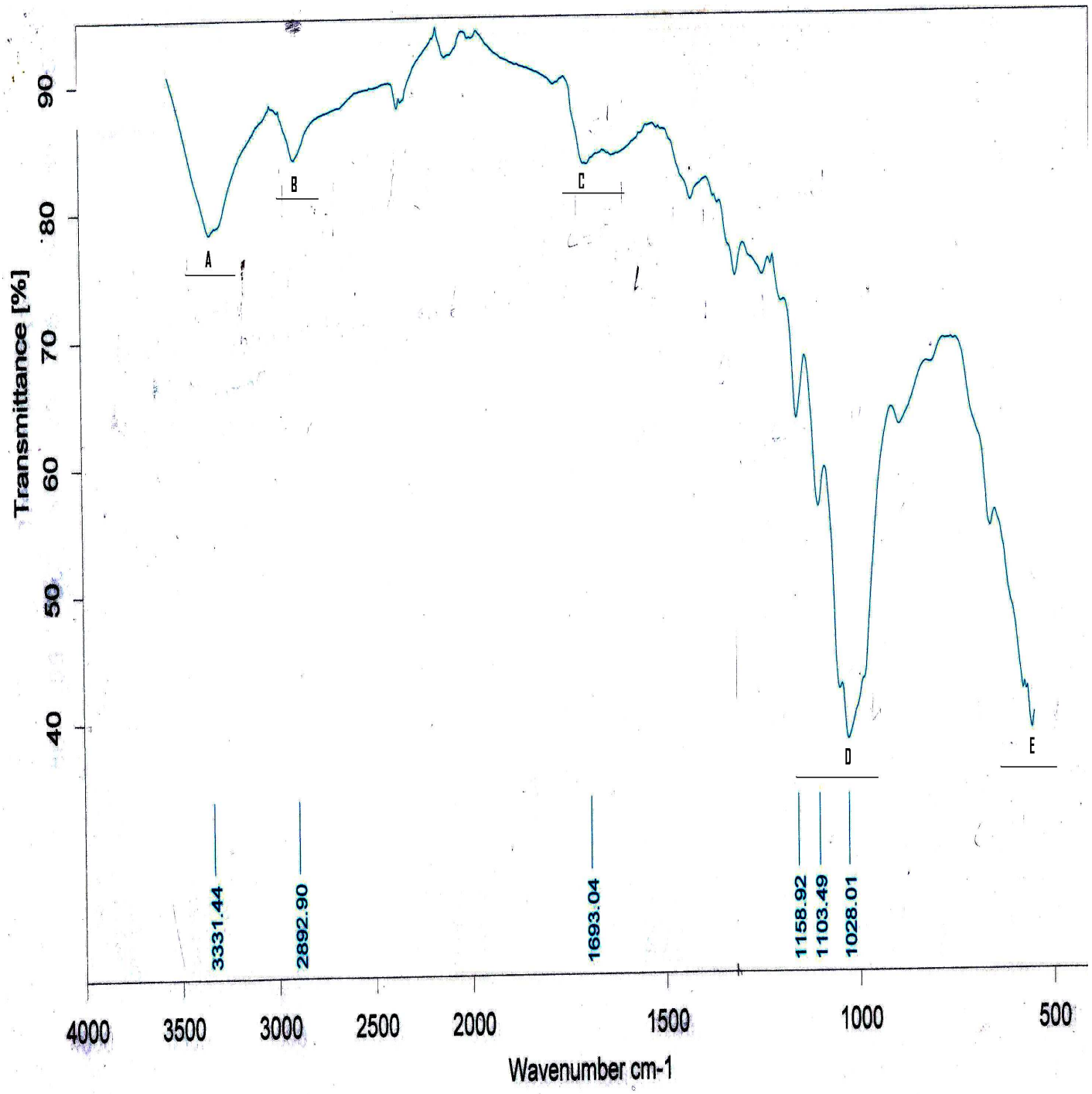


**Figure 4.21(a): Infrared Peaks of *f-CNTs* ($H_2SO_4/HNO_3$) at 50°C**

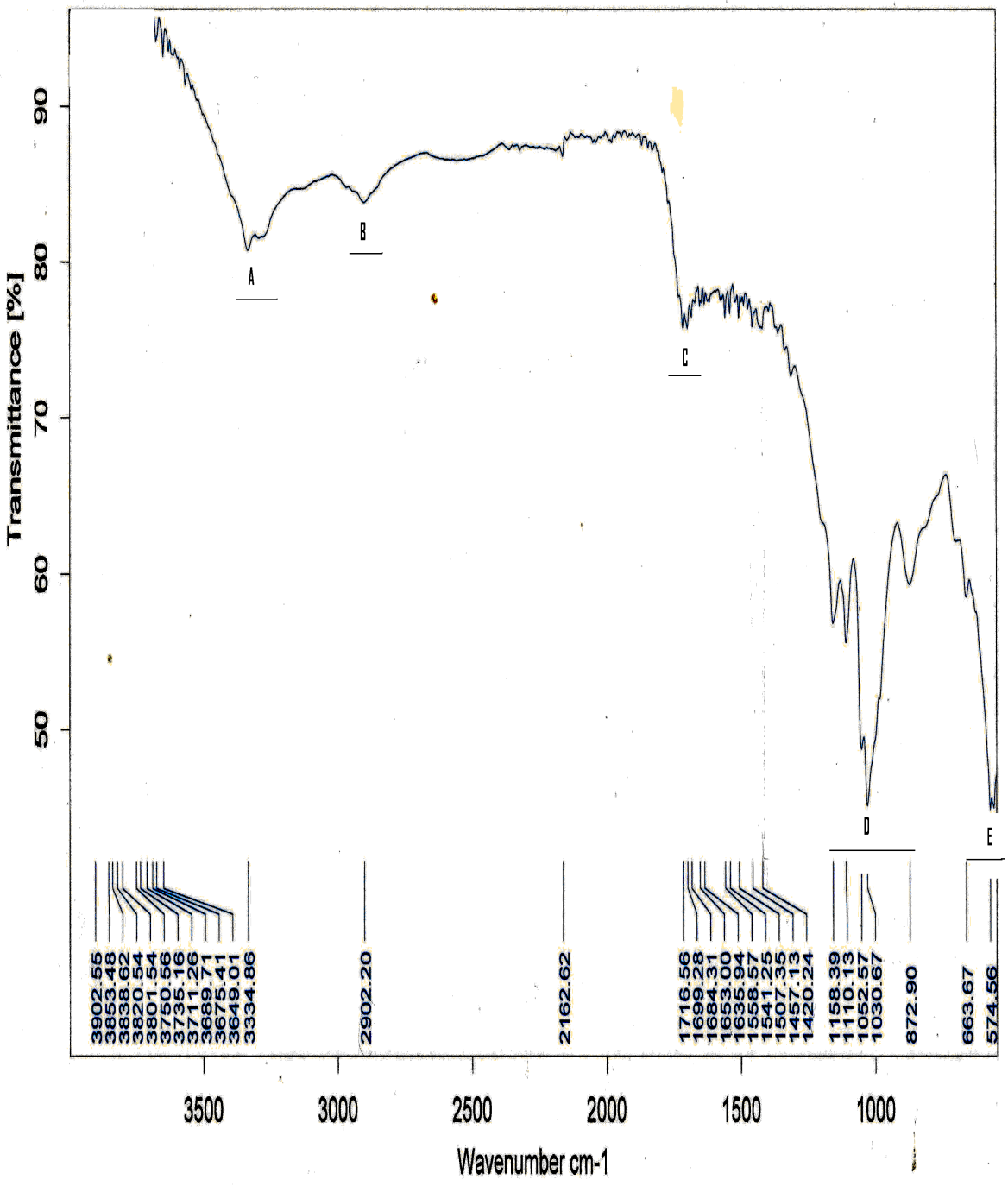


**Figure 4.22(b): Infrared Peaks of *f-CNTs* ($H_2SO_4$/$HNO_3$) at 100°C**

b) Discussion of Results of Functionalization of CNTs with concentrated nitric acid and sulfuric acid

Figure 4.20 elaborated from the TEM results (Fig. 4.17, 4.18 and 4.19), shows the increase of the size of nanotubes when the temperature was decreasing. This is because self-diffusion of guest molecules inside of CNTs can be possible. The carbon nanotubes (CNTs) can be aligned to form a well-ordered nanoporous membrane [186, 187], which can be incorporated in a macroscopic structure [188] for separation devices. The study of self-diffusivity can explain well the influence of nanotube sizes and temperature. Yashonath and co-workers had examined this effect in more detail for diffusion zeolites [189, 190] using molecular dynamics simulations. They termed this behaviour the "Levitation effect". If the guest molecule fits perfectly in the window of the zeolite, the molecule appears to be "floating"; increasing or decreasing the diameter of the guest molecules causes the diffusion coefficient to decrease. This effect is temperature dependent [191]. A similar effect has been observed by Bride et al. [192] for carbon nanotubes.

With regard to Figure 4.20, the self-diffusivity was subsequently increasing with the decreasing of temperature. Since the self-diffusion explains the incorporation of guest molecule in CNTs through nanoporous membrane, the diameter of CNTs has to increase in the tendency where the self-diffusion will increase. It results in the increase of diameter with the decrease of temperature as shown in figure 4.20. Regarding the objective to develop the surface of CNTs for further utilization, more importance was given to the trend where the adsorption (surface phenomenon) was possible, rather than where absorption was evident. The increase of temperature, causing the diameter to decrease, led to higher collision frequencies due to faster motion. In addition, the probability to find a particle close to the pore wall is enhanced (higher collision probability). In order to have the drug (folic acid) bonded on the surface of CNTs, the functionalized carbon nanotubes (CNTs) made at 100°C were selected, due to their small size and the adsorption developed on their surface.

The $^{1}H$ NMR Spectra 26, 27 and 27 were obtained with $D_2O$ as solvent. Therefore COOH group and OH group directly attached on the surface of CNTs were shifted in δ/ppm (4.5-5.5) for $D_2O$ peaks. Expecting to get f-CNTs covered on surfaces only with COOH and OH groups as shown in Scheme 2.4, the $^{1}H$ NMR analysis for all f-CNTs made at different temperatures (100ºC, 50ºC and RT) have shown the presence of $CH_2COOH$ and $CH_2OH$. This has guided to set the structure as shown in Scheme 4.4. More investigation was needed to disclose the cause of the presence of $CH_2COOH$ and $CH_2OH$ on the surface as well as COOH and OH as shown in the scheme 4.4. When the purification stage is not reliable, there is possibility to have the amorphous carbon mixed with carbon nanotubes. The purification of pristine made using HCl (32%) and further the presence of $HNO_3$ (55%) in the operation of functionalization were enough to remove the amorphous carbon. Dravid et al. [193], however, suggested an alternative model described as 'paper roll' where nanotubes are composed of spiral scrolls of graphene sheets. Amelinckx [194] has proposed an intermediate model where the nanotubes consist of cylindrical sheets, with scrolls of constant helicity interspersed between them. This structure as presented, grants to CNTs an exceptional mechanical property that their high degree of stiffness combines with resilience, and the ability to buckle and collapse in a reversible manner: even largely distorted configurations (axially compressed, twisted) can be due to elastic deformations with virtually no atomic defects involved [195, 196, 197, 198].

The motion of dislocation edges in a strained structure is a well-known phenomenon in the theory of dislocations. This can cause as well the crack of some hexagonal symmetry C-C in order to have simple carbon attached to other hexagonal, keeping the nanotubes structure. Indeed, the presence of strong acid for CNTs functionalization can cut the tubes in shorter pieces and generate carboxylic functions at the tips and around the sidewalls where the curvatures of the tubes present a higher strain.

In addition, the infrared analysis from Figure 4.21(a) and (b), and the $^{1}H$ NMR Spectra 26, 27 and 28, have confirmed that the produced f-CNTs was constituted of MWNTs covered on the surface with $CH_2OH$ and $CH_2COOH$ and with OH and COOH as shown in Scheme 4.4.

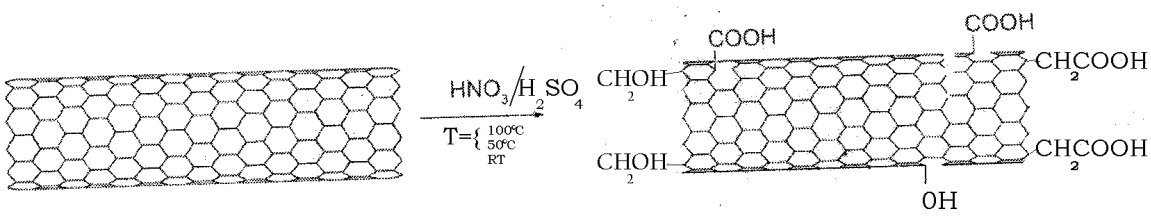


**Scheme 4.4: f-CNTs ($H_2SO_4/HNO_3$) structure.**

In comparison with the result from Figure 4.22, it was found that both fractions of OH and COOH incorporation in f-CNTs were increasing with the increase of temperature. At room temperature, the fraction of OH group incorporation was much neglected and the mol ratio COOH/OH was 32.4, this was rapidly reduced to 1.1 at 50ºC until dropping down to 0.35 at 100°C. It means that though the weak presence of OH in f-CNTs at room temperature, this increased very rapidly when the temperature started increasing. This shows that when working at room temperature or below there is possibility of getting f-CNTs covered only with COOH.

The OH (phenol group) is a polar group, and plays an important role for water solubility of the functionalized carbon nanotubes. It was experimentally proved that the f-CNTs obtained at 100°C, having more mol of OH on the surface, was more soluble in water than those obtained below 100°C. Thus, the abundance of OH and COOH groups on the surface will facilitate more covalent attachment to polymers or drugs according to their different electronegativities. This granted the f-CNTs made at 100ºC to be more useful than those made at low temperatures. The scope of this reaction was very broad and produces f-CNTs that possess high solubility in a wide range of different solvents. This was preferentially selected for the next phase of the drug binding to carbon nanotubes.

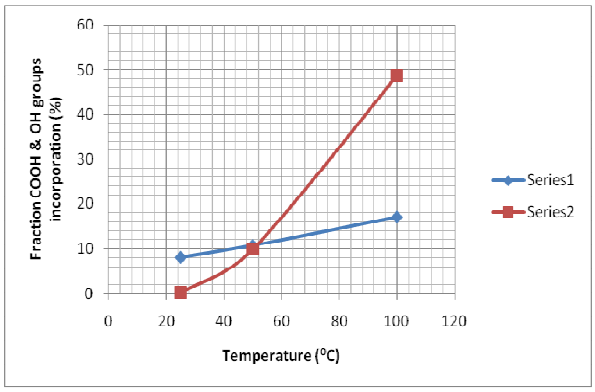


**Figure 4.23: Fraction of COOH & OH group incorporation versus temperature**

Series 1: Fraction incorporation of carboxyl group (COOH) on the surface of CNTs.
Series 2: Fraction incorporation of phenol group (OH) on the surface of CNTs.

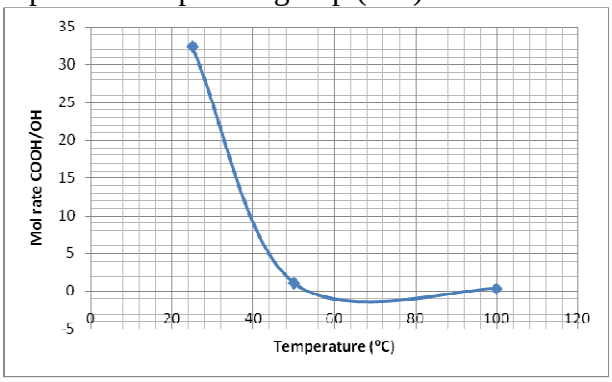


**Figure 4.24: Mol rate COOH/OH versus temperature**

**B. Functionalization of CNTs with Aspartic acid**

The functionalized carbon nanotubes (f-CNTs) were also obtained by heating MWNTs with aspartic acid as amino acid in DMF at 220ºC. This resulted to the structure as shown in Scheme 4.5.

a) Results of *f-CNTs* by Aspartic acid

After collecting a yield of 183mg soluble in water from pH 10, different analysis were performed to investigate the sample obtained.

The microscopic image obtained after TEM analysis confirmed the nanotube structure with the diameter of 60nm as shown in Figure 4.24.

**Figure 4.25: f-CNTs (MWNTs +Aspartic acid in DMF at 220°C)**

The $^{1}$H NMR Spectra 29 (in appendix) showed peaks A in chemical shift (δ/ppm) 3.050-2.200 for –**$CH_2$**COOH and B in chemical shift (δ/ppm) 4.40-4.70 for =N-**CH $CH_2$** $(COOH)_2$ as expected.

Different peaks including A, B, C, D, E, F and G were shown in the infrared (IR) investigation as presented in Figure 4.25.

A: N-H stretch, at 3331.44 $cm^{-1}$.

B: C-H stretch in the region 3015.95-2902.20$cm^{-1}$

C: Overtone region usually contains a prominent band in the region 2337.23-2119.11$cm^{-1}$

D: C=O bond stretch, at 1738.63 $cm^{-1}$

E: C-N stretch, at 1436.30$cm^{-1}$

F: C-O (acetate) stretch, in the region 1228.93-1216.70 $cm^{-1}$

G: O-H out of plane bend, 1011.82-912.05 $cm^{-1}$

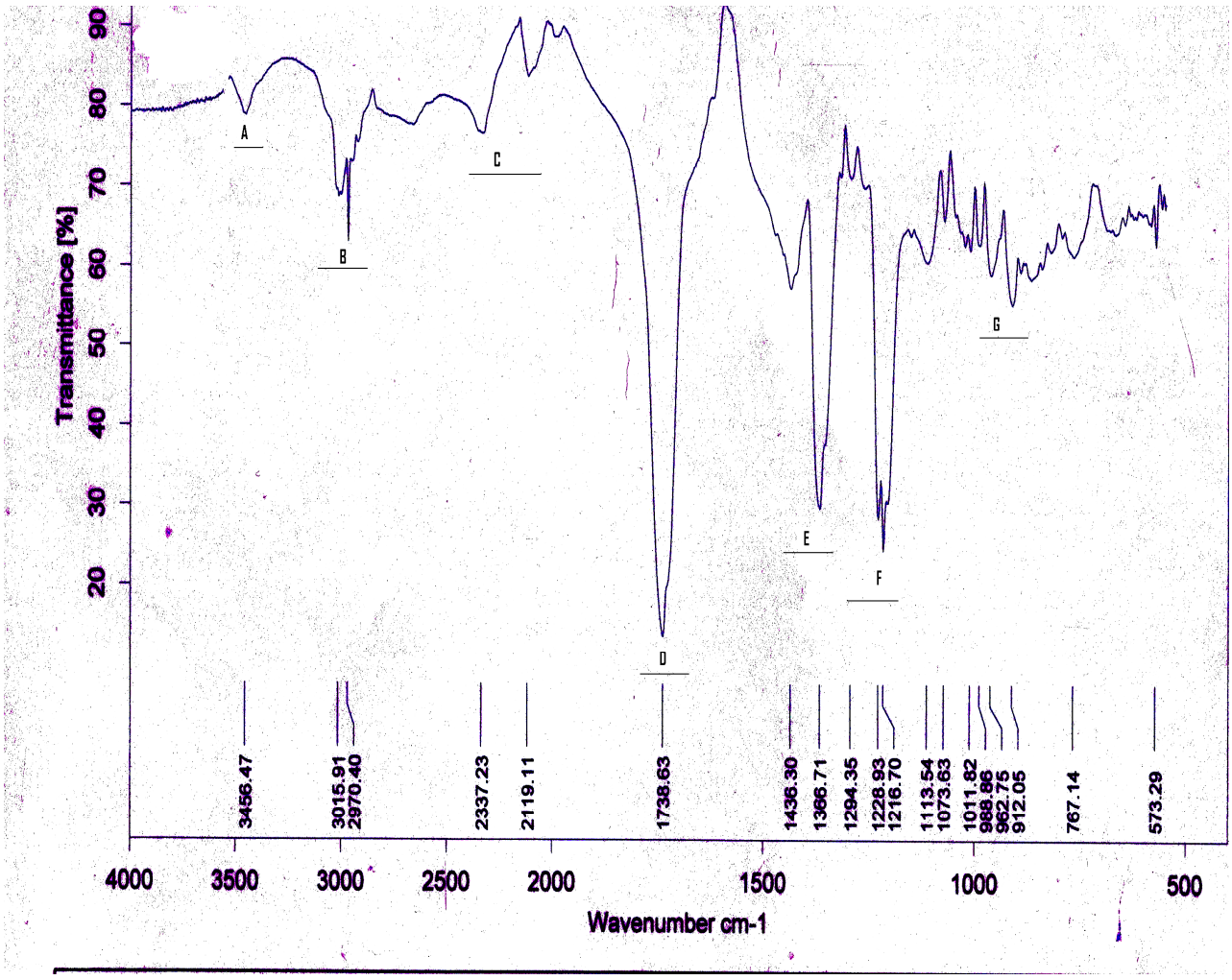


**Figure 4.26: IR f-CNTs (aspartic acid)**

Using titration formula Y= 1-0.04X[f], when working with 200mg of f-CNTs 0.88 mmol of COOH corresponding to 20% of COOH was incorporated on the surface of CNTs after the neutralization of excess NaOH with 3ml of HCl. The carboxyl group incorporated in the f-CNTs was intended to be bound with the solubilising group and the drug. Then the quantity of solubilising group and drug will be evaluated in terms of 20% of fraction of COOH in f-CNTs. The test of solubility showed that the f-CNTs obtained were water soluble at pH =10. The attachment to a solubilising group was beneficial to increase the solubility.

[f] Y is the quantity of COOH in mmol incorporated on the surface of f-CNTs and X is the volume of HCl in ml

b) Discussion of Results of *f-CNTs* by Aspartic acid

The diameter of f-CNTs obtained from MWNTs heated at 220°C in aspartic acid with DMF was 60nm. This was bigger than the diameter obtained for MWNTs in sulfuric and nitric acids at 100°C and 50°C, and lesser than MWNTs in sulfuric and nitric acids at RT. According to the findings from Figure 4.20, the diameter was decreasing with the increase of temperature. At 220°C as a very high temperature, the diameter should be very small. To explain this contrast, Derouane and co-workers [199, 200] were the first to mention an enhanced mobility for cases where the dimensions of guest particles match closely the host structure dimensions. They called this effect the "floating molecule". When the temperature rises to very high, the dimension of the diameter of the guest can increase or decrease and affects the diffusion coefficient. The diameter of f-CNTs obtained differently when varying molecules at different temperatures, was attributed to the phenomena of guest molecules inside CNTs in detail by means of molecular dynamics simulation.

The investigation of peaks in $^{1}H$ NMR Spectra 29 and infrared (IR) as shown in Figure 4.25 confirmed the structure elaborated in Scheme 4.5.

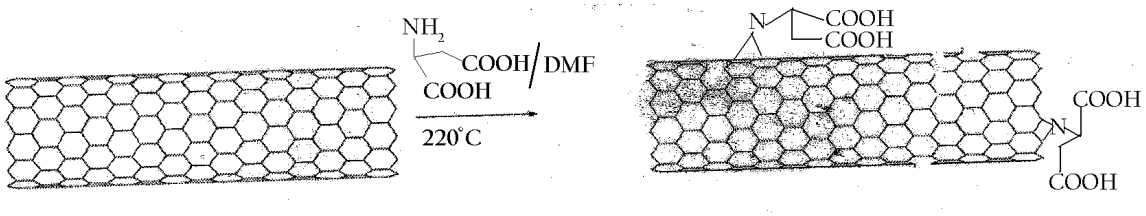


**Scheme 4.5: f-CNTs (aspartic acid) structure**

Overall, the use of strong acid and amino acid to functionalize the carbon nanotubes generates carboxylic groups (Schemes 4.4 and 4.5), which increase their dispersibility in aqueous solutions [201]. Solubility under physiological conditions is a key prerequisite to make CNT biocompatible. In addition, functionalised carbon nanotubes (f-CNTs) can be linked to a wide variety of active molecules, including peptides, proteins, nucleic acids and other therapeutic agents.

#### 4.3.2.2. Noncovalent functionalization of carbon nanotubes

The poly-DL-succinimide, due to the ability to provide ring-opening process when applying one type of amine reactant, was selected as polymer to make noncovalent functionalization of carbon nanotubes. The opening-ring through the application of both solubilizing group and drug anchoring site were necessary to provide long side chains. Consequently, the coating molecules could present functional groups available for bioconjugation with peptides or other molecules such as amines, to create various functional CNT conjugates for different biological applications.

**A. Results of Noncovalent functionalization of carbon nanotubes**

The functionalization of carbon nanotubes (scheme 4.6) was done at 160ºC via the dissolution of poly-DL-succinimide in DMF, the solution wherein CTNs were dispersed. The yield was 216mg. The product was partially water soluble at pH=10. The sample was submitted to different analysis to investigate the quality of f-CNTs.

The TEM analysis recorded in Figure 4.26 showed that CNTs were covered with poly D.L. succinimide to make f-CNTs with outer diameter of $d_o$= 60nm and inner diameter of $d_{in}$= 40nm.

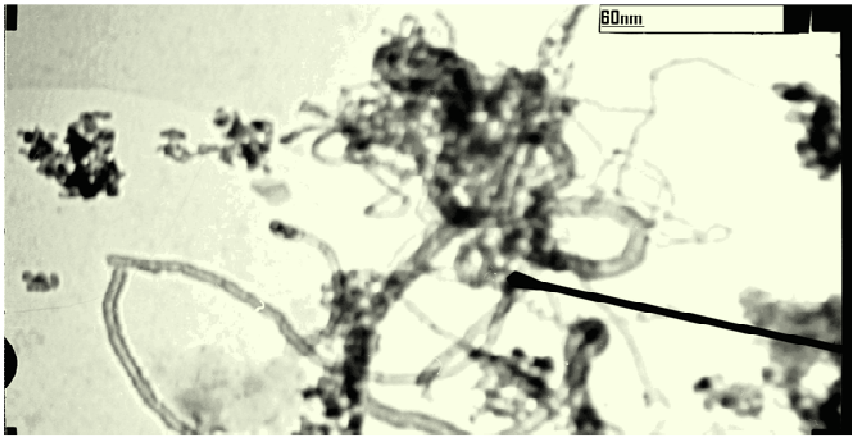


**Figure 4.27: f-CNTs (Polysuccinimide) microscopic image**

Three peaks were shown in the $^{1}H$ NMR Spectra 30 which corresponds to f-CNTs (Polysuccinimide), and the chemical shifts (δ/ppm) related to those peaks were analysed as follow:

A: (3.030-2.650) confirmed the expected group band –CO-$CH_2$- with 2H expected.

B: (4.5-4.45) confirmed the expected group band CH-N with 0.82 H calculated while 1H was expected.

C: 7.940, showed H in aromatic region.

Different characteristic peaks were shown in the infrared (IR) analysis as presented in Figure 4.27.

a) The characteristic absorption peaks appear at 2941.63 $cm^{-1}$, due to C-H vibration, and at 1707.82 $cm^{-1}$, due to C=O vibration of poly-DL-succinimide.
b) The characteristic peaks at 1654.53 $cm^{-1}$, due to C=C on the end cap.
c) The peaks at 1387.39 $cm^{-1}$ are due to C-N stretch.
d) The characteristic peaks `at 1211.25 $cm^{-1}$, and at 1164.00 $cm^{-1}$, due to C-C stretching vibration.
e) The peaks at 694.79 $cm^{-1}$and 633.12 $cm^{-1}$, due to C=C of carbon nanotubes with graphene structure.

**B. Discussion of results of Noncovalent functionalization of carbon nanotubes**

The dark part in Figure 4.26 related to TEM analysis confirmed the coating molecule on the carbon nanotubes surface.

The H of aromatic group of peak C shown in $^{1}H$ NMR Spectra 30 was not expected to be appeared though the number of H calculated is negligible (0.05H). It was defined in section 4.3.2.1 that the CNTs were structurally constituted of graphene (graphite-ene) and the rupture of nanotubes started to occur at the end cap which after dislocating the C-C of some hexagonal. To achieve the electronic configuration, an H should be attached to carbon (C=C) stayed in hexagonal. In addition, the nanotubes are very vulnerable at the cape more than anywhere else. The use of an ultrasonic bath to disperse f-CNTs could sometimes be the cause of a rupture of some link C-C in hexagonal on the end cap.

Definitively, the peaks A, B as illustrated in $^{1}H$ NMR Spectra 30 confirm the structure detailed in the Scheme 4.6.

The infrared (IR) in Figure 4.27 has shown all the expected peaks as the structure illustrated in Scheme 4.6.

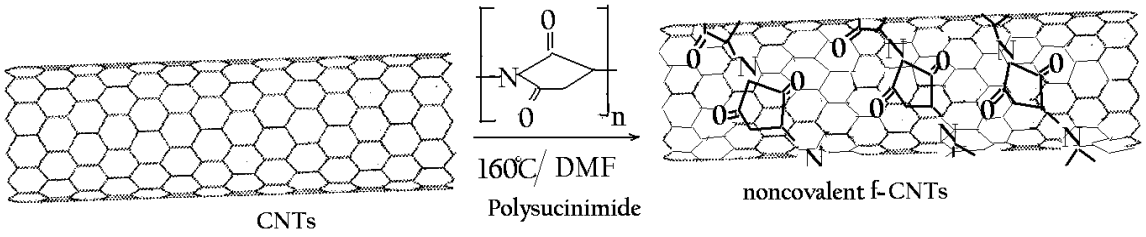


**Scheme 4.6: f-CNTs (Polysuccinimide)**

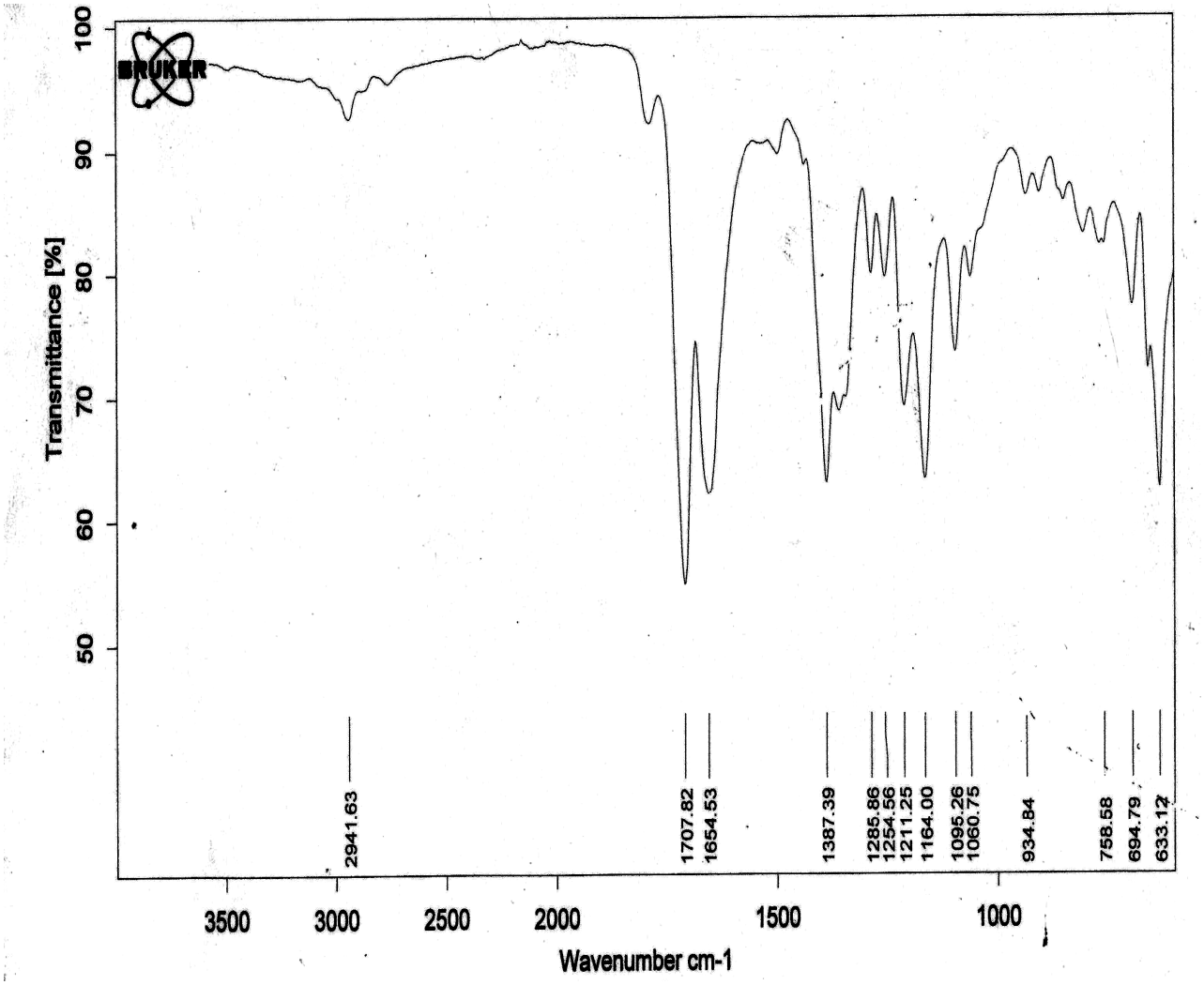


**Figure 4.28: IR f-CNTs (Polysuccinimide)**

### 4.3.3. Functionalized carbon nanotubes (f-CNTs) bound Folic acid conjugates

The carboxyl group found after developing the covalent functionalization of carbon nanotubes (Schemes 4.4 and 4.5) was attached to the amines to generate the peptide group for further use. The tertiary amine was attached through carboxyl group at a certain mol ratio to enhance the solubility of the f-CNTs. With respect to cover the total ratio to 100%., the folic acid was added to complete the electronic configuration. The choice was made on 3-dimethylamino-1-propylamine (DMP) as a strong base; this can render the amino group positively charged by carrying more cationic, and will preferentially approach surfaces of certain types of cancer cells that are negatively charged.

Since the noncovalent functionalization was developed by coating CNTs with poly-DL-succinimide (Scheme 4.6), the opening of the ring was required to enhance water-solubility and provide available site for anchoring of the drug. This was completed by the application of 3-dimethylamino-1-propylamine (DMP) as solubilizing group and 1, 3-propylenediamine (PDA) as drug anchoring site.

#### 4.3.3.1. f-CNTs ($H_2SO_4$+$HNO_3$ at 100˚C) bound folic acid conjugates

Given that the estimation of the percentage of –COOH in a quantity of f-CNTs was done by the titration, the assessment of the quantity of DMP and folic acid was rendered possible. In fact, the reversible covalent attachment was achieved by the reaction between –COOH and $NH_2$ via the coupling agent 0-benzotiazol-1-yl-tetramethylurorium hexafluorophosphate (HBTU). With the objective to raise the water solubility of f-CNTs, 30% of –COOH was evaluated to be attached to DMP as solubilizing group. Therefore the folic acid was used in excess with the objective to complete all the 70% of -COOH that did not react with DMP. The removal of excess folic acid was made possible by washing the solid obtained with tetramethylurea (TMU) dissolving free folic acid. Thus, the achievement of this reaction has led to the product with the yield of 163mg, and the chemical structure is presented in Scheme 4.7. Several tests were performed including water-solubility, TEM and $^1$H NMR analysis.

**A. Results of f-CNTs ($H_2SO_4$+$HNO_3$ at 100˚C) bound folic acid conjugates**

The water-solubility was successful at pH 6-7, while the TEM analysis of Figure 4.28 gave $d_0$=50nm and $d_{in}$=20nm and $^1$H NMR Spectra 31 confirmed the expected peaks with chemical shift shown in Scheme 4.7 as illustrated in Table 4.11.

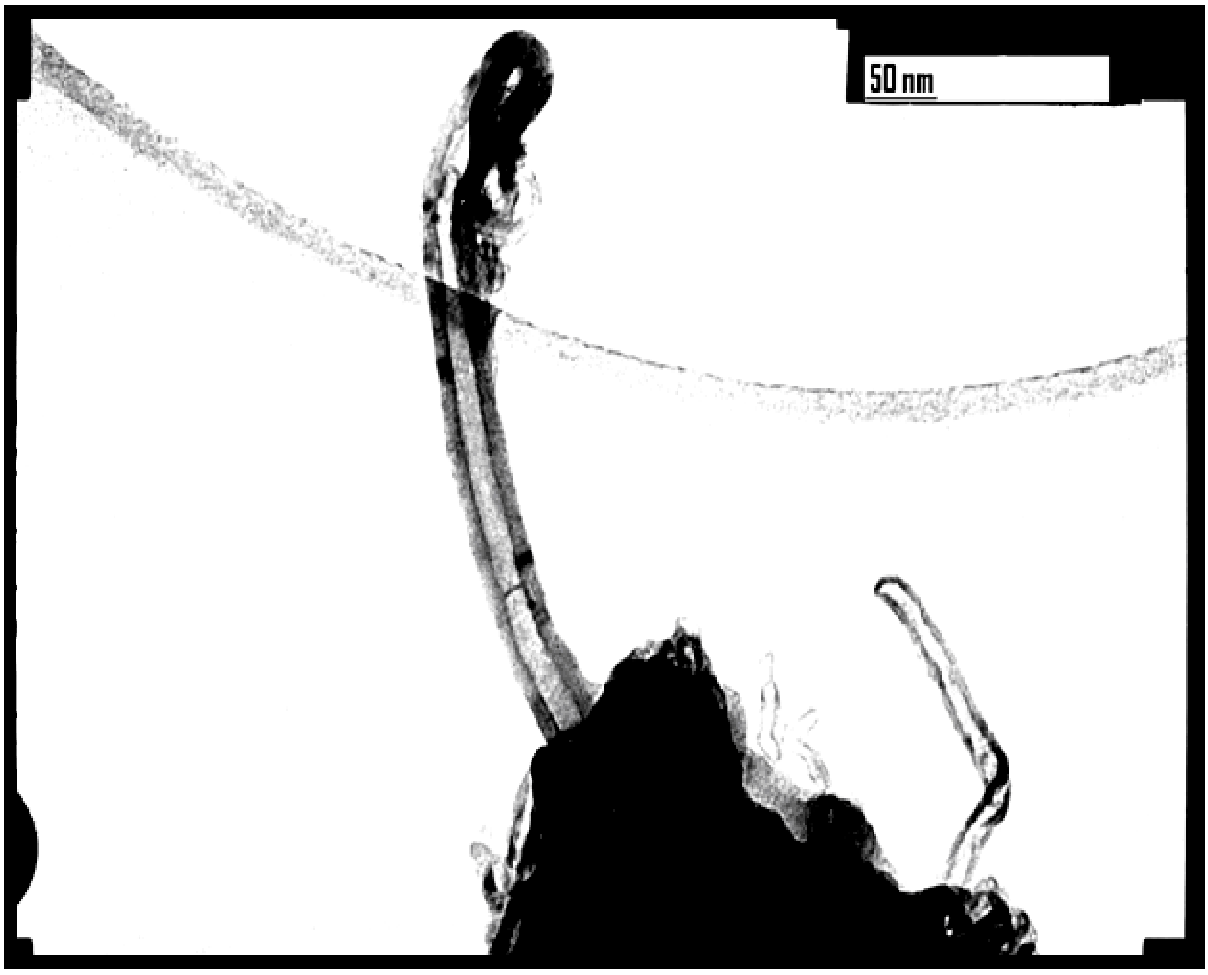


**Figure 4.29: f-CNTs ($H_2SO_4$/$HNO_3$)-FA**

**Table 4.11: HNMR spectra of *f-CNTs* ($H_2SO_4$/$HNO_3$)-FA**

| Chemical Shift δ/ppm | $^1$H NMR peacks identification | Assignment |
|---|---|---|
| 8.60-6.75 | G, F, E | **CH** Aromatic |
| 4.85 -4.28 | C | **CH** Asp, **CH** Folic acid and **$CH_2$**OH |
| 3.25-2.75 | D | -CONH**$CH_2$**, NH**$CH_2$**, -**$CH_2$**NH |
| 2.25-1.8 | B | -**$CH_2$**COOH, **$CH_2$**CONH, NH**$(CH_3)_2$** |
| 1.8-1.7 | A | COOH$CH_2$**$CH_2$**CH, $CH_2$**$CH_2$**$CH_2$ |

**B. Discussion of results of f-CNTs ($H_2SO_4$+$HNO_3$ at 100˚C) bound folic acid conjugates**

The coupling obtained after conjugation of folic acid to f-CNTs (Scheme 4.7) has completed the nanotubes shape as shown in Figure 4.28. The micrograph image showed the dark color at the end cap of the nanotubes; this is due to the attachment through the amide formation of the covalent reversible attachment of the f-CNTs with the drug. With the size of 50nm as outer diameter and 20nm as inner diameter the conjugate can be easily tracked into the cytoplasm and the nucleus.

With regard to the $^{1}H$ NMR Spectra (31), the fraction of incorporation of folic acid was calculated by using the integration of A that is 1 and the sum of integration of aromatic group E, F and G which is 1.64. With 30% of DMP and 70% of folic acid, the mol ratio was 3/7 and the number of H expected was 20H for A and 35H for the sum of E, F, and G as it is shown in the structure (Scheme 4.7). Referring to A as 20H calculated with integration 1, the sum of E, F and G with integration of 1.64 gave 32.8H calculated which corresponded to 94% incorporation.

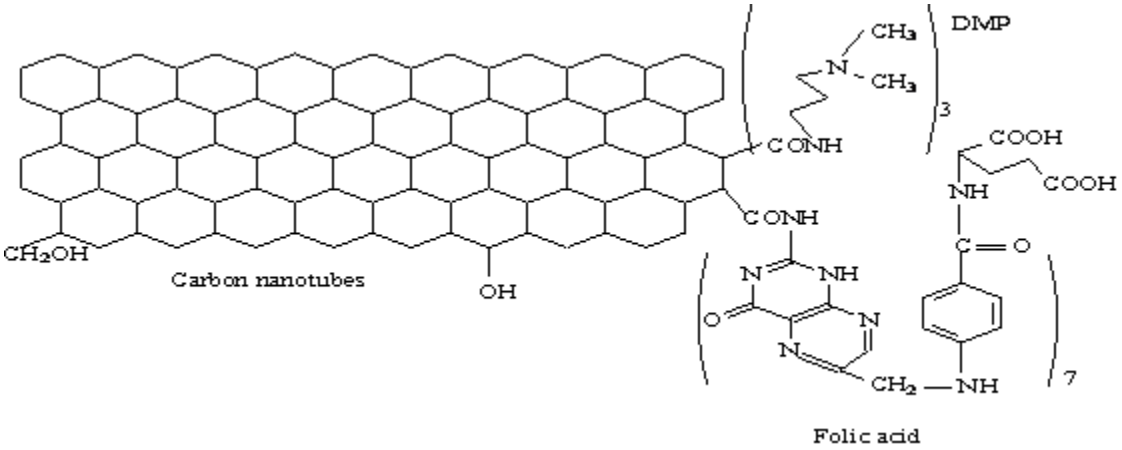


**Scheme 4.7: f-CNTs ($H_2SO_4/HNO_3$)-DMP (30)-FA (70) Structure**

#### 4.3.3.2. f-CNTs (Aspartic acid) bound folic acid conjugates

In this case, the estimation of the percentage of –COOH in a quantity of f-CNTs was also evaluated by the titration; and it was possible to assess the necessary quantity of DMP and folic acid. In fact, the reversible covalent attachment was achieved by the reaction between –COOH and $NH_2$ via the coupling agent 2-(1H-benzotriazol-1-yl)-1,1,3,3-tetramethyluronium fluorophosphates (HBTU). With the objective to raise the water solubility of f-CNTs, 40% of –COOH was evaluated to be attached to DMP as solubilizing group. Thus, the fraction of solubilising group was bigger than that attached in section 4.3.3.1, because the previous f-CNTs were more soluble than the later f-CNTs when both considered in their initial condition. Therefore the folic acid was used in excess with the objective to complete all the 60% of -COOH that did not react with DMP. The removal of excess of folic acid was made possible by washing the solid obtained with tetramethylurea (TMU) which could dissolve all free folic acid in the solution.

**A. Results of f-CNTs (Aspartic acid) bound folic acid conjugates**

This reaction gave a product with the yield of 231mg, and the chemical structure is presented in Scheme 4.8. Several tests were performed including water-solubility, TEM and $^{1}$H NMR analysis. The water-solubility was successful at pH 6-7.

After TEM analysis, the average diameter of nanotubes in Figure 4.29 was evaluated to 170nm.

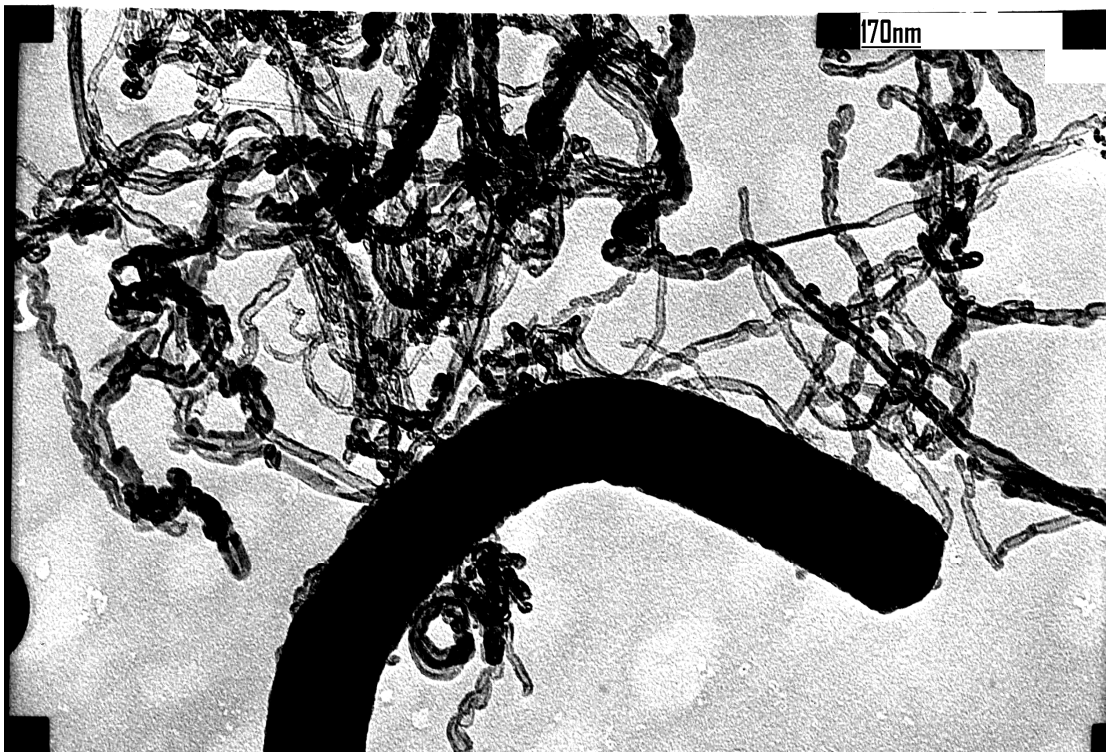


**Figure 4.30: f-CNTS (Aspartic acid)-DMP (40)-FA (60) microscopic image**

The $^{1}$H NMR Spectra (32) showed all expected chemical bands as illustrated in Table 4.12. Thus, this confirms that the reversible attachment between f-CNTs with DMP and folic acid was possible via the formation of amide group. To calculate the fraction incorporation of folic acid, the integration of peak A evaluated to 1 was chosen as reference and corresponded to 4H as expected, and the integration of aromatic peaks (E, F, G) evaluated to 3.8 was calculated 15.2H while the expected was 15H as shown in Scheme 4.8, and then the fraction incorporation of folic acid was 101.3%. The error was 1.3%.

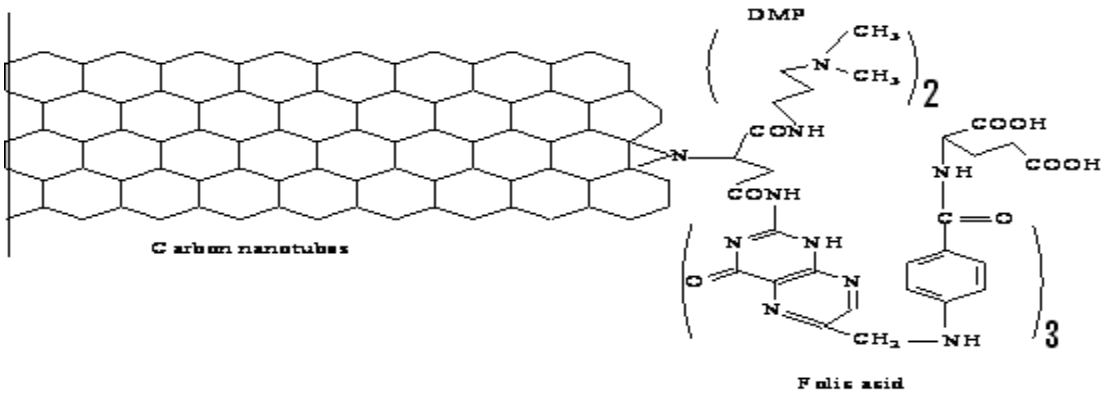


**Scheme 4.8: f-CNTs (Aspartic acid)-DMP (40)-FA (60) Structure**

**Table 4.12: HNMR data f-CNTs (aspartic acid)-DMP (40)-FA (60)**

| Chemical Shift δ/ppm | $^1$HNMR peaks identification | Assignment |
|---|---|---|
| 8.7-6.8 | G, F, E | **CH** Aromatic |
| 4.7-4.25 | D | **CH** Asp, **CH** Folic acid |
| 3.2-2.9 | C | -CONH**$CH_2$**, NH**$CH_2$**, **$CH_2$**NH**$(CH_3)_2$** |
| 2.3-1.8 | B | -**$CH_2$**COOH, **$CH_2$**CONH, COOH$CH_2$**$CH_2$**CH |
| 1.8-1.7 | A | $CH_2$**$CH_2$**$CH_2$ |

**B. Discussion of results of f-CNTs (Aspartic acid) bound folic acid conjugates**

With small size of 170nm, the f-CNTs-drug conjugate, being biocompatible, can easily penetrate the cells until the delocalisation of cancerous cells for the release of the drug to the target. The f-CNTs-drug conjugate from aspartic acid (Fig. 4.29) showed the dark spot spread along the nanotubes while Figure 4.28 related to the f-CNTs of conjugate made from $H_2SO_4/HNO_3$ at 100˚C has shown more dark spot at the end cap comparatively. Since in section 4.3.2.1 the incorporation of COOH (17.1%) in f-CNTs with $H_2SO_4/HNO_3$ at 100˚C (Table 4.10) was lesser than the one (20%) in f-CNTs with aspartic acid, more quantity of DMP and folic acid will be needed in total to cover all the carboxyl group, and this can result to a structure with nanotube more dark.

**4.3.3.3. f-CNTs (Poly-DL- succinimide) bound folic acid conjugates**

The f-CNTs for this case was obtained by coating the MWCNTs with the polymer poly-DL-succinimide whose opening of the ring required the attachment of DMP and PDA in a certain proportion. The attachment of both DMP as solubilising group and PDA drug anchoring site led to the formation peptide groups able to reinforce the antibody. The challenge was to evaluate the quantity of polymer coated to the MWCNTs for functionalization, accordingly to determine the quantity of DMP and PDA. In order to ensure more space for the anchoring drug the mol ratio was 40% for solubilising group (DMP) and 60% for drug anchoring site (PDA). The reaction was running at below room temperature while PDA was added in excess and drop-wise. This could prevent the crosslinking capable to occur during the reaction. After elimination of excess of PDA by washing with hot toluene and then hot acetone, folic acid was added in excess relative to the quantity of PDA.

**A. Results of f-CNTs (Poly-DL- succinimide) bound folic acid conjugates**

After the collection of a product with a yield of 35mg, different tests were performed including water-solubility, TEM and $^1H$ NMR analysis. The water-solubility was successful at pH 6-7.while the TEM analysis gave Figure 4.30 with outer diameter ($d_o$) of 80nm and inner diameter ($d_i$) 40nm, and $^1H$ NMR Spectra 33.

After TEM analysis, the evaluation of micrograph image (Figure 4.30) confirmed the nanotubes structure of 80nm as outer diameter and 40nm as inner diameter, with the presence of lines in transversal of nanotubes.

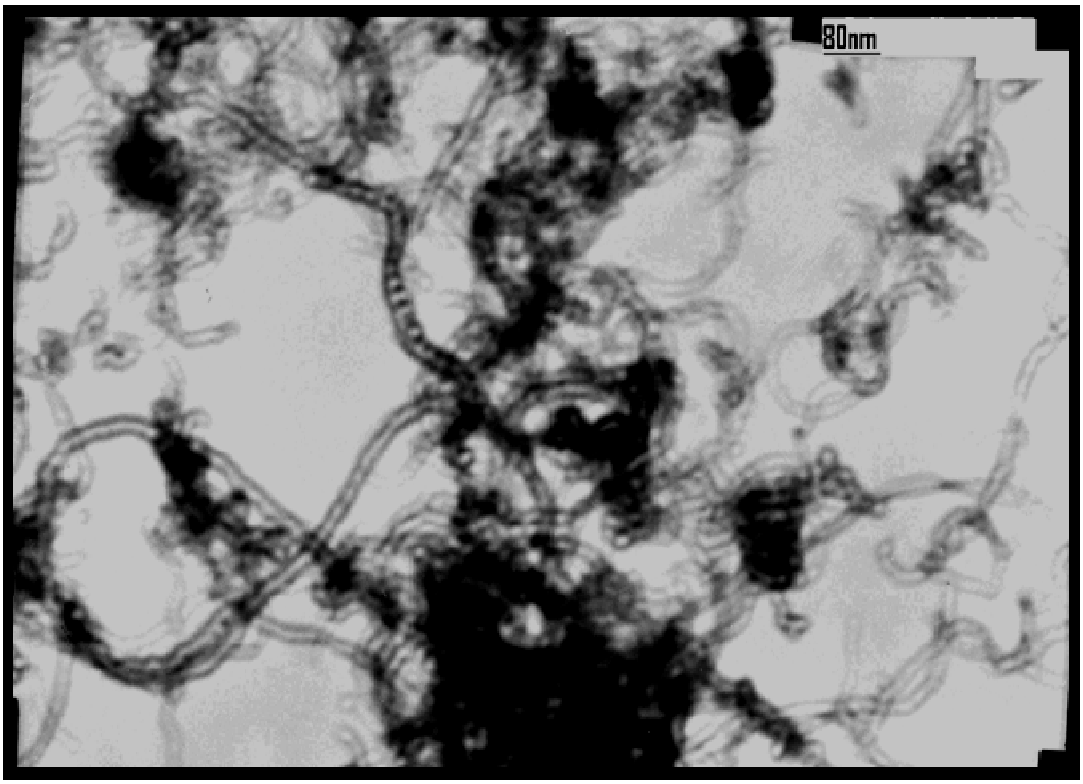


**Figure 4.31: f-CNTs (PSI)-DMP (40)-PDA (60)-FA microscopic image**

The $^{1}$H NMR Spectra (33) showed different peaks as follows:

A: - $CH_2$-**$CH_2$**-$CH_2$; B: **$CH_2$**-N **$(CH_3)_2$**; $NH_2$**$CH_2$**; CONH**$CH_2$**; C: **$CH_2$**CONH; D: CO**CH**NH and E, F, G: **H** aromatic.

To calculate the fraction incorporation of folic acid, the integration of pick A evaluated to 1 was chosen as reference and corresponded to 10H as expected, and the integration of aromatic peaks (E, F, G) evaluated to 1.58 was calculated 15.8H while 15H was expected according to the Scheme 4.10. This has resulted to the fraction incorporation of folic acid of 105.3% with the error of 5.8%.

**B. Discussion of results of f-CNTs (Poly-DL- succinimide) bound folic acid conjugates**

The presence of lines in transversal of nanotubes has shown that MWCNTs have been coated with polymer bound folic acid (drug). This confirms the theoretical structure that was previously illustrated in Figure 2.1. When taking in to account both the average weight of polymer which can prevent the layer of the drug in the kidney, and the small size of nanotubes which can facilitate the translocation of the drug in the cell, the synthetic polymer bound folic acid (methotrexate) coating the CNTs are more beneficial in therapy to improve the condition of drug uptake in the cells. All chemical bands shown in Scheme 4.9 were illustrated in the $^{1}H$ NMR Spectra (33).

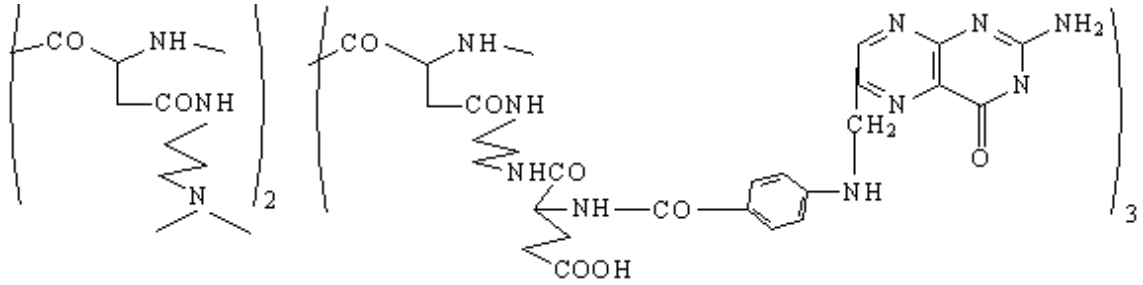


**Scheme 4.9: f-CNT (PSI-DMP (40)-PDA (60))-FA structure**

# CHAPITER 5

# CONCLUSION AND RECOMMENDATIONS

## 5.1 Conclusion

The current research was undertaken to investigate the formation of biofissionable amide in polymer and carbon nanotubes bound folic acid and methotrexate. Considering the structural approach of MTX (Schemes 1.1) as compared to folic acid (Schemes 1.2) which is very expensive, folic acid was used as drug and the results were comparable to MTX drug. In order to prove the formation of bioreversible bond (CONH) between the polymer and the drug, the kinetics study was found necessary. This was achieved since the incorporation of folic acid in polymeric carrier evolved the time of reaction.

The polymer has been chosen as drug carrier due to its molecular weight capable of preventing high concentration of drug in the kidney. Carbon nanotubes, taking advantage of its small size capable of penetrating the cell membrane, has also been utilized as drug carrier to reach the target. Especially when the carbon nanotube is covered on the surface by a polymer bound to the drug, more advantage can be held up relating to the small size and molecular weight. Therefore, the primary objective of this research was the use of carbon nanotubes as drug carrier as compared to polymeric drug carrier.

The completion of this research was possible through the functionalization of both polymeric and carbon nanotubes carriers in respect of certain requirements, capable of rendering the drug conjugates bioactive through covalent attachment.

To realize the total functionalization, X% of Polyaspartamide was covered with 3-dimethylamino-1-propylamide (DMP) and Y% as outstanding available site was covered with 1,3 diaminopropane (PDA). This was done by varying the mol ratio X/Y (19/1, 9/1, 17/3 and 4/1) which led to 94%, 98%, 102% and 101% incorporation of PDA

in the polymer respectively after NMR analysis. In addition, a variety of polymers were chosen to be conjugated to folic acid. This was made possible by using an ester, 2-(1H-benzotrial-1-yl)-1,1,3,3-tetramethylurium hexafluorophosphate (HBTU), as coupling agent. The challenge is that the long chain can be subjected to cleavage during the reaction. The kinetic study was found necessary to optimize the time of reaction for a minimum cleavage with a maximum incorporation of folic acid giving an optimum yield. Thus, the time of reaction was set within the range of 120 to 130 minutes. In this time, the incorporation of folic acid varyied between 90% and 104% for a yield within the range of 80 to 85%.

The carbon nanotubes, due to its small size, were also used as drug carrier to the target. Two methods have been developed to functionalize the carbon nanotubes, and these included covalent and noncovalent functionalization. The covalent functionalization was developed on the surface of CNT the carboxyl group that was able to react through HBTU as coupling agent with the amines of DMP in one part and folic acid in other part. The formation of CONH as bioreversible bond between the f-CNTs and folic acid has been investigated by the use of $^{1}$H NMR and IR analysis. This was successful, especially when after the enhancement of water solubility the nanotube shape of the structure has been conserved within the diameter range of 50nm to 170nm after TEM investigation. Particular attention was to f-CNT prepared with CNT dispersed in the mixture of sulphuric acid and nitric acid at variable temperatures. The phenol (OH) and carboxyl (COOH) groups were attached on the surface of CNT making the rate COOH/OH to decrease with increasing temperature. Hence, the f-CNT covered on the surface with OH and COOH was more water soluble than the f-CNT covered with COOH.

In order to achieve the noncovalent functionalization, the polysuccinimide was added to the carbon nanotubes and thereafter DMP as solubilising group and PDA as drug anchoring site were both used for the polymer ring-opening. The f-CNT obtained was subjected to $^{1}$H NMR, IR and TEM analysis. After analysis, selected f-CNTs were bound to folic acid through HBTU. This led to the folic acid carrier conjugation with formation of CONH as biofissionable bond investigated after $^{1}$H NMR analysis. The TEM result

has illustrated the conservation of nanostructure with the diameter of 80nm. The f-CNTs functionalized with polymer can be more beneficial as drug carrier due to the small size and the high average molecular weight.

## 5.2 Recommendation

There are many recommendations which can be made both to improve the current work and to extend it somewhat further into new areas of research.

### 5.2.1. Recommendation for the current work

These recommendations are necessary for the improvement of this work:

- The polymer carrier has to be water soluble at pH within the range 6 and 7.
- In order to provide a maximum incorporation of folic acid, the polymeric carrier has to be conserved in the anhydrous desiccators.
- The required quantity of HBTU as coupling agent must be in the ratio of 1:1.1 (carrier:HTBU) because a large quantity can cause more cleavage of polymer.
- The sonication was useful for the dispersion of carbon nanotubes in the solvent, but it must be observed in a short time, approximately 15 minutes to prevent the carbon nanotubes from being brittle.
- To prevent destruction of nanotubes, the functionalization of carbon nanotubes using the mixture of sulphuric acid and nitric acid must not go beyond 4 hours when working at 100°C.

### 5.2.2. Recommendation for further work

This was not sufficient to conclude that the prodrugs obtained using polymer or carbon nanotubes as carriers, could easily penetrate the cell membrane and release the drug to the target because no biomedical evaluation has been done. Therefore it is recommended that future work be focused on investigating the cytotoxic performance of carbon nanotubes carrier drug conjugates.

The phenol group and carboxyl group generated on the surface of f-CNTs made with the mixture of sulphuric acid and nitric acid can be a subject of selection of drugs due to their different electronegativities. Hence the application of different drugs for a good selection is recommended for future work.

**REFERENCES**

(1). Shaw, G.M.; Schaffer; D.; Velie, E.M.; Morland, K.; Harris, J.A. (1995). Periconceptional vitamin use, dietary folate, and the occurrence of neutral tube defects. *Epidemiology*, **6**: 219-26.

(2). Zittoun, J. (1993). Anemias due to disorder of folate, vitamin B12 and transcobalamin metabolism. *La Revue du praticien*, **43** (11): 1358-63.

(3). Smith, C.; Lieberman, M.; Marks, D.B.; Marks, A.D. (2007). *Marks' essential medical biochemistry*. Hagerstown, MD: Lippincott Williams & Wilkins. *Clinical:Malaria*, 1-7

(4). Jennings E. (1995). Folic acid as a cancer-preventing agent. *Med Hypotheses*, **45** (3): 297-303.

(5). Johnston, A.; Gudjonsson, J.E.; Sigmundsdottir, H.; Ludviksson, B.R.; Valdimarsson, H. (2005). The anti-inflammatory action of methotrexate is not mediated by lymphocyte apoptosis, but by the suppression of activation and adhesion molecules. *Clin Immunol*, **114** (2): 154-163.

(6). Ma, Z.; and Taylor, J.S. (2001). Nucleic acid triggered catalytic drug and probe release: A new concept for the design of chemotherapeutic and diagnostic agents. *Bioorganic & Medicinal Chemistry*, **9**: 2501-2510.

(7) Chu, B.C.F.; Whiteley, J.M. (1977). High molecular weight derivatives of methotrexate as chemotherapeutic agents. *Mol. Pharmacol*, **13**: 80-88

(8) Ringsdorf, H.J.; et. al. (1975). In Site-specific drug delivery. *Polym. Sci Polym. Sym*, **51**: 135.

(9) Maeda, H. (1989). Tumoritropic and lymphotropic principles of macromolecular drugs. *Crit. Revs. Therapeut. Drug Carrier Systems*, **6**: 193.

(10) Christie, R.J. ; Grainger, D.W. (2003). Design strategies to improve soluble macromolecular delivery constructs. *Adv. Drug Delivery Revs*, **55**: 421-437.

(11) Allen, T.M.; Cullis, P.R. (2004) Drug delivery systems; entering the mainstream. *Science*, **303**: 1818-1822.

(12) Kostarelos, K. (2003). Rational design and engineering of delivery systems for therapeutics: biomedical exercises in colloid and surface science. *Adv Colloid Interface Sci*; **106**: 147-168.

(13)Pouton, C.W. ; Seymour, L.W. **(**2000). Key issues in non-viral gene delivery, *Adv. Drug. Deliv. Rev*, **46**: 187-203.

(14) Pantarotto, D.; Briand, J.P.; Prato, M.; Bianco, A. (2004). *Translocation of bioactive peptides across cell membranes by carbon nanotubes. Chem Commun (Camb)*, 16-17.

(15) Shi; Kam, N.W.; Jessop, T.C.; Wender, P.A.; Dai, H. (2004). Nanotube Molecular transporters: internalization of carbon nanotubes-protein conjugates into mammalian cells. *J Am Chem Soc*, **126**: 6850-6851.

(16) Ferrari, M. (2005). Cancer nanotechnology: opportunities and challenges. *Nat Rev Cancer*, **5**: 161-171.

(17) Wu, W.; Wieckowski, S.; Klumpp, C.; Benincasa, M.; Briand, J.P.; Gennaro, R.; Prato, M.; Bianco, A. (2005). Targeted delivery of amphotericin B to clls using functionalized carbon nanotubes. *Angew Chem Int Ed Engl; in press, doi:* **10:** 1002/*anie. 200501613*.

(18) World Health Organisation (WHO). Fact sheet No 297, February 2009.

(19) Health 24-Cancer facts and figures (2001); Type of Cancer prevalent in South Africa.

(20) Louie, J.K.; Hsu, L.C.; Osmond, D.H.; Katz, M.H.; Schwarcz, S.K. **(**2002). Trends in causes of death. *J Infect Dis*., **186**: 1023-1027.

(21) Grisham, C.M.; Reginald, H.G. (1999). Enzyme. *Biochemistry*. *Philadelphia: Saunders College Pub*, 426–427

(22) Koshland D. E. (1958). Application of a Theory of Enzyme Specificity to Protein Synthesis. *Proc. Natl. Acad. Sci.* **44** (2): 98–104.

(23) Chabner, B. A. (1982). Methotrexate. *In Pharmacologic Principles of Cancer Treatment. B. A. Chabner, editor. W. B. Saunders Co., Philadelphia*, 229-255.

(24) Foye, W.D. (1995*). In cancer Chemotherapeutic Agents*. Ed., Am. Chem. Soc., Washington, DC, 9-45.

(25) Embleton, M.J.; and Garnett, M.C. (1985). *In Monoclonal antibodies for cancer detection and therapy* (R.W. Baldwin, and V.S. Byers, Eds.). Academic Press, London, 317-344.

(26) Diamond, L.K.; Mercer, R.D.; et al. (1948). Temporary remission in acute leukaemia in children produced by folic acid antagonists. *N. Engl. J Med*, **238**: 787-793.

(27) Ward, J.R. (1985). Historical perspective on the use of methotrexate for the treatment of rheumatoid arthritis.*J. Rheumatol*, **12**: 3-6

(28) Kremer, J.M. (1996). Historical overview of the treatment of rheumatoid arthritis with emphasis on methotrexate. *J. Rheumatol*, **44**: 34-37.

(29) Moss, R.B. (1995). Alternative pharmacotherapies for steroid-dependent asthma. *Chest,* **107**: 817-825.

(30) Leeman, L.M.; Wendland, C.L. (2000). Cervical ectopic pregnancy. *Arch. Fam. Med*, **9**: 72-77.

(31) Mathews, D.A.; Alden, R.A.; Bolin, J.T.; Freer, S.T; et al. (1977). In Molecular basis of differential resistance to cycloguanil and pyrimethamine in Plasmodium falciparum malaria. *Science,* **197**: 452-455.

(32) Reynolds, J.E.F.; Parfitt, K.; Parsons, A.V.; Sweetman, S.C. (1996). The protective role of folic acid and vitamin E against toxic. *The royal pharmaceutical Society*, **19**: 1361-1362.

(33) Lewisohn, R.; Leuchtenberger, C.; Leuchtenberger, R.; and Keresztezy, J.C. (1946). The influence of Liver L. casei factor on spontaneous Breast.. *Science,* **104**: 436-437.

(34) Butterworth, C.E. Jr.(1992). Effect of folate on cervical cancer. Synergism among risk factors. *Ann NY Acad Sci*, **669**: 293-299.

(35) Anderson, R.G.W.; Kamen, B.A.; Rothberg, K.G. (1992). Caveolin, a protein component of caveolac membrane coats. *Science,* **255**: 410-411.

(36) Ross, J.F.; Chaudhuri, P.K.; Ratnam, M. (1994). Differential regulation of folate receptor. *Cancer,* **73**: 2432-2443.

(37) Donaldson, K.; Stone, V.; Tran, C.L.; Kreyling, W. and Borm, P.J. (2004). Nanotoxicology, Occup. *Environ. Med*, **61**: 727-728.

(38) Donaldson, K.; Stone, V.; Tran, C.L.; Kreyling, W. and Borm, P.J. (2004). Nanotoxicology, Occup. *Environ. Med*, **61**: 727-728.

(39) Georgakilas, V.; Tagmatarchis, N.; Pantarotto, D.; Bianco, A.; Briand, J.P.; Prato, M. (2002). Amino acid functionalization of water soluble carbon nanotubes. *Chem Commun*, **24**: 3050-3051.

(40) Pantaroto, D.; Briand, J.P.; Prato, M.; Alberto, B. (2004). Translocation of bioactive peptides across cell membranes by carbon nanotubes. *Chem commun*, **1**:16-17.

(41) Pantarotto, D.; Partidos, C.D.; Graff, R.; Hoebeke, J.; Briad, J.P.; Prato, M.; et al. (2003). Synthesis, structural characterisation, an immunological properties of carbon nanotubes functionalized with peptides. *J AM Chem Soc*, **125** (20): 6160-4.

(42) Lu, G.; Moore, J.M.; Huang, G.; Mount, A.S.; Rao, A.M.; Larcom, L.L.; et al. (2004) RNA polymer translocation with single-walled carbon nanotubes. *Nano Lett*, **4**(12): 2473-2477.

(43) Dumitriu, S.; and Dumitriu, M. (1994). Polymeric drug carrier. *In Polymeric Biomaterials.* (S. Dumitriu, Ed.) marcel Dekker, New York, 435-724.

(44) Dunn, L.; and Ottenbrite, R. M.; Eds (1991). *In Polymeric drug and Drug Delivery Systems*. ACS Symp.: Ser. **469**: 3-10.

(45) Takakura, Y.; and Hashida, M. (1995). Drug targeting: Organ-specific strategies. *Crit. Rev. Oncol. Hematol*, **18**: 207-231.

(46) Ouchi, T.; and Ohya, Y. (1995). Macromolecular prodrugs. Prog. Polym. *Sci*, **20**: 211-257.

(47) Gabisson, A.; In: Roerdink, F.H.D.; and A.M.; Eds. (1989). Drug carrier systems. *John Wiley, New York*, **9**: 185-212.

(48) Brannon Peppas, L.; Int. J. (1995). Recent advances on the use of biodegradable. *Pharm*, **116**: 1-9.

(49) Kerr, D.J.; and kaye, S.B. (1991). Chemoembolism in cancer chemotherapy. *CRC Crit. Rev. Ther. Drug Carrier Sys.* **8**: 19-39.

(50) Yang, M.B.; Tamargo, R.J.; and Brem, H. (1989). Controlled delivery of 1,3-bis (2-choroethyl)-1-nitrosourea. *Cancer Res*, **49**: 5103-5107.

(51) Springer, C.J.; Bagshawe, K.D.; Sharma, S.K.; Searle, F.; Sherwood, R.F.; and Melton, R.G. (1991). Ablation of human choriocarcinoma xenografts in nude mice. *Eur. J. Cancer*, **27**: 1361-1366.

(52) Harris, J.M.J. (1985). Laboratory Synthesis of Polyethylene Glycol Derivatives. *In Macromol*. Sci. Rev. Macromol. Chem. Phys., **25**: 325-373.

(53) Davidson, R.L.; O'Malley, K.A.; and Wheeler, T.B. (1976). Polyethylene glycol-induced mammalian cell hybridization: Effect of polyethylene glycol molecular weight and concentration. *Somatic Cell Genetics*, **2**: 271-280.

(54) Peppas, L.B. (1997). *Polymer in Controlled Drug Delivery*. Medical Plastics and Biolmaterials Magazine, **215**: 191-201.

(55) Abuchowski, A.; Van Es, T.; Plozuk, N.C.; and Davis, F.F. (1977). Alteration of immunological properties of bovine serum albumin by covalent attachment of polyethylene glycol. *J. Biol. Chem*, **252**: 3578-3581.

(56) Lee, R.J.; and Low, P.S. (1994). Delivery of liposomes to cultured KB cells via folate receptor mediated endocytosis. *J. Biol. Chem*, **269** (5): 3198-3204.

(57) Hirano, T.; Klesse, W.; Ringsdorf, H. (1979). Polymeric derivatives of activated. Cyclophosphamide as drug delivery systems in anti-tumor chemotherapy. *Makromol. Chem*, **180**: 1125-1131.

(58) Ohaya, Y.; Nakao, T.; Ouchi, T.; et al. (2003). Preparation and characterization of Polypseudorotaxanes Based on Biodegradable Poly(L-lactide)/Poly(ethyleneglycol) Triblock Copolymers. *Macromol,* **36**(25) :9313-9318.

(59) Katayose, S.; Kataoka, K. (1998). Polyion Complex Micells with reaction Aldehyde Groups. *J. Pharm. Sci*, **97**: 160-163.

(60) Rejmanovà, P.; Kopecek, J.; Duncan, R.; Lloyd, J.B. (1985). Stability in rat plasma and serum. *Biomaterial*, **6**: 45-48.

(61) Kopecek, J. (1984). Controlled biodegradability of polymers-a key to drug delivery systems. *Biomaterials*, **5**:19-25.

(62) Krinick, N.L.; Rihova, B.; Ulbrich, K.; Strohalm, J.; Kopecek, J. (1990). Targetable photoactivatable drugs.2. *Makromol. Chem*, **191**: 839-856.

(63) McCormick, L.A.; Seymour, L.C.W.; Duncan, R.; Kopecek, J. (1986). Polymer conjugates as anticancer nanomedecines. *J. Biaact. Comp. Polym*. **1**: 467-497.

(64) Ohkawa, K.; Hatano, T.; Tsukada, Y.; Matsuda, M. (1993). In Chemotherapeutic efficacy. *Br. J. Cancer*, **67**: 274-278.

(65) Song, Y.; Onishi, H.; Nagai, T. (1993). Pharmacokinetic characteristics and antitumor. *Biol. Pharm*. Bull, **16**: 48-54.

(66) Sezaki, H., and Hashida, M. (1984). Macromolecular-drug conjugates in targeted cancer chemotherapy. *CRC Crit. Rev.Ther. Drug Carrier Syst*, **1**: 1-38.

(67) Goddard, P.; Petrak, K. (1989). Biodegradation of drug-modified polymers in drug delivery-a critical analysis. *J. Bioaact. Compat. Polym*. **4**: 372-402.

(68) Thomas, H. (1992). New horizons in cancer therapy. *Drugs of today*. **28**: 311-331.

(69) Dept of Chemistry, Wright-Rieman Laboratories, Rutgers University, Piscataway, NJ 08854-8087, ETATS-UNIS.

(70) Ringsdorf, H. (1975). Structure and properties of pharmacologically active polymers. *J. Polym.Sci. Polym. Symp*, **51**: 135-153.

(71) Neri, P.; Antoni, G.; Benvenuti, F.; Cocola, F.; Gazzei, G. (1973). Synthesis of α,β-poly[(2-hydroxyethyl)-DL-aspartamide], a new plasma expander. *Journal of Medicinal Chemistry*, **16**(8): 893-897.

(72) Kàlal, J.; Drobnik, J.; Kopecek, J.; Exner, J. (1978) Water soluble polymers for medicine. *British Polymer Journal*, **10** (2): 111-114.

(73) Neri, P.; Antoni, G. (1982). *α,β*-poly(2-Hydroxyethyl)-DL-aspartamide. *Macromolecular Syntheses*, **8**: 25–28.

(74) Machado, Mdel; Neuse, E.W.; Perlwitz, A.G. (1992). Water-soluble polyamides as potential drug carriers, V. Caboxy-functionalized polyaspartamides and copolyaspartamides. *Angewandte Makromolekulare Chemie*, **195**(1): 35-56.

(75) Neuse, E.W. (2008). Synthetic Polymers as Drug-Delivery Vehicles in Medicine. *Met. Based Drugs*,1-19

(76) Caldwell, G.; Neuse, E.W.; Perwitz, A.G. (1997). Water soluble polyamides as potential drug carriers. IX. Polyaspartamides grafted with amine-terminated poly(ethylene oxide) chains. *Journal of Applied Polymer Science,* **66**(5): 911-919.

(77) Pytela, J.; Saudek, V.; Drobnik, J.; Rypacek, F. (1989). Poly(N5-hydroxyalkylglutamines). IV. Enzymatic degradation of n5-(2-hydroxyethyl)-L-glutamine homopolymers and copolymers. *Journal of Controlled release*; **10**(1): 17-25.

(78) Danusso, F.; Ferruti, P. (1970). Synthesis of tertiary amino polymers. *Polymer,* **11**: 88-113.

(79) Ferruti, P.; Marchisio, M.A.; Barbucci, R. (1985). Synthesis and physicochemical charaterization of a hydrophilic. *Polymer*, **26**: 1336-1348.

(80) Hill, I.R.C.; Garnett, M.C.; Bignotti, F.; Davis, S.S. (1999). In vivo cytotoxicity of poly(amidoamine)s: Relevance to DNA. *Biochem. Biophys. Acta,* **1427**: 161-174.

(81) Ranucci, E.; Ferruti, P.; et. al. (1994). Recent results on functional polymers and macromonomers of interest as biomaterial or for biomaterial modification. *J. Biomat. Sci. Polym*, **15**: 1235-1241.

(82) Ferruti, P.; Barbucci, R. (1984). Linear Amino Polymers-Synthesis, Protonation and Complex-Formation. *Adv. Polym. Sci*, **58**: 55-92.

(83) Ferruti, P.; Maria, A.; Marchisio; Duncan, R. (2002). Poly(amido-amine)s : Biomedical applications. *Macromol. Rapid Commun,* **23** : 332-335

(84) Cadwell, G.; Neuse, E. W. (1992). Preparation of Nanocomposite Ply(allylamine)-Poly(ethylene). *S. Afr. Chem*, **45**: 93-102.

(85) Malgesini, B.; Verpilio, L; Duncan, R.; Feruti, P. (2003). Formulation of new bioactive polymeric materials for applications in tissue engineering. *Macromol. Biosci*, **3**: 59-66.

(86) Ferruti, P.; Marchchisio, M.A.; Duncan, R. (2002). Poly(amido-amine)s carrying primary. *Macromol. Rapid commun*, **23** : 332-335.

(87) Ferruti, P.; et al. (2000). Amphoteric linear poly(amido-amine)s as endosomolytic polymers: correlation between physicochemical and biological properties. *Macromolecules,* **33** (21): 7793-7800.

(88) Kulkarni, P.N.; Blair, A.H.; and Ghose, T.I. (1981). Covalent binding of methotrexate to immunogenobulins and the effect of antibody-linked drug on tumor growth in vivo. *Cancer Res*, **41**: 2700-2706.

(89) Upeslacis, J.; Hinman, L. (1988). Annual reports in Medical Chemistry (N. Saltzman, Ed.), *Academic Press, New York*, 151-160.

(90) Garnett, M.C.; Baldwin, R.W. (1986). An improved synthesis of a methotrexate – albumin -791T/36 monoclonal antibody-conjugate cytotoxic to osteogenic sarcoma cell lines. *Cancer Res,* **46**:2407-2412.

(91) Bures, I.; Lichy, A.; Bostik, J. (1990). The use of protein as a acrrier of methotrexate for experimental cancer chemotherapy V. Alternative method of serum albumin-methotrexate derivative. *Spundova, M.;Neoplasma,* **37**: 225-231.

(92) Chakraborty, P.; Bhaduri, A.N; Das, P.K. (1990). Neoglycoproteins as carriers for receptor-mediated drug targeting in the treatment of experimental visceral Leishmaniasis. *Biochem. Biophys. Res. Commun*, **166**: 404-410.

(93) Sanzgiri, Y.; Blaton, C.D.; Gallo, J.M. (1990). Targeting tumors using magnetic drug delivery. *Pharm. Res*, **7**: 418-421.

(94) Caldwell, G.; Meirim, M.G.; Neuse, E. W. (1998). Water-soluble polymer-ferrocene conjugates based on polyamide carriers containing intrachain-type secondary amine functions as binding sites. Journal of Inorganic and Organic Polymers, **8**(4): 225-236.

(95) Meirim, M.G.; Neuse, E.W.; N'Da, D.D. (2001). Carrier-bound methotrexate I. water-soluble polyaspartamide-methotrexate conjugates with Ester links in the polymer-drug spacer. *J. Appl. Polym. Sc*, **82**: 1844-1849.

(96) Kono, K.; Liu, M.; Fréchet, J.M.J. (1999). Design of dendritic macromolecules containing folate or methotrexate residues. *Bioconjugate Chem*, **10**: 1115-1121.

(97) Okamoto, C.T. (1998). Endocytosis and transcytosis. *Adv. Drug Del. Rev*, **29**: 215-228.

(98) Okamoto, C. T. (1998). Endocytosis and transcytosis. *Adv. Drug Del. Rev;* **29**: 215-228.

(99) Wang, S.; Luo, J.; Lantrip, D.A.; Waters, D.J.; Low, P.S.; et. al. (1997). Efficient syntheses of pyrofolic acid and pteroyl azide, reagents for the production of carboxyl-differentiated derivatives of folic acid. *Bioconjugate Chem*, **8**: 673-679.

(100) Sudimack, J.; Lee, R.J. (2000). Targeted drug delivery via the folate receptor. *Adv. Drug Delivery Rev*, **41**: 147-162.

(101) Coney, L.R.; Tomasetti, A.; Carayannopoulos, L.; Frasca, V.; Kamen, B.A.; et. al. (1991). Cloning of a tumor-associated antigen. *Cancer Res*, **51:** 6125-6132.

(102) Leamon, C.P.; Parker, M.A.; Vlahov, I.R.; Xu, L.C.; Reddy, J.A.; Vetzel, M; Douglas, N. (2002). Synthesis and Biological Evaluation of EC20: A New Folate-Derived 99mTc-Based Radiopharmaceutical. *Bioconjugate Chem*, **13**: 1200-1210.

(103) Anderson, K.E., Stevenson, B.R., Rogers, J.A. (1999). In Targeted delivery of proteins by nanosized carriers. *J. Controlled Release, **60**: 189-198.*

(104) Caliceti, P.; Salmaso, S.; Semenzato, A.; Carofiglio, T.; Fornasier, R.; Fermeglia, M.; et. al. (2003). Synthesis and physicochemical characterization of folate-cyclodextrin. *Bioconjugate Chem*, **14**: 899-908.

(105) David Dago N'Da (2004). Synthesis of methotrexate and ferrocene conjugates as potential anticancer agents. *A thesis submitted to the faculty of science, Wits Univ*, 34-46.

(106) Allen, T.M. ; and Cullis, P.R. (2004). Drug delivery Systems : Entering the Mainstream. *Science Magazine 19 March 2004, 1818-1822*.

(107) Varde, N.K. ; and Pack, D.W. (2004). Microspheres for controlled-release drug delivery. *Expert Opinion in Biological Therapy,* **4**, 35-51

(108) Chen J.M.; et al. (2001). Mutational screening of the cationic trypsinogen gene in a large cohort of subjects with idiopathic chronic pancreatitis. *Mar*, **59**(3):189-93.

(109) Iijima, S. (1991). Helical microtubules of graphitic carbon. *Nature*, **354**: 56-58

(110) Chem, S; She, W.; Wu, G.; Chen, D.; and Jiang, M. (2005). A new approach to the functionalization of single-walled carbon nanotubes with both alkyl and carboxyl groups. *Chemical Physics Letters*, **402**: 312-317.

(111) Serp, P.; Corrias, M.; and Kalck, P. (2003). Carbon nanotubes and nanofibers in catalysis. *Applied Catalysis A: General*, **253**: 337-358.

(112) Iijima, S. and Ichihashi, T. (1993). Single-shell carbon nanotubes of 1-nm diameter. *Nature,* **363**: 603-605.

(113) Bethune, D.S.; Klang, C.H.; de Vries, M.S.; Gorman, G.; Savoy, R.; Vazquez J.; and Beyers, R. (1993). Cobalt-catalysed growth of carbon nanotubes with single-atomic-layer walls. *Nature,* **363**: 605-607.

(114) Iijima, S. ; Brabec, C. ; Maiti, A. ; Bernholc, J. (1996). Structural flexibility of carbon nanotubes. J. Chem, Phys, **104**(5) : 2089-2092.

(115) Colvin, V.L. (2003). The potential environmental impact of engineered nanomaterials. *Nat Biotechnol*, **21**: 1166-1170.

(116) Lin, Y.; Taylor, S.; Li, H.; Fernando, K. Qu, A.; Wang, L.; Gu, L.; Zhou B. and. Sun, Y.P (2004). Advances toward bioapplications of carbon nanotubes. *J Mater Chem*, **14**: 527-541.

(117) Bianco, A.; Kostarelos, K.; Partidos C.D.; and Prato, M. (2005). Biomedical applications of functionalized carbon nanotubes. *Chem Commun*, 571-577.

(118) Kostarelos, K.; Lacerda, L.; Partidos, C.D.; Prato, M.; and Bianco, A. (2005). Carbon nanotubes mediated delivery of peptides and genes to cells: translating nanobiotechnology to therapeutics. *J Drug Deliv Sci Technol*, **15**: 41-47.

(119) Bianco, A. (2004). Carbon nanotubes for the delivery of therapeutic molecules. *Expt opin Drug Deliv*, **1**: 57-65.

(120) Xia, W.; Wang, Y.; Bergstra, R.; Kundu, S.; and Muhler, M. (2007). Surface characterization of oxygen-functionalized multi-walled carbon nanotubes by high-resolution X-ray photoelectron spectroscopy and temperature-programmed desorption. *Applied Surface Science*, **254**: 247-250.

(121) Che, G.; Lakshmi, B.B.; Martin, C.R.; and Fisher, E.R. (1998). Chemical Vapor Deposition Based Synthesis of Carbon Nanotubes and Nanofibers. *Chem. Mater*, **10**: 260-267.

(122) IiJima, S. (1991). Helical microtubules of graphitic carbon. *Nature*, **354**: 56-58.

(123) Collins, Philip G. (2000). Nanotubes for electronics. *Scientific American*, 67-69.

(124) Statishkumar, B.C.; Govindaraj, A.; Sen, R. And Rao, C.N.R. 1998). In Organometallic precursor route to carbon nanotubes. *Chem. Phys. Lett.*, **293**: 47-52.

(125) Nikolaev, P.; Bronikowski, M.J.; Bradley, E.K.; Rohmund, F.; Colbert, D.T.; Smith, K.A.; and Smalley, R.E (1999). *Chem. Phys. Lett.*, **313**: 91-97.

(126) Guo T, Nikolaev P., Rinzler D. Tomanek D.T., Colbert D.T., Smalley R.E. (1995). Self- Assembly of Tubular Fullerenes. *J. Phys. Chem.*, **99**: 10694-10697.

(127) Guo T., Nikolaev P., Thess A., Colbert D.T., Smalley R.E. (1995). Catalytic growth of Single-Walled nanotubes by laser vaporization. *Chem. Phys. Lett.*, **243**: 49-54.

(128) Zieggler, K.J.; Gu, Z.; Peng, H.; Flor, E.L.; Hauge, R.H.; Smalley, R.E (2005). Controlled oxidative cuting of single-walled carbon nanotubes. *J. Am. Chem. Soc*. **127**: 1541-1547.

(129) Heald, C.G.R.; Wildgoose, G.G.; Compton, R.G.; Jiang, L.; Jones, T.G.J. (2004) Chemical derivatisation of multiwalled carbon nanotubes using diazonium salts. *Chem. Phys. Chem*, **5**: 1794-1799.

(130) Niyogi, S.; Hamon, M. A.; Hu, H.; Zhao, B.; Bhowmik, P.; Sen, R.; Itkis, M.E.; Haddon, R. C. (2002) Chemistry of single-walled carbon nanotubes. *Acc. Chem. Res.,* **35**: 1105-1113.

(131) Rosca, I. D.; Watari, F.; Uo, M.; Akasaka, T. (2005). Oxidation of multiwalled carbon nanotubes by nitric acid. *Carbon*, **43**: 3124-3131.

(132) Zeng, L.; Alemany, L. B.; Edwards, C. L.; Barron, A. R. (2008). Demonstration of covalent sidewall functionalization of single wall carbon nanotubes by NMR spectroscopy: Side chain length dependence on the observation of the sidewall sp3 carbons. *Nano Res.*, **1**: 72-88.

(133) Siegrist, R.L.; Urynowicz, M.A.; West, O.R.; Crimi, M.L. and Lowe, K.S. (2001) Principles and Practices of In Situ Chemical Oxidation Using Permanganate. *Journal of Environmental Engineering*, **128**(11): 1068-1079.

(134) Hiura, H.; Ebbesen, T.W.; and Tanigaki, K. (1995). Opening and purification of carbon nanotubes in high yields. *Adv. Mater*, **7**: 275-6.

(135) Zhang, N.; Xie, J.; and Vadaran, V.K. (2002) Functionalization of carbon nanotubes by potassium permanganate assisted with phase transfer catalyst Smart Mater. *Struct*, **11**: 962-5.

(136) Tshang, S.C.; Chem, Y.K.; Harris, P.J.F.; and Green, M.L.H. (1994). A simple chemical method of opening and filling carbon nanotubes. *Nature,* **372**: 159.

(137) Lago, R.M.; Tsang, S.C.; Lu, K.L.; Chem, Y.K.; and Green, M.L.H. (1995). In Fullerene-based materials as new support media in heterogeneous. *J. Chem. Soc. Chem. Commun*, 1355

(138) Liu, J.; et al. (1998). Fullerene pipes. *Science* **280**: 1253-6.

(139) Satishkumar, B.C; Govindaraj, A.; Mofokeng, J.; Subbama, G.N.; and Rao, C.N.R. (1996). Novel experiments with carbon nanotubes: opening, filling, closing and functionalizing nanotubes. *J. Phys. B: At. Mol. Opt. Phys*, **29**: 4925-34

(140) Xie, J.; Zang, N.; Guers, M.; and Varadan, V.K. (2002). Ultraviolet-curable polymers with chemically bonded carbon nanotubes for microelectromechanical system applications Smart Mater. **11**: 575-80

(141) Nguyen, G.; Delarue, F.; Burcklé, C.; Bouzhir, L.; Giller, T.; Sraer, J.D. (2002). Pivotal role of the renin/prorenin receptor in angiotensin II. *Institut National de la Santé et de la Recherche Médicale (INSERM) U489, Jun*, 1**09**(11):1417-27.

(142) Dyke, C.A.; Stewart, M.P.; Tour, J.M. (2005). Separation of single-walled carbon nanotubes on silica gel. Materials morphology and raman excitation wavelength affect data interpretation. *J. Am. Chem. Soc.***, 127:** 4497-4509.

(143) Tagmatarchis, N.; Prato, M. (2004). Functionalization of carbon nanotubes via 1,3-dipolar cycloadditions. *J. Mater. Chem.,* **14**: 437-439.

(144) Hudson, J.L.; Casavant, M.J.; Tour, J.M. (2004). Water-soluble, exfoliated, nonroping single-wall carbon nanotubes. *J. Am. Chem. Soc.*, **126**: 11158-11159.

(145) Heald, C.G.R.; Wilgoose, G.G.; Compton, R.G.; Jiang, L.; Jones, T.G.J. (2004). Chemical derivatisation of multiwalled carbon nanotubes using diazonium salt. *Chem. Phys. Chem*., **5**: 1794-1799.

(146) Liang, F.; Sadana, A.K.; Peera, A.; Chattopadhyay, J.; Gu, Z.; Hauge, R.H.; Billups, W.E. (2004). A convenient route to functionalized carbon nanotubes. *Nano Lett.*, **4**: 1257-1260.

(147) Lee, K.M.; Li, L.; Dai L. (2005). Asymmetric end-functionalization of multiwalled carbon nanotubes. *J. Am. Chem. Soc.*, **127**: 4122-4123.

(148) Chen, R. J.; Zhang, Y. G.; Wang, D. W.; Dai, H. J. 2001, Noncovalent sidewall functionalization of single-walled carbon nanotubes for protein immobilization. *J. Am. Chem. Soc*, 123: 3838-3839.

(149) Chen, J.; Liu, H. Y.; Weimer, W. A.; Halls, M. d.; Waldeck, D. H.; Walker, G. C. (2009). Noncovalent engineering of carbon nanotube surfaces by rigid, functional conjugated. *12 Mar 2009.*

(150) Chen, R. J.; Zhang, Y. G.; Wang, D. W.; Dai, H. J. (2001). Noncovalent sidewall functionalization of single-walled carbon nanotubes for protein immobilization. *J. Am. Chem. Soc.*, **123**: 3838-3839.

(151) Wu, P.; Chem, X.; Hu, N.; Tam, U. C.; Blixt, O.; Zettl, A.; Bertozzi, C. R. (2008). Biocompatible carbon nanotubes generated by functionalization with glycodendrimers. *Angew. Chem. Int. Ed.*, **47**: 5022-5025.

(152) Islam, M.F.; Rojas, E.; Bergey, D.M.; Johnson, A.T.; Yodh, A.G. (2003). High weight fction surfactant solubilization of single-wall carbon nanotubes in water. *Nano Lett.*, **3**: 269-273.

(153) Moore, V.C.; Strano, M.S. Haroz, E.H.; Hauge, R.H. Smalley, R.E.; Schmidt, J.; Talmon, Y. (2003). Individually suspended single-walled carbon nanotubes in various surfactants. *Nano Lett.*, **3**: 1379-1382.

(154) Richard, C.; Balavoine, F.; Schultz, P.; Ebbesen, T. W.; Mioskowski, C. **(**2003) Supramolecular self-assembly of lipid derivatives on carbon nanotubes. *Science*, **300**: 775-778.

(155) Minko, T. (2005). Soluble polymer conjugates for drug delivery. *Curr. Drug Discov. Technol.*, **2**: 15-20.

(156) Moore, V.C.; Strano, M.S. Haroz, E.H.; Hauge, R.H.; Smalley, R.E.; Schmidt, J.; Talmon, Y. (2003). Individually suspended single-walled carbon nanotubes in various surfactants. *Nano Lett.* **3**: 1379-1382.

(157) Shvartzman-Cohen, R.; Nativ-Roth, E.; Yerushalmi-Rozen, R.; Baskaran, E.; Szleifer, I.; Levi-Kalisman, Y. (2004). Selective dispersion of single-walled carbon nanotubes in the presence of polymers: the role of molecular and colloidal length scales. *J. Am. Chem. Soc.*, **126:** 14850-14857.

(158) Sinani, V.A.; Kotov, N.A.; Yaroslavov, A.A.; Rakhnyanskaya, A.A.; Gheith, M.K.; Wicksted, J.P.; Sun, K.; Mamedov, A.A. Aqueous dispersions of single-wall and multiwall carbon nanotubes with designed amphiphilic polycations. (2005). *J. Am. Chem. Soc.* **127:** 3463-3472.

(159) Didenko, V.V.; Moore, V.C.; Baskin, D.S.; Smalley, R.E. (2005). Visualization of individual single-walled carbon nanotubes by fluorescent polymer wrapping. *Nano Lett.*, **5**: 1563-1567.

(160) Zheng, M.; Jagota, A.; Semke, E.D.; Diner, B.A.; McLean, R.S.; Lustig, S.R. Richardson, R.E.; Tassi, N.G. (2003). DNA-assisted dispersion and separation of carbon nanotubes. *Nat. Mater*, **2**: 338-342.

(161) Zheng, M.; Jagota, A.; Diner, B.A.; McLean, R.S.; Onoa, G.B.; Semke, E.D.; Watts, D.J.; Strano, M.S. arone, P.; Usrey, M. Santos, A.P.; Chou, S.G.; Dresselhaus, M.S.; Samsonidze, G.G. **(**2003). Structure-based carbon nanotubes sorting by sequence-dependent DNA assembly. *Science*, **302**: 1548-1548.

(162) Dieckmann, G.R.; Razal, J.; Giordano, G.M.; Musselman, I.H.; Baughman, R.H.; Dalton. A.B.; Munoz, E.; Johnson, P.A.; Draper, R.K.; Chen, J. (2003). Controlled assembly of carbon nanotubes by designed amphiphilic peptide helices, *J. Am. Chem. Soc.*, **125**: 1770-1777.

(163) Wang, S.; Delduco, D.F.; Lustig, S.R.; Wang, H.; Parker, K.N.; Rizzo, N.W.; Subramonet, S.; Jagota, A.; Humphreys, E.S.; Chung, S.; Chiang, Y.-M. (2003) Peptides with selective affinity for carbon nanotubes. *Nat. Mater*, **2**: 196-200.

(164) Dieckmann, G.R.; Razal, J.; Giordano, G.M. Musselman, I.H. Baughman, R.H. Dalton. A.B. Munoz, E. Johnson, P.A. Draper, R.K. Chen, J. (2003). Controlled assembly of carbon nanotubes by designed amphiphilic peptide helices. *J. Am. Chem. Soc.*, **125**: 1770-1777.

(165) Dalton, A.B.; Razal, J.M.; Draper, R.K.; Musselman, I.H.; Dieckmann, G.R.; Ortiz-Acevedo, A.; Zorbas, V.; Brunner, E.; Sampson, W.M.; Collins, S.; Yosshida, M.M.; Jose-Yacaman, M. (2004). Hierarchical self-assembly of peptide-coated carbon nanotubes. *Adv. Funct. Mater*, **14**: 1147-1151.

(166) Ortiz-Acevedo, A.; Xie, H.; Zorbas, V.; Sampson, W.M.; Dalton, A.B.; Baughman, R.H.; Draper, R.K.; Musslman, I.H.; Dieckmann, G.R. (2005). Diameter-

selective solubilization of single walled carbon nanotubes by reversible cyclic peptide. *J. Am. Chem. Soc.*, **127**: 9512-9517.

(167) Pantarotto, D.; Partidos, C.D.; Graff. R.; Hoebeke, J.; Briand J.P.; and Prato M.; and Bianco, A. (2003). Synthesis, Structural characterization and immunological properties of carbon nanotubes functionalized with peptides. *J Am Chem Soc* **125**: 6160-6164.

(168) Pantarotto, D.; Partidos, C.D.; Hoebeke, J.; Brown, F.; Kramer, E.; Briand, J.P.; Muller, S.; Prato M.; and Bianco, A. (2003). Immunization with peptide-functionalized carbon nanotubes enhances virus-specific neutralizing antibody responses. *Chem Biol.*, **10**: 961-966.

(169) Salvador-Morales, C.; Flahaut, E.; Sim, E.; Sloan, J.; Green, M.L.H. and Sim, R.B. (2006) Complement activation and protein adsorption by carbon nanotubes *Mol. Immunol.* **43** 193–201

(170) Salvador-Morales, C.; Flahaut, E.; Sloan, J.; Green, M.L.H.; Sim, R.B. (2005). Complement activation and protein adsorption by carbon nanotubes. *Mol immunol, in press*, **288** : 354-365

(171) Wong, J.M. (2005). Methotrexate in systemic lupus erythematosus. *Lupus*, **14**: 101-105.

(172) Pignatello, R; Guccione, S; Forte, S: Di Giacomo, C.; Sorrenti, V.; Vicari, L.; Uccello Barretta, G.; Balzano. F.; Puglisi, G. (2004). Lipophilic conjugates of methotrexate with short-chain alkylamino acids as DHFR inhibitors. Synthesis, biological evaluation, and molecular modelling. *Bioorg. Med. Chem.*, **12**: 2951-2964.

(173) Sirotnak, F.M.; Moccio, D.M.; Kellcher, L.E.; Goutas, L.I. (1981). Relative frequency and kinetic properties of transport-defective phenotypes among methotrexate-resistant LI 210 Clonal cell lines derived in vivo. *Cancer Res.*, **41** : 4447-4454

(174) Pignatello, R.; Toth, T.; Pugliss, G. (2001) Structural effects of lipolphilic methotrexate conjugates on model phospholipid biomembranes. *Thermochim. Acta*, **380** : 255-264.

(175) Pastorin, G. ; Wu, W. ; et al. (2006). Double functionalization of carbon nanotubes for multimodal delivery. *Chem. Commun*, **11**: 1182-1184.

(176) Prato, M.; Kostarelos, K.; Bianco, A. (2008). Functionalized carbon nanotubes in drug design and discovery. *Acc. Chem. Resi.*, **41** : 60-68.

(177) Quintara, A.; Raczika, E.; Piehler, L.; Lee, I.; Myc. A.; Majoros, I.; Patri, A. K.; Thomas, T.; Mule, J.; Baker, J.R. (2002). Design and function of a dendrimer-based therapeutic nanodevice target to tumor cells through the folate receptor. *Pharm. Res.*, **19**: 1310-1316.

(178) Jaspreet, K.V.; Maram, K.R.; and Vinod, D.L. (2005). Nanosystems in drug targeting: opportunities and challenges. *Current Nanoscience*, **1**: 47-64.

(179) Kricheldorf, H.R. (1987). In: α-amino acid N-carboxyanhydride and related heterocycles. *Springer-verlag*, 3-58.

(180) Neri, P.; Antoni, G.; Benvenutti, F.; Cocola, F.; and Gazzei, G. (1973). Synthesis of α,β-poly[(2-hydroxyethyl)-DL-aspartamide], a new plasma expander. *J. Med. Chem.* **16:** 893–897.

(181) Tomida, M.; Nakato, T. ; Matshunami, S.; Kakuchi, T. (1997). In Convenient synthesis of high molecular weight polymer. *Polymer*, **38**: 4733-4736.

(182) Machado, M.; De L.; Neuse, E.W.; Perlwitz, A.G. (1992). Water-soluble polyamides as potential drug carriers. *Die Angewandte Makromolekulare Chemie* **195**: 35-56.

(183) Shen, W.C.; Ballou, B.; Ryser, H. J.P.; Hakala, T.R. (1986). Targeting, Internalization, and Cytotoxicity of Methotrexate-Monoclonal Anti-Stage-specific Embryonic Antigen-1 Antibody Conjugates in Cultured F-9 Teratocarcinoma Cells. *Cancer Res.*, **46** (8): 3912-3916.

(184) Dickinson, E.; and Eriksson, L. (1991). Particle flocculation by adsorbing polymers. *Adv. Colloid Interface SCi.* **34:** 1-29.

(185) Moudgil, B.M.; and Somasundaran, P. (Eds.) (1986). *Flocculation, Sedimentation and Consolidation*. Am. Inst. Chem. Eng., New York. 229-248.

(186) Hinds, B.J.; Chopra, N.; Rantell, T.; Andrews, R.; Gavalas, V.; Bachas, L.G. (2004). Aligned multiwalled carbon nanotube membranes. *Science*, **303**: 62-65.

(187) Casavant, M.J.; Walters, D.A.; Schmidt, J.J.; Smalley, R.E. (2003). In Temperature and Size Effects on Diffusion in Carbon Nanotubes. *J. Appl. Phys.*, 93, 2153-2156.

(188) Srivastava, A.; Srivastava, O.N.; Talapatra, S.; Vajtai, R.; Ajayan, P. (2004). In Enhanced Fluid Flow through Nanoscale Carbon Pipes - Nano Letters. *Nat. Mater*, **3**: 610-614.

(189) Yashoanath, S.; Santikary, P.J. (1994). Diffusion of Sorbates in Zeolites Y and A: Novel Dependence on Sorbate Size and Strength of Sorbate-Zeolite Interaction. *Phys. Chem.*, **98**: 6368-6376.

(190) Yashonath, S.; Rajappa, C. (1997). In Neutron Scattering and Molecular Dynamics Evidence for Levitation Effect in Nanopores. *Faraday Discuss*, **106**: 105-118.

(191) Yashonath, S.; Rajappa, C. (1997). In Neutron Scattering and Molecular Dynamics Evidence for Levitation Effect in Nanopores. *Faraday Discuss*, **106**: 105-118.

(192) Derouane, E.G.; André, J.M.; Lucas, A.A. (1988). In Temperature and Size Effects on Diffusion in Carbon Nanotubes. *J. Catal.*, **110** : 58-73.

(193) Dravid, V. P.; Lin, X.; Wang, Y.; Yee A.; and Chang, R.P.H. (1993). Buckytubes and Derivatives: Their Growth and Implications for Buckyball Formation. *Science*, **259**: 1601- 1604.

(194) Amelinckx, S.; Bernaerts, D.; Zhang, X. B.; Tendeloo, G. and Landuyt, J. (1995). Electron microscopy of carbon nanotubules and related structures. *Science*, **267**: 1334-1338.

(195) Iijima,S.; Brabec, C.; Maiti, A.; and Bernholc, J. (1996). Structural flexibility of carbon nanotubes. *J. Chem. Phys.*, **104**: 2089-2092.

(196) Yakobson, B.I.; Brabec, C.J.; and Bernholc, J. (1996). In High strain rate fracture and C-chain unraveling in carbon nanotubes. *Phys. Rev. Lett.*, **76**: 2511-2514.

(197) Falvo, M.R.; Clary, G.J.; Taylor II, R.M.; Chi, V.; Brooks, F.P.; Washburn, S.; and Superfine, R. (1997). In situ resistance measurements of strained carbon nanotubes. *Nature (London)* **389**: 582-584.

(198) Despres, J. ; Daguerre, E. ; and Lafdi, K. (1995). In Nanomechanics of Carbon Tubes: Instabilities beyond Linear Response. *Carbon*, **33** : 87-92.

(199) Derouane, E.G.; André, J.M. (1987). In Temperature and size effects on diffusion in carbon nanotubes. *Chem. Phys. Lett.*, **137** : 336-340.

(200) Hunger, B. ; Heuchel, M. ; Louis, A.C. ; and Randall, Q.S. (2002). Characterization of Acidic OH Groups in Zeolites of Different Types: An Interpretation of $NH_3$-TPD Results in the Light of Confinement Effects. *J. Phys. Chem. B*, **106** (15): 3882–3889.

(201) Liu, J.; Rinzler, A.G.; Dai, H.; Hafner, J.H.; Bradley, R.K.; Boul, P.J.; Lu, A.; Iverson, T.; Shelimov, K.; Huffman, C.B.; et al. (1998). Fullerene pipes. *Science*, **280**: 1253-1256.

## APPENDIX:

## $^{1}$H NMR SPECTRA

## $^{1}$H NMR SPECTRA (1): PSI-DMP (90)-EDDA (10)

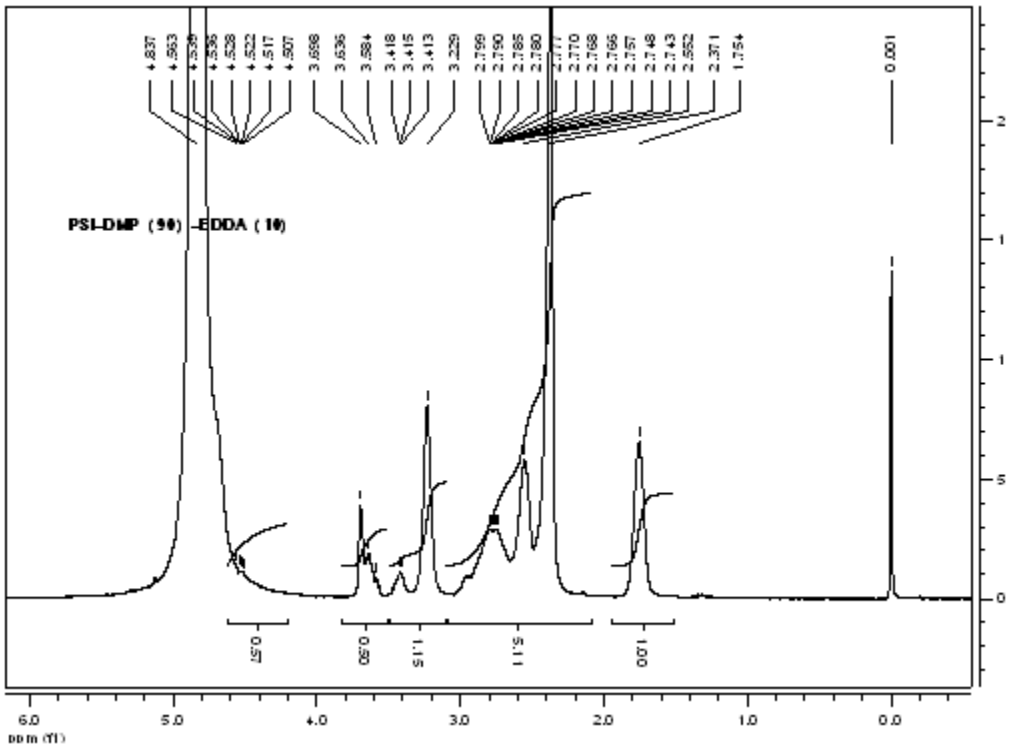

## $^{1}$H NMR SPECTRA (2): PSI-DMP (80)-EDDA (20)

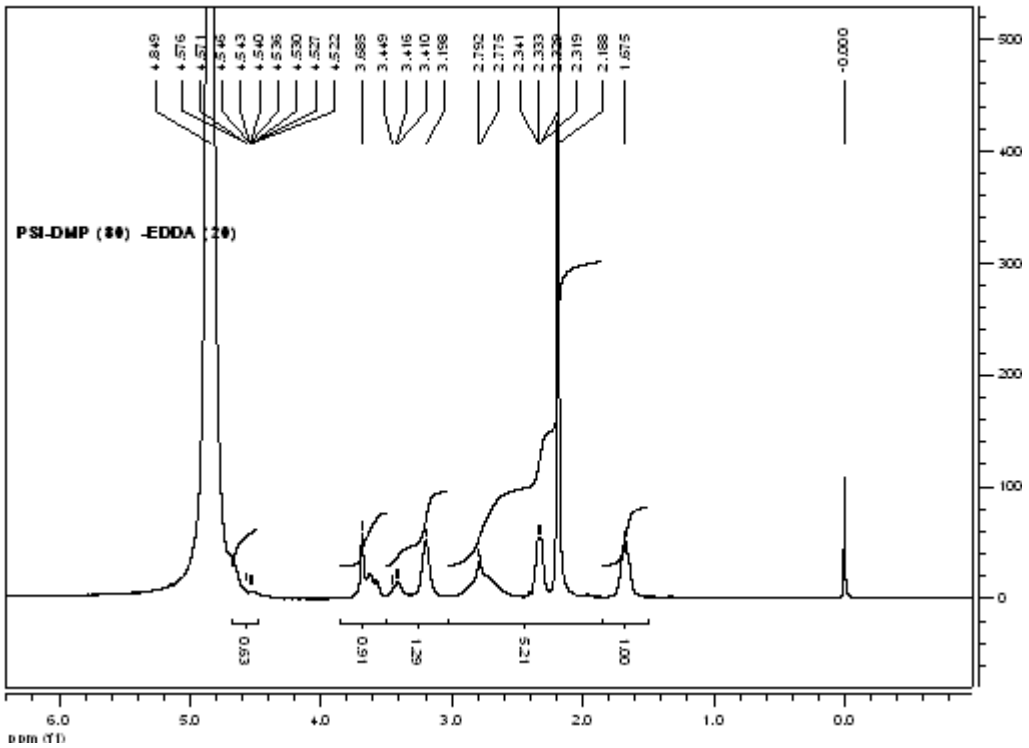

## $^{1}$H NMR SPECTRA (3): PSI-DMP (95)-PDA (5)

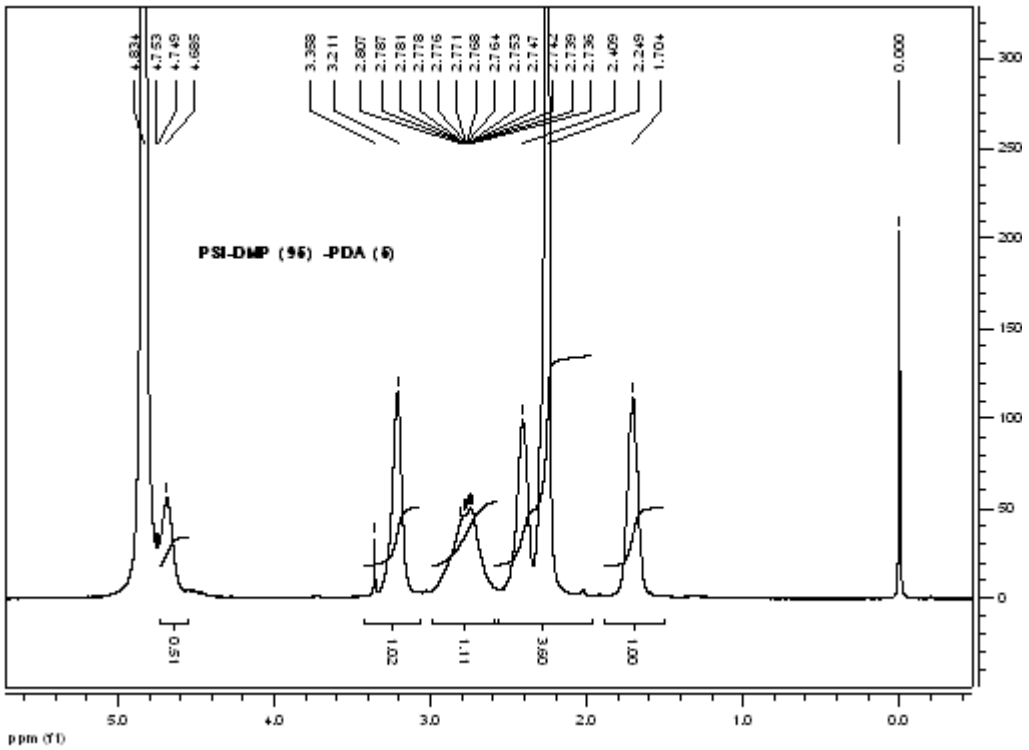

**$^1$H NMR SPECTRA (4): PSI-DMP (90)-PDA (10)**

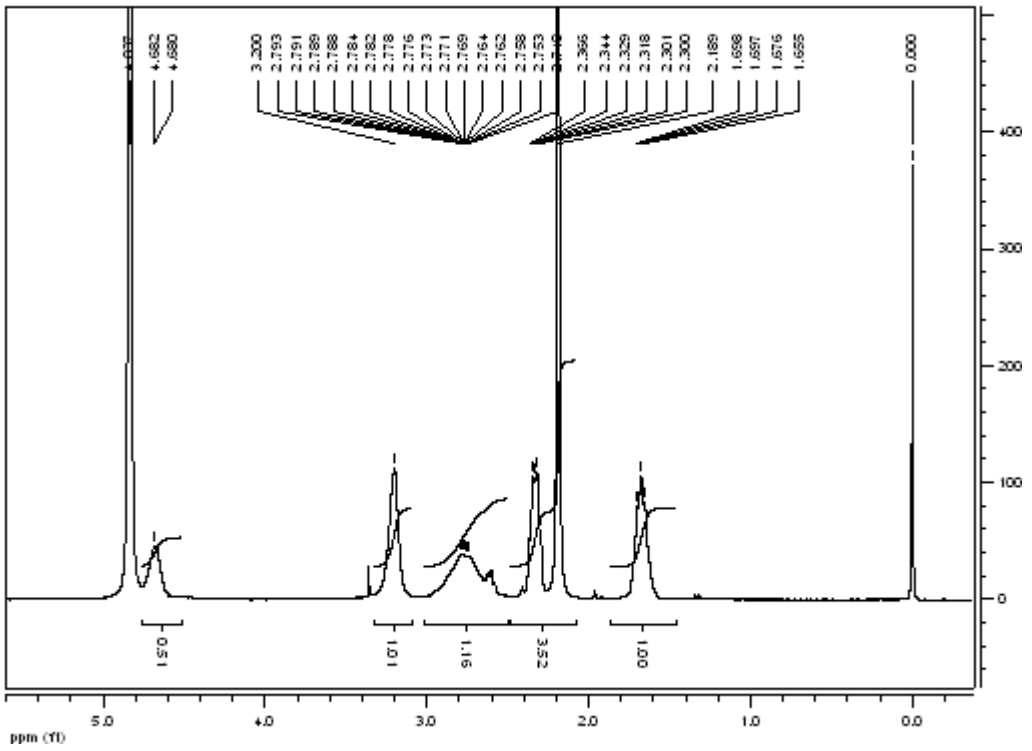

## $^{1}$H NMR SPECTRA (5): PSI-DMP (85)-PDA (15)

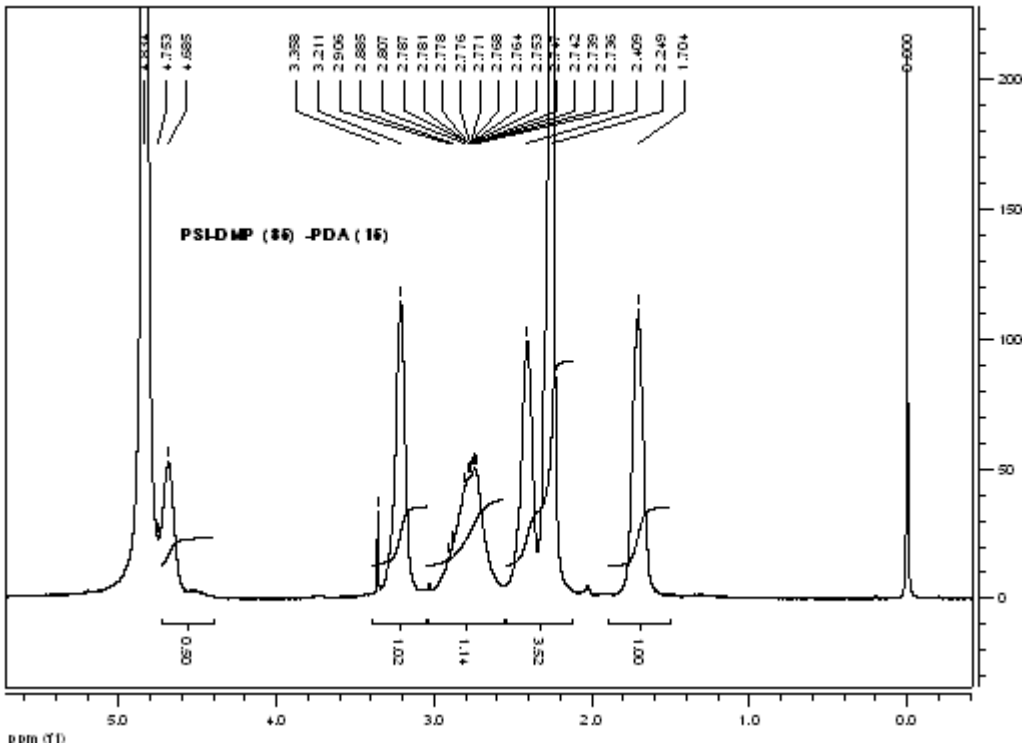

## $^{1}$H NMR SPECTRA (6): PSI-DMP (80)-PDA (20)

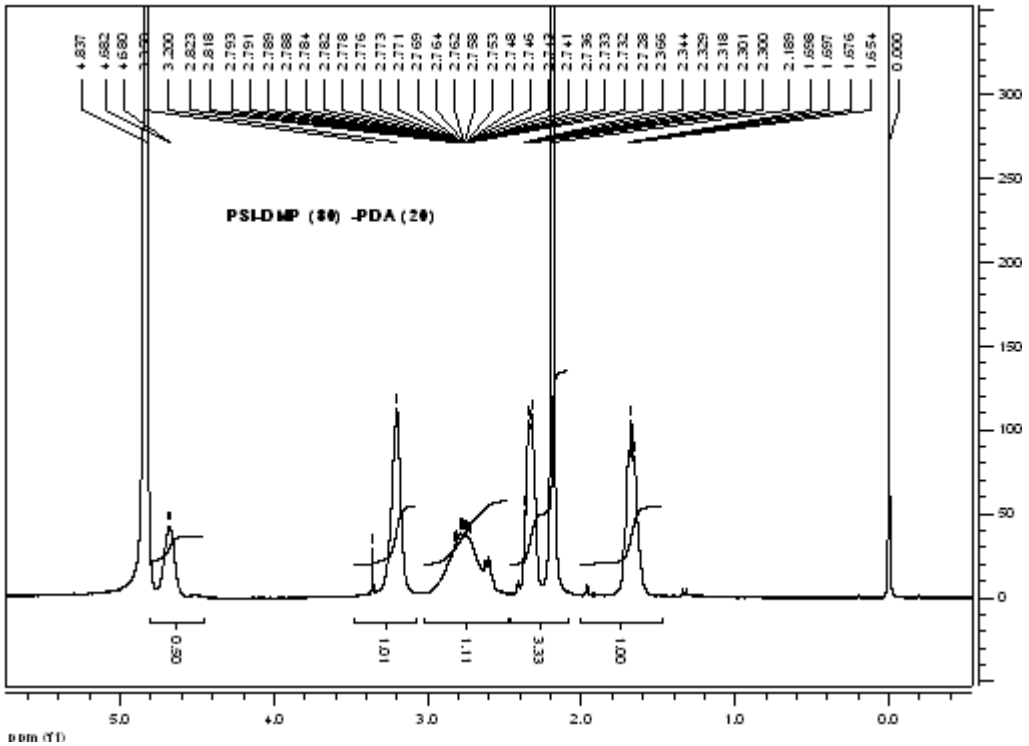

## $^{1}$H NMR SPECTRA (7): PSI-DMP (95)-PDA (5)-FA

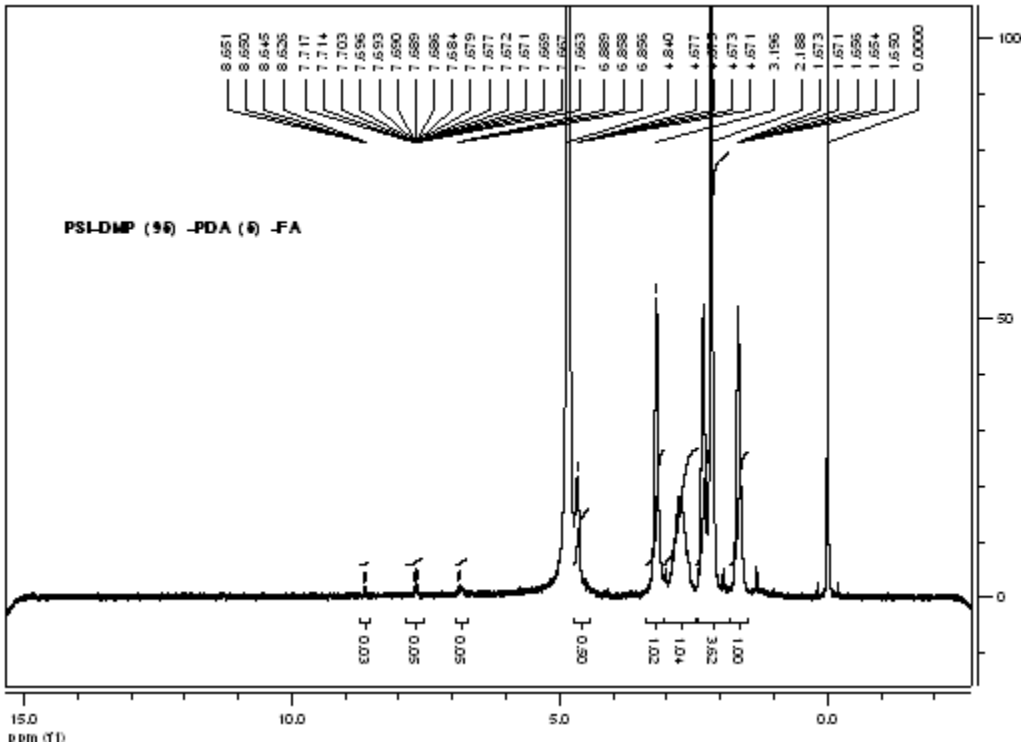

**$^{1}$H NMR SPECTRA (8): PSI-DMP (85)-PDA (15)-FA**
**(After 10 minutes of reaction) (8% FA incorporation)**

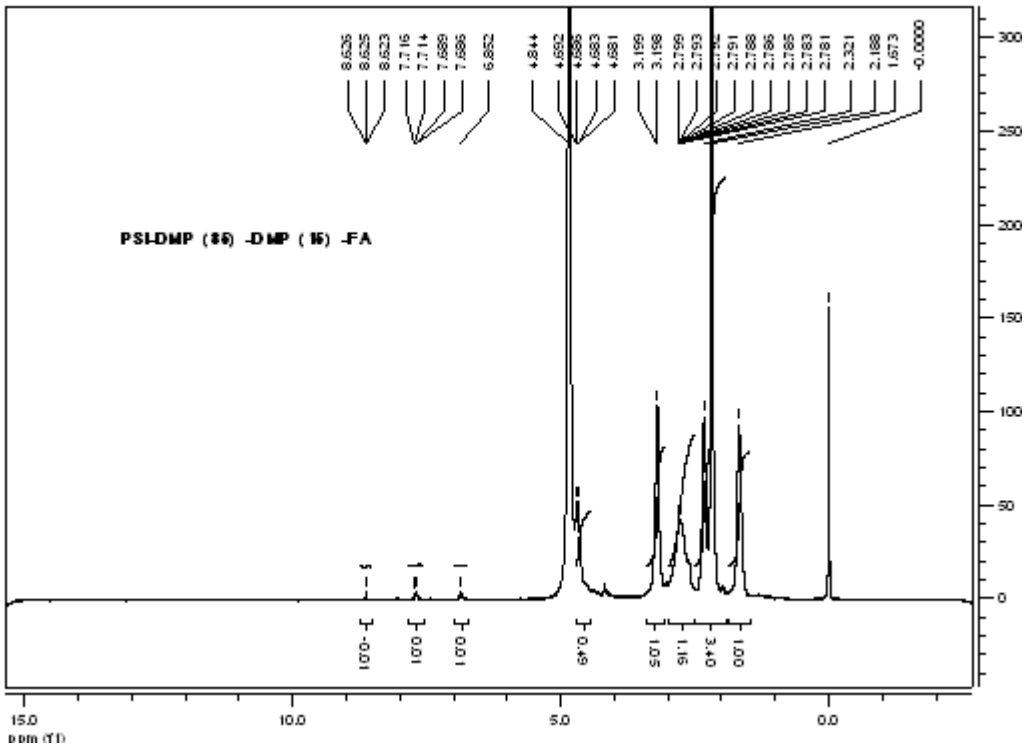

**$^{1}$H NMR SPECTRA (9): PSI-DMP (85)-PDA (15)-FA**
**After 20 minutes of reaction (21.3% FA incorporation)**

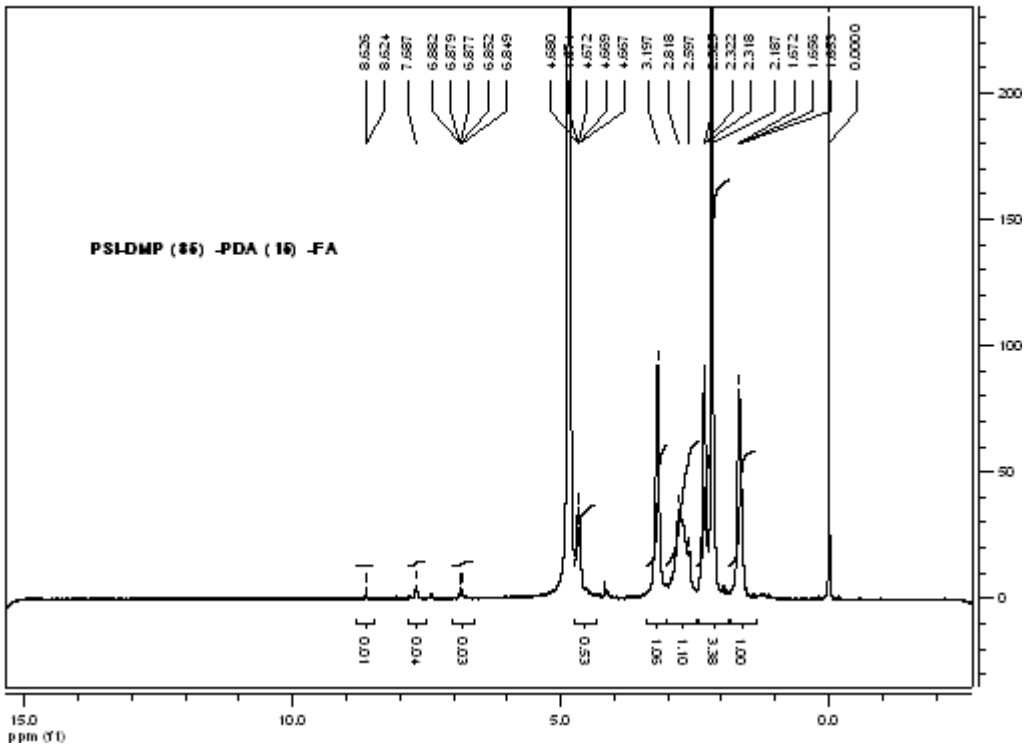

**$^{1}$H NMR SPECTRA (10): PSI-DMP (85)-PDA (15)-FA**
**After 30 minutes of reaction (26.7% FA incorporation)**

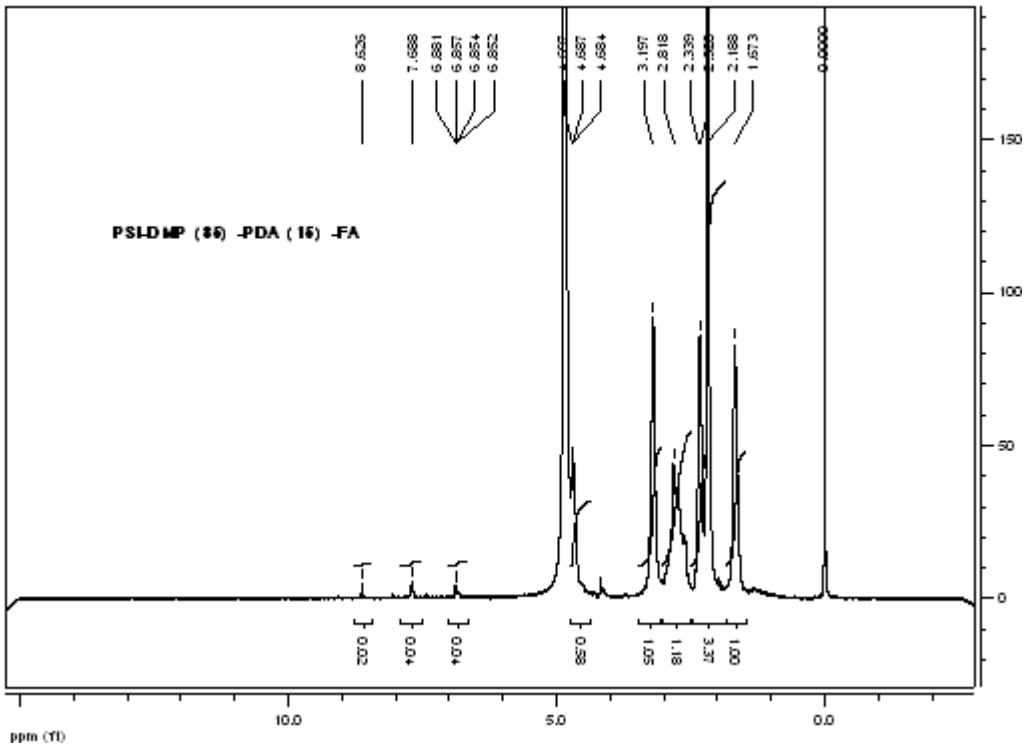

**$^{1}$H NMR SPECTRA (11): PSI-DMP (85)-PDA (15)-FA**
**(After 40 minutes of reaction) (29.3% FA incorporation)**

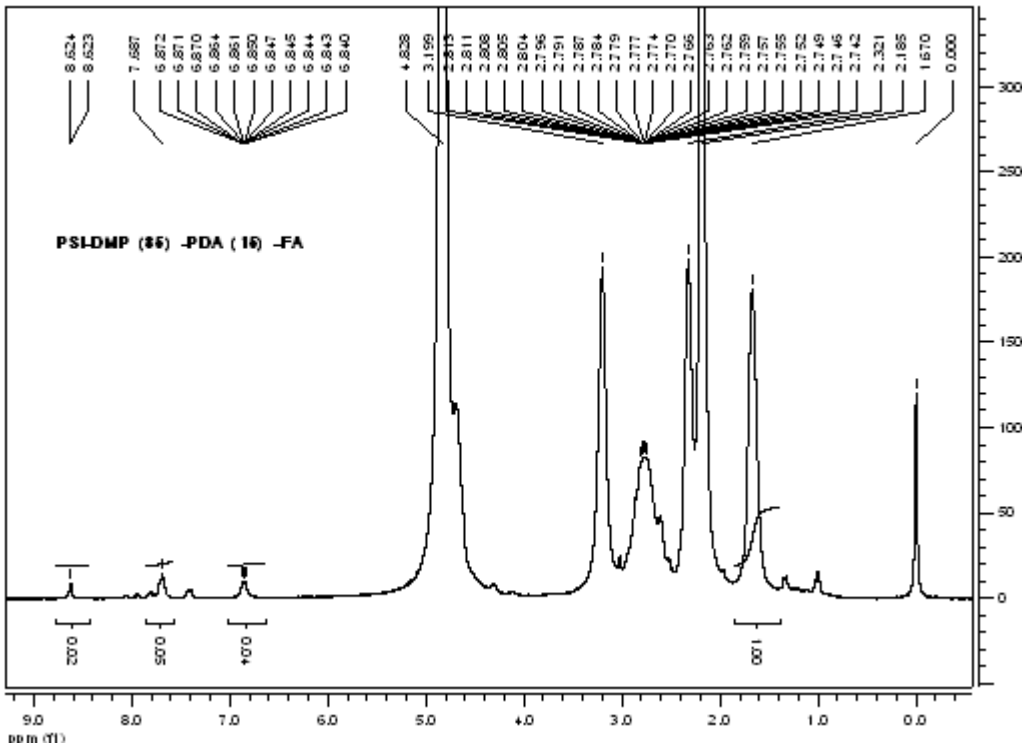

**$^{1}$H NMR SPECTRA (12): PSI-DMP (85)-PDA (15)-FA**
**After 50 minutes of reaction (32% FA incorporation)**

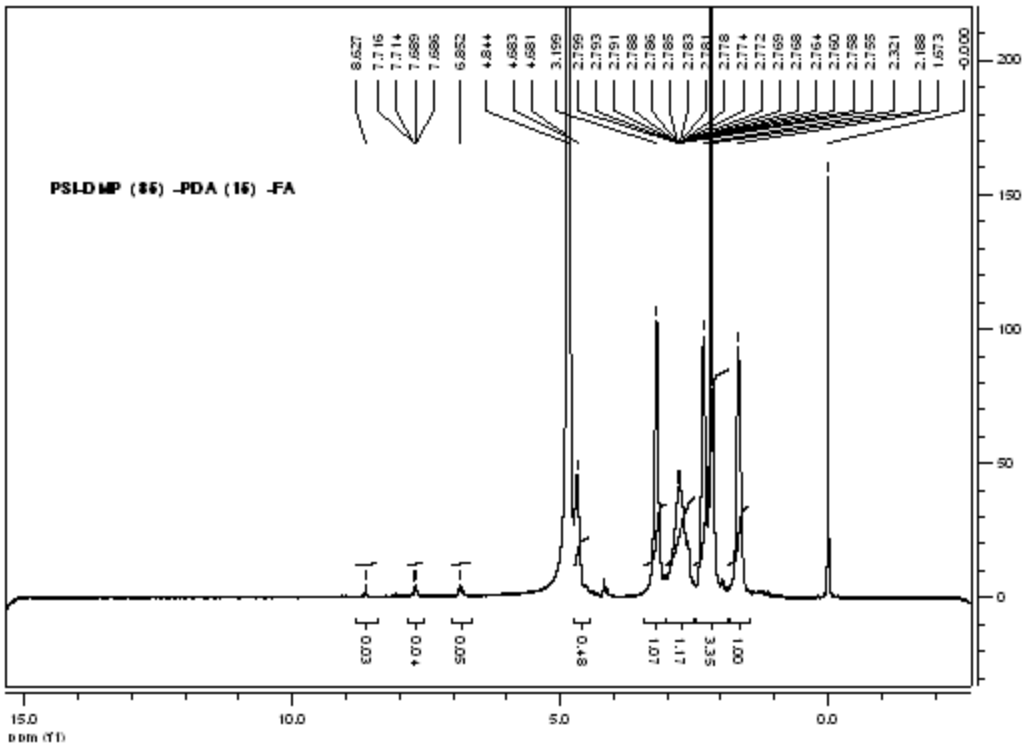

**$^{1}$H NMR SPECTRA (13): PSI-DMP (85)-PDA (15)-FA**
**After 60 minutes of reaction (34.7% FA incorporation)**

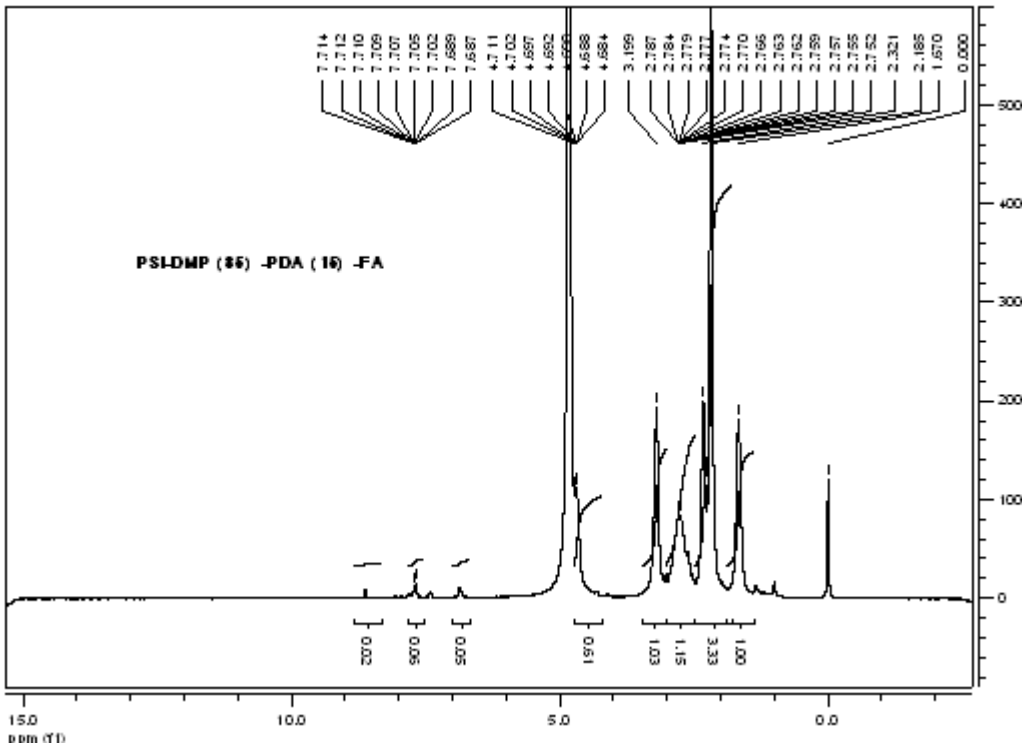

**$^{1}$H NMR SPECTRA (14): PSI-DMP (85)-PDA (15)-FA**
**(After 70 minutes of reaction) (48% FA incorporation)**

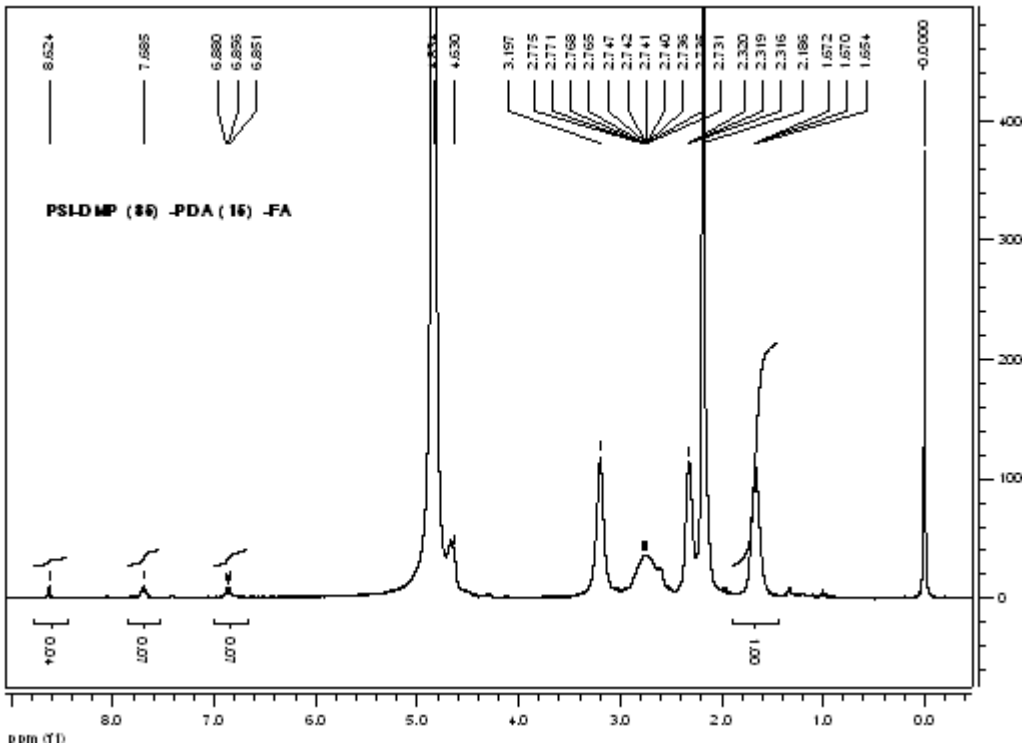

**$^{1}$H NMR SPECTRA (15): PSI-DMP (85)-PDA (15)-FA**
**(After 80 minutes of reaction) (53.3% FA incorporation)**

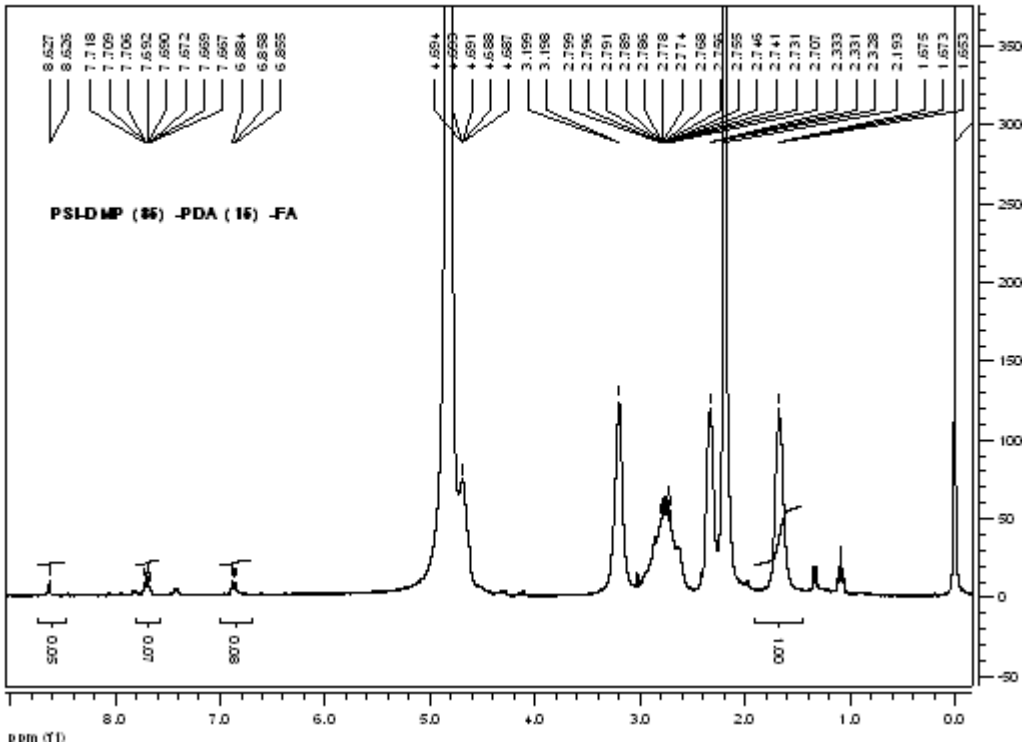

**$^{1}$H NMR SPECTRA (16): PSI-DMP (85)-PDA (15)-FA**
**(After 90 minutes of reaction) (61.3% FA incorporation)**

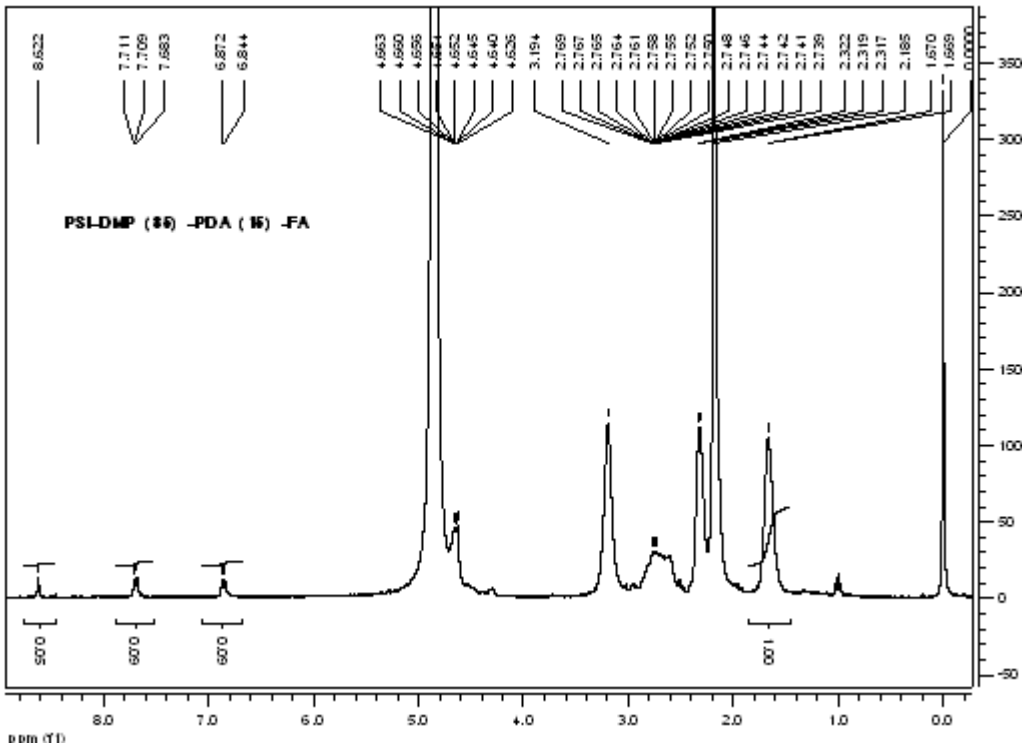

**$^{1}$H NMR SPECTRA (17): PSI-DMP (85)-PDA (15)-FA**
**(After 100 minutes of reaction) (82.7% FA incorporation)**

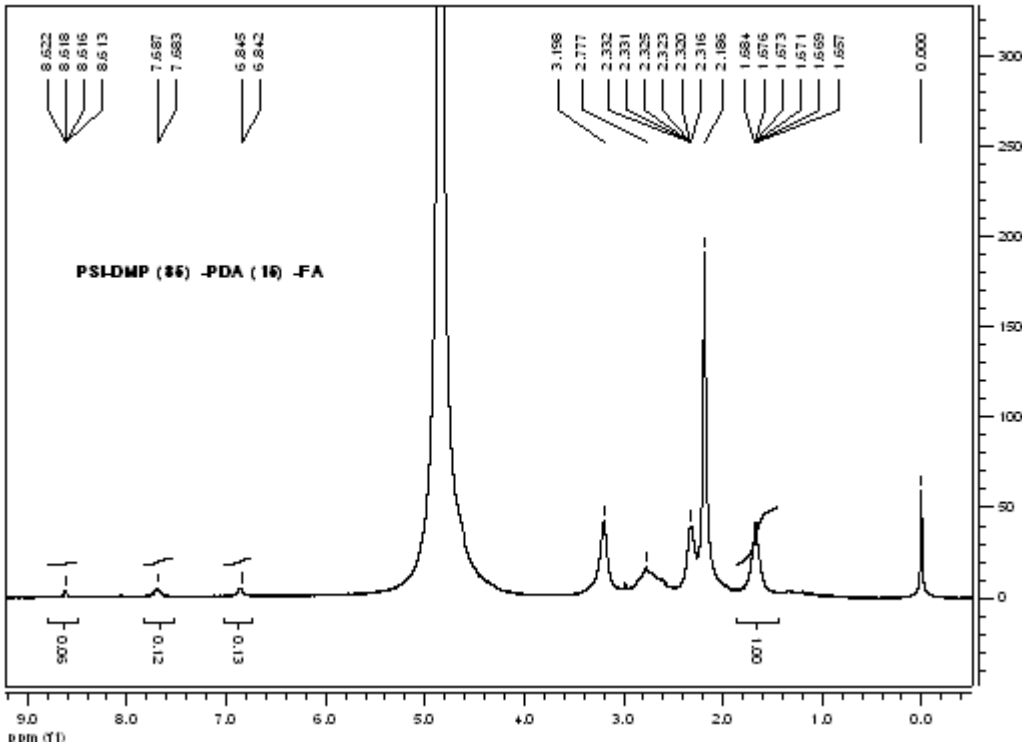

**$^{1}$H NMR SPECTRA (18): PSI-DMP (85)-PDA (15)-FA**
**(After 110 minutes of reaction) (85.3% FA incorporation)**

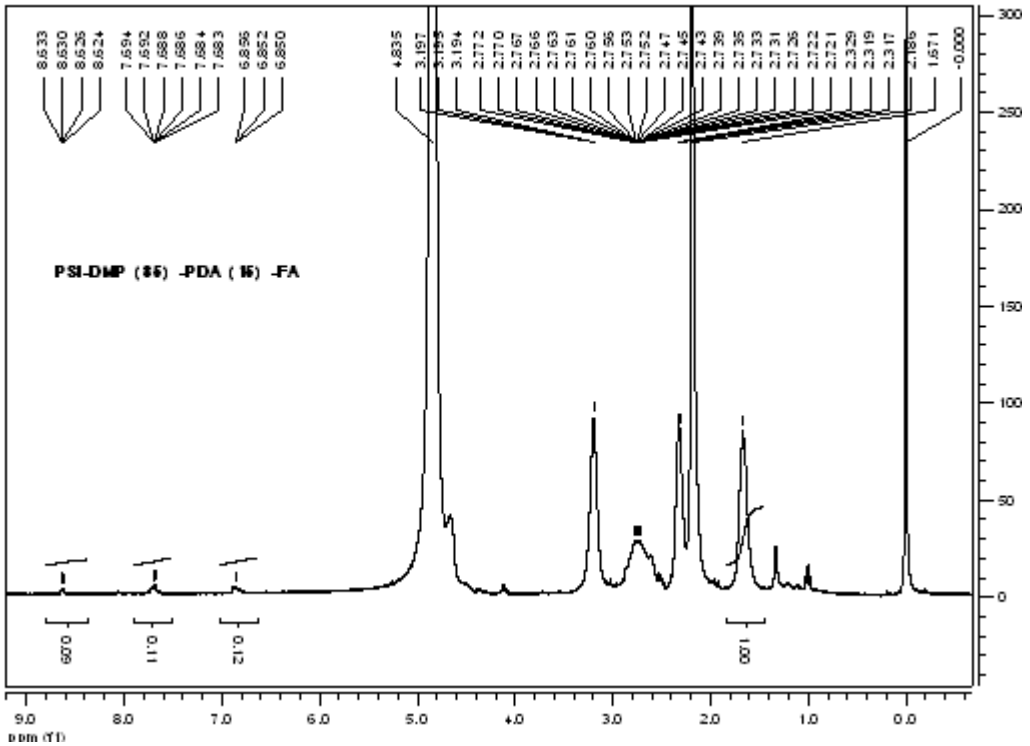

**$^{1}$H NMR SPECTRA (19): PSI-DMP (85)-PDA (15)-FA**
**(After 120 minutes of reaction) (90.6% FA incorporation)**

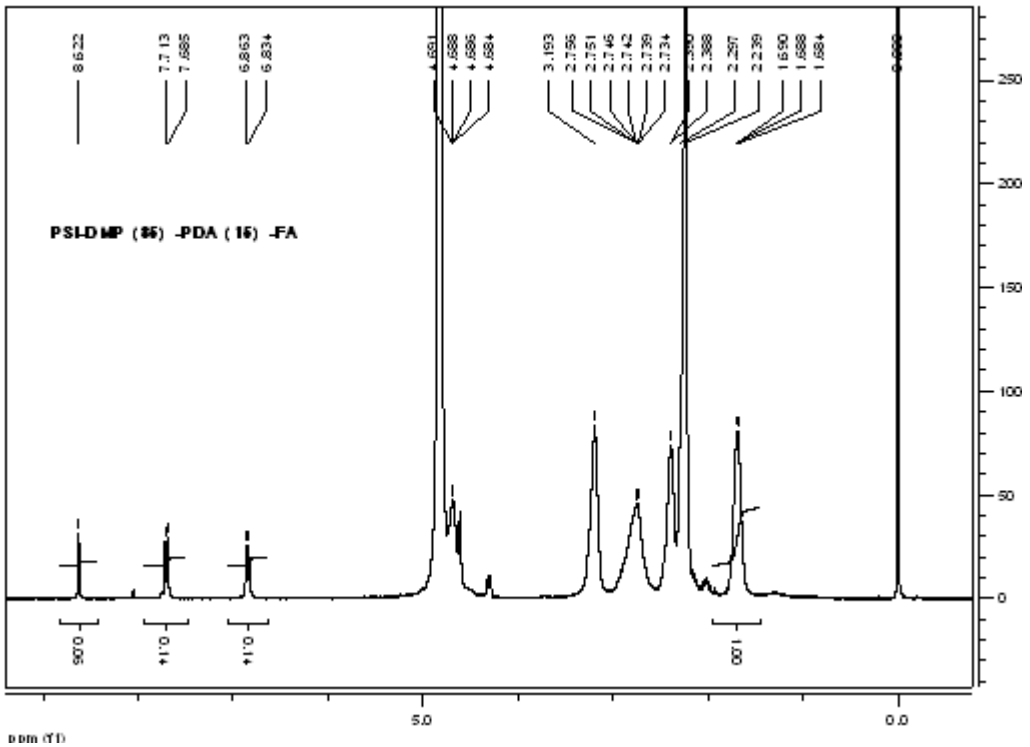

**$^{1}$H NMR SPECTRA (20): PSI-DMP (85)-PDA (15)-FA**
**(After 130 minutes of reaction) (96% FA incorporation)**

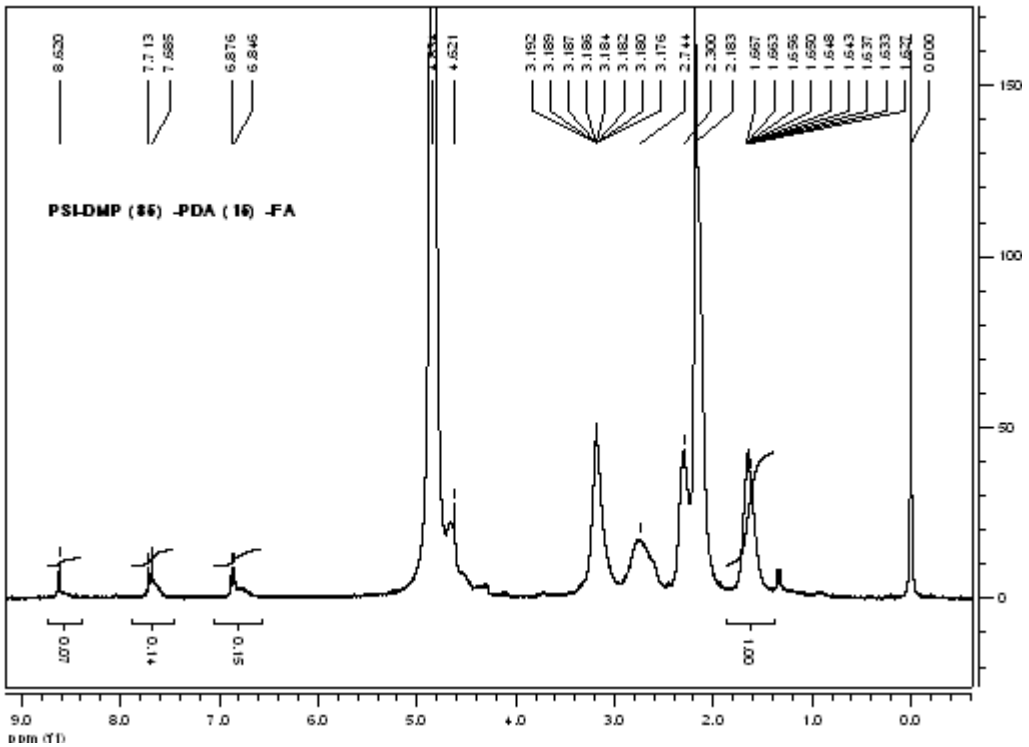

**$^{1}$H NMR SPECTRA (21): PSI-DMP (80)-PDA (20)-FA**
**After 10 minutes of reaction**

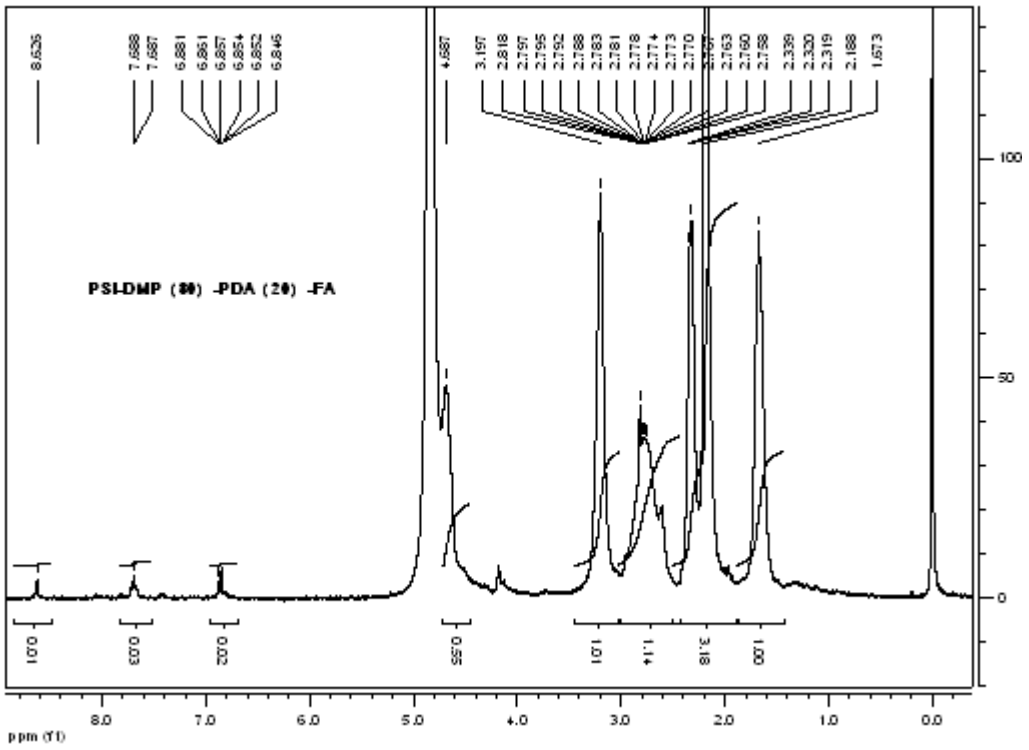

**$^{1}$H NMR SPECTRA (22): PSI-DMP (80)-PDA (20)-FA**
**After 25 minutes of reaction**

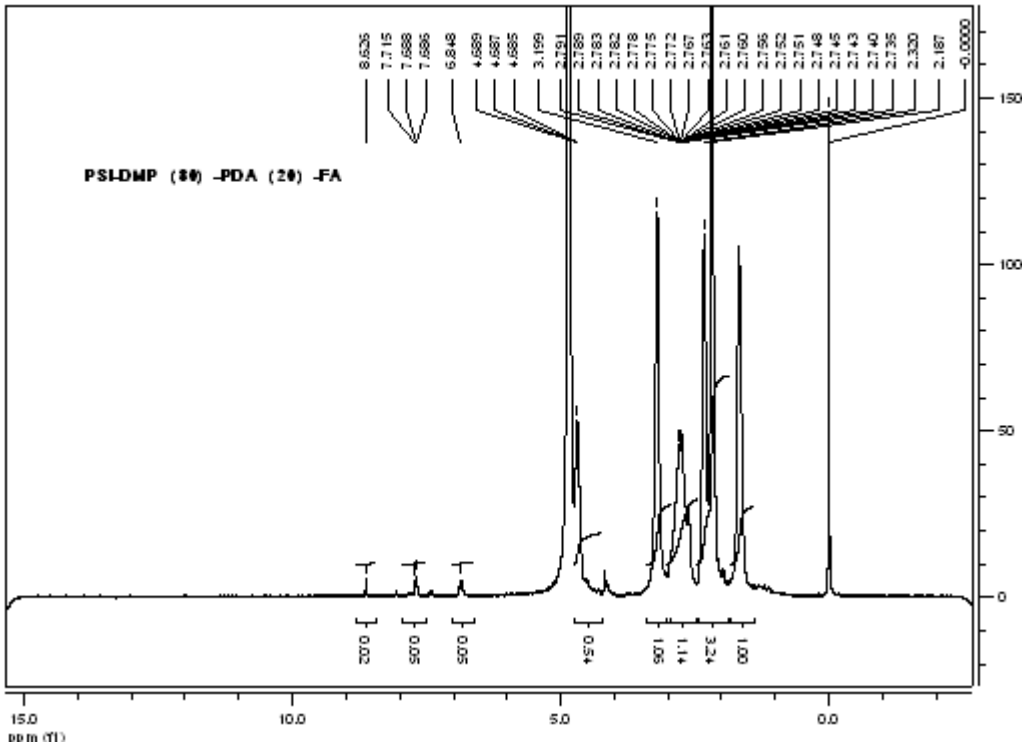

**$^{1}$H NMR SPECTRA (23): PSI-DMP (80)-PDA (20)-FA**
**After 50 minutes of reaction**

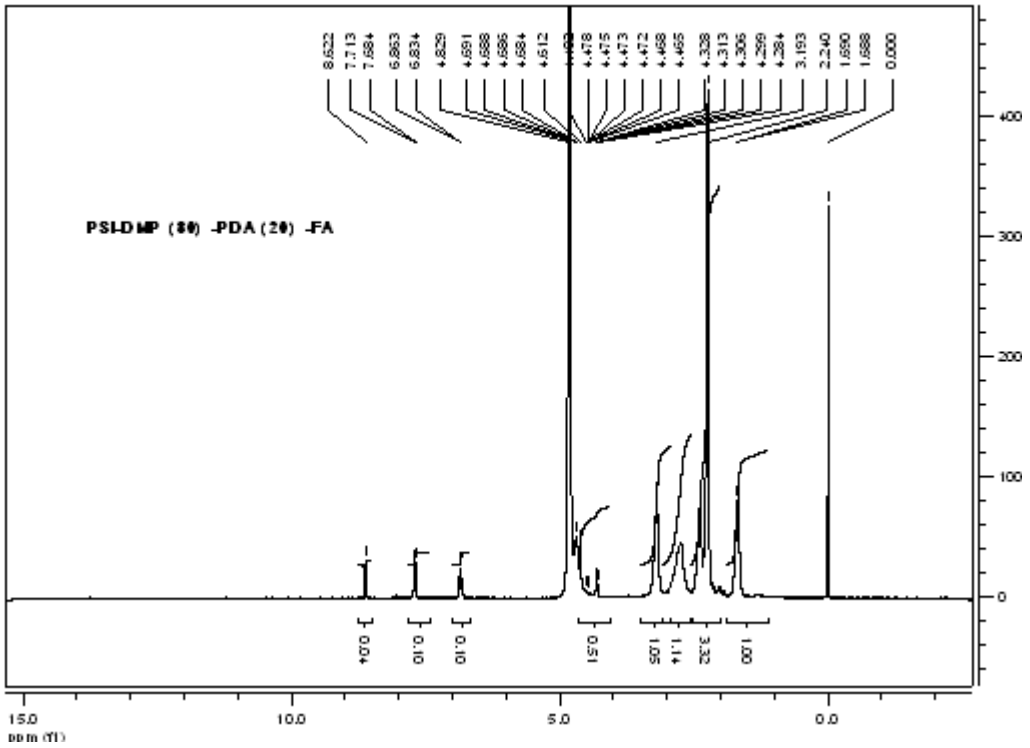

**$^{1}$H NMR SPECTRA (24): PSI-DMP (80)-PDA (20)-FA)**
**After 60 minutes of reaction**

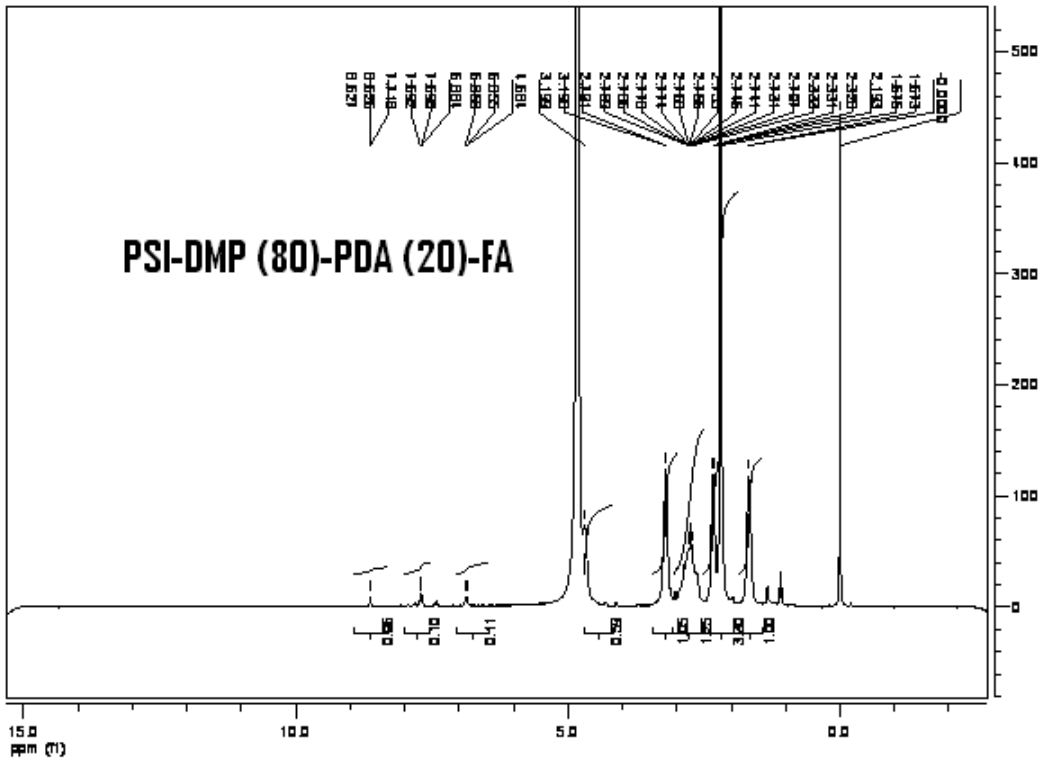

**$^{1}$H NMR SPECTRA (25): PSI-DMP (80)-PDA (20)-FA**
**After 120 minutes of reaction**

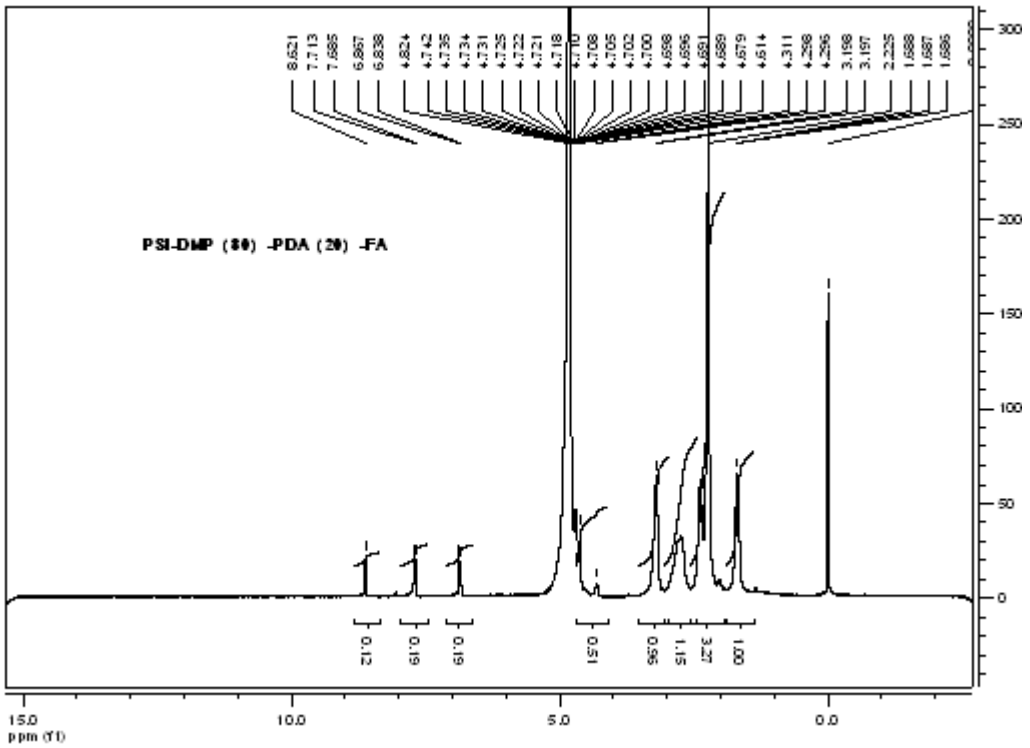

## $^{1}$H NMR SPECTRA (26): f-CNTs: MWCNTs in $H_2SO_4$ / $HNO_3$ at 100°C

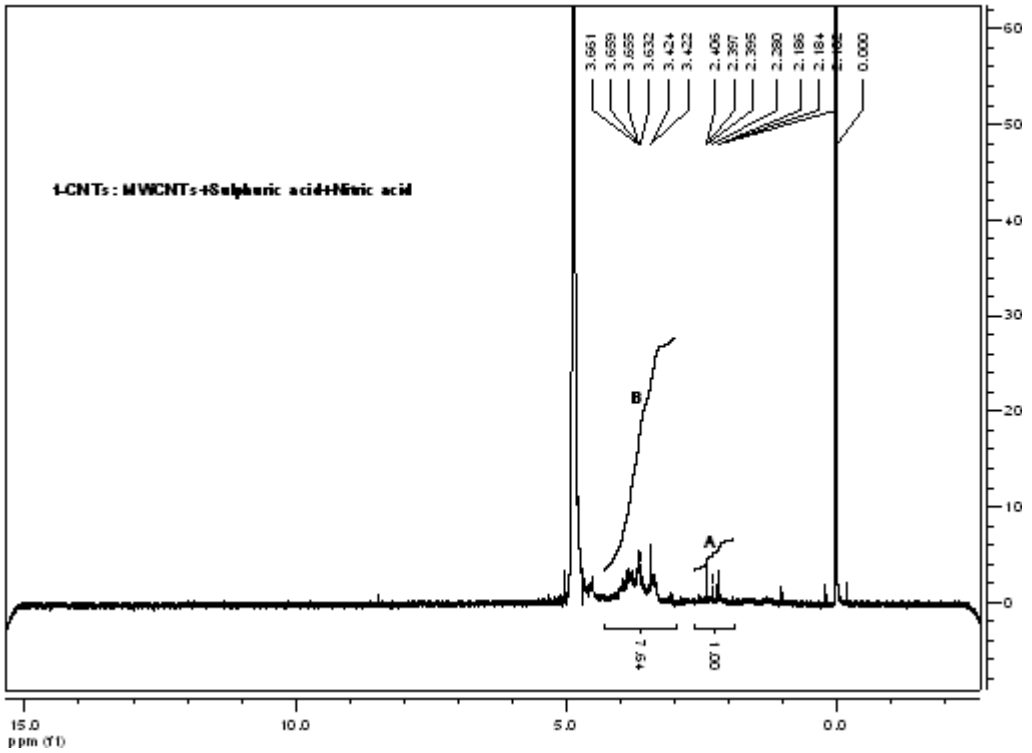

**$^{1}$H NMR SPECTRA (27): f-CNTs: MWCNTs in $H_2SO_4/HNO_3$ at 50°C**

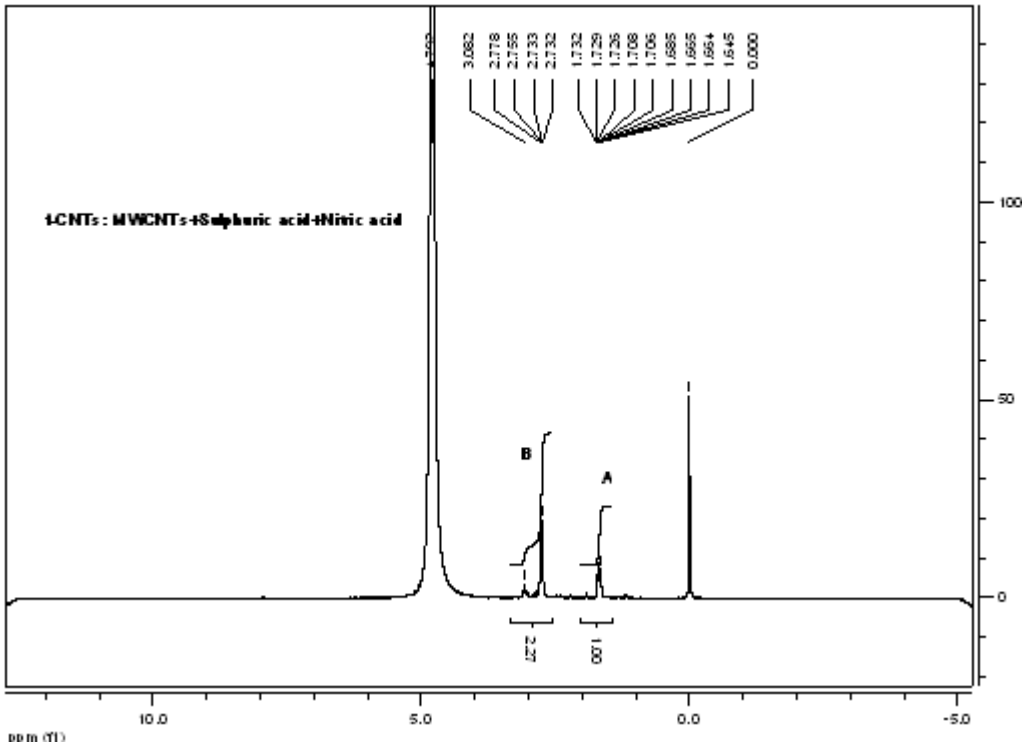

## $^{1}H$ NMR SPECTRA (28): f-CNTs: MWCNTs in $H_2SO_4/HNO_3$ at RT

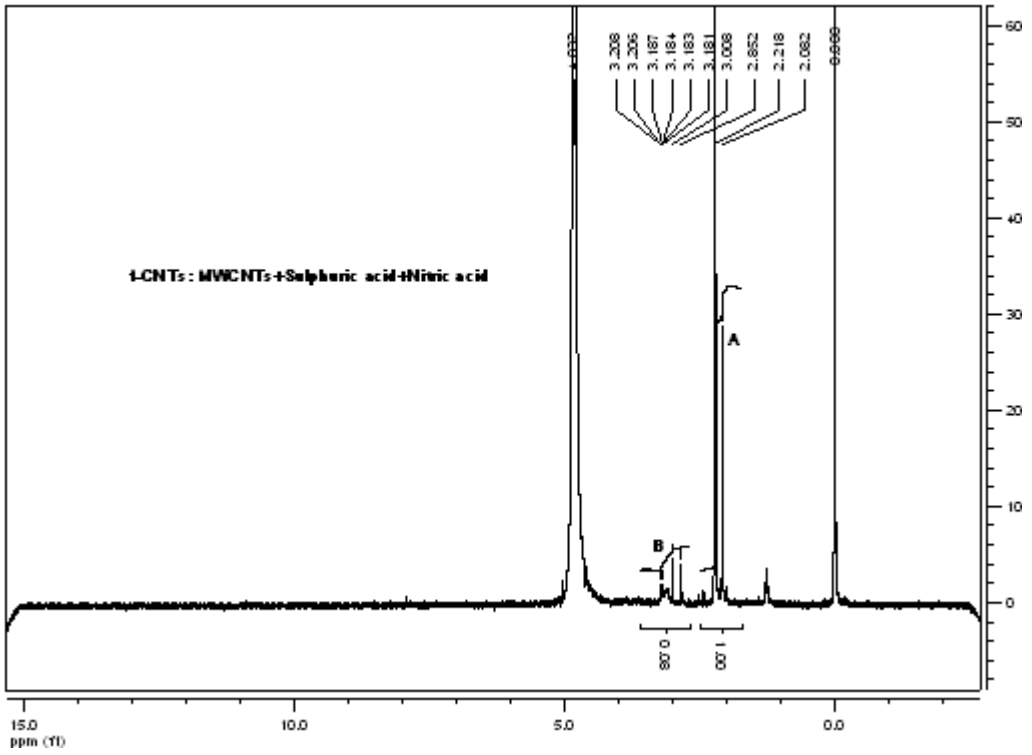

**$^{1}$H NMR SPECTRA (29): f-CNTs: MWCNTs + Aspartic acid in DMF at 230˚C.**

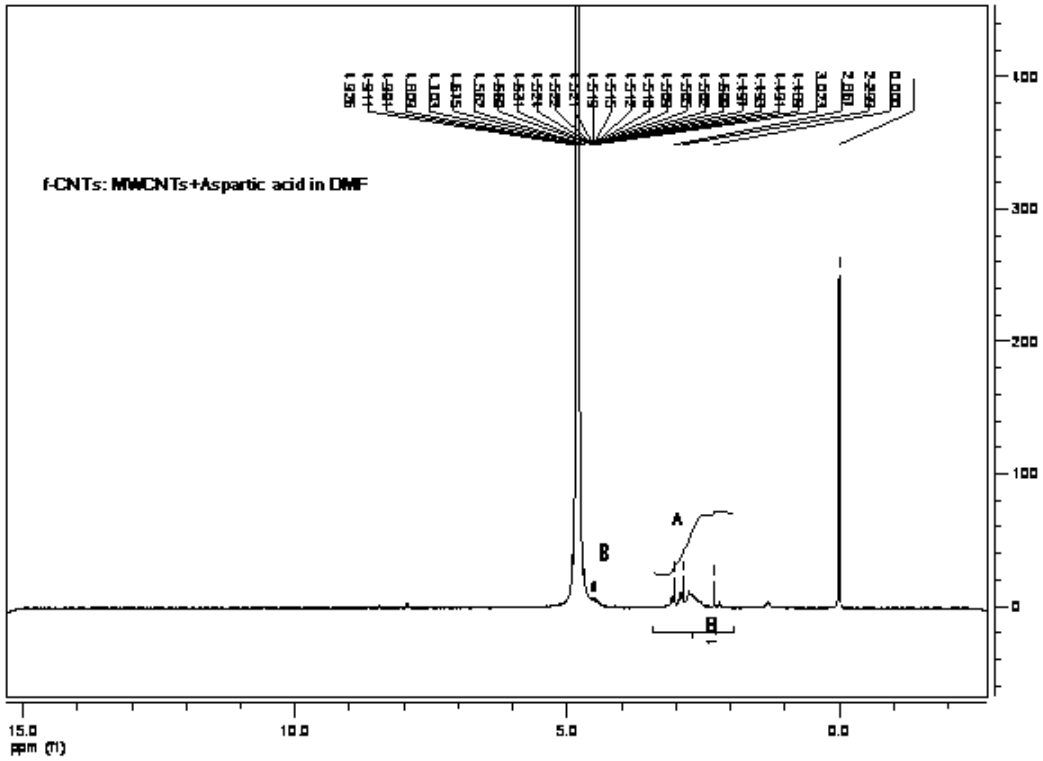

## $^{1}$H NMR SPECTRA (30): f-CNTs: MWCNTs + PSI in DMF at 160˚C

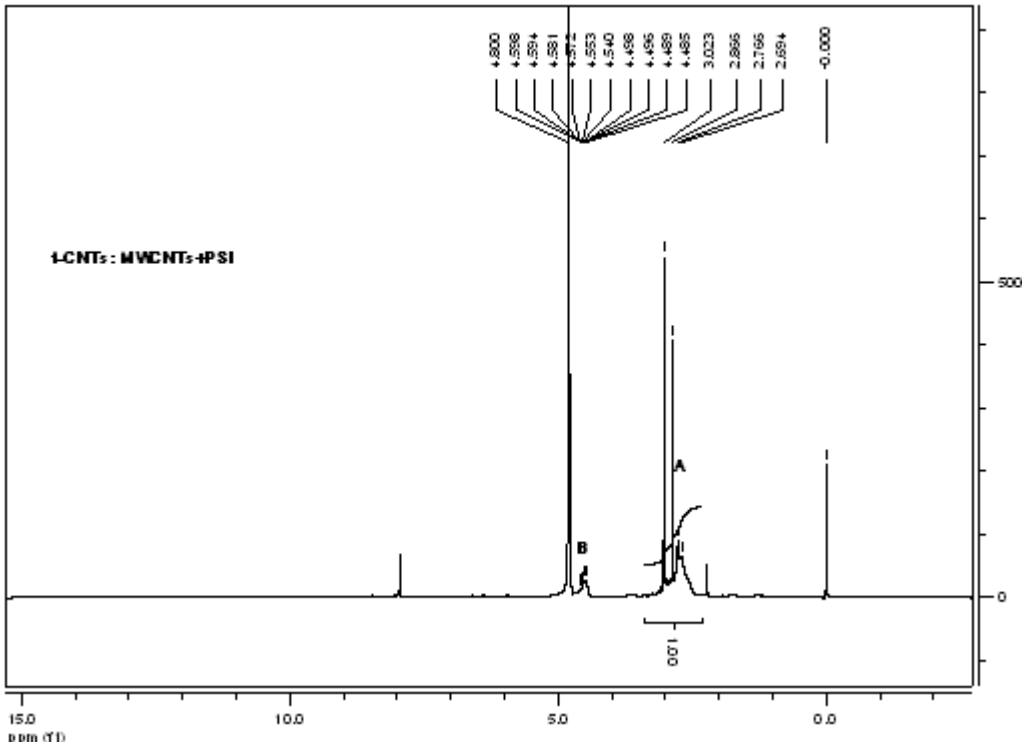

**$^{1}$H NMR SPECTRA (31): f-CNTs (MWCNTs+$H_2SO_4$+$HNO_3$)-DMP (30)-FA (70)**
**94% FA incorporation**

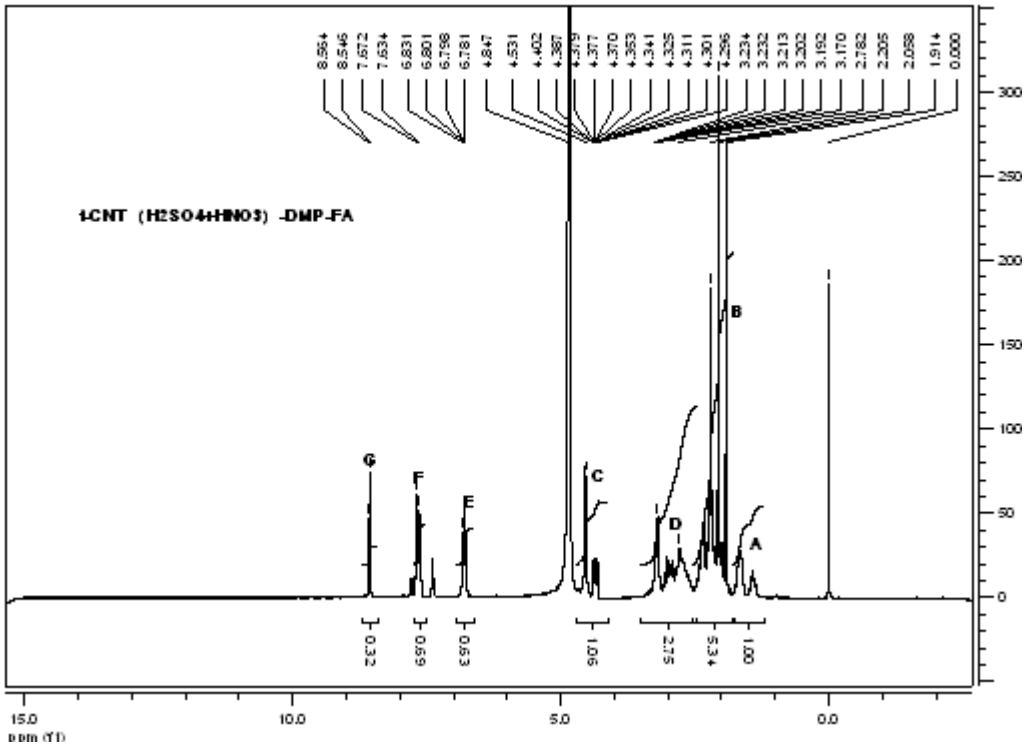

**$^{1}$H NMR SPECTRA (32): f-CNTs (MWCNTs+Aspartic Acid)-DMP(40)-FA(60) Incorporation FA 101,3%**

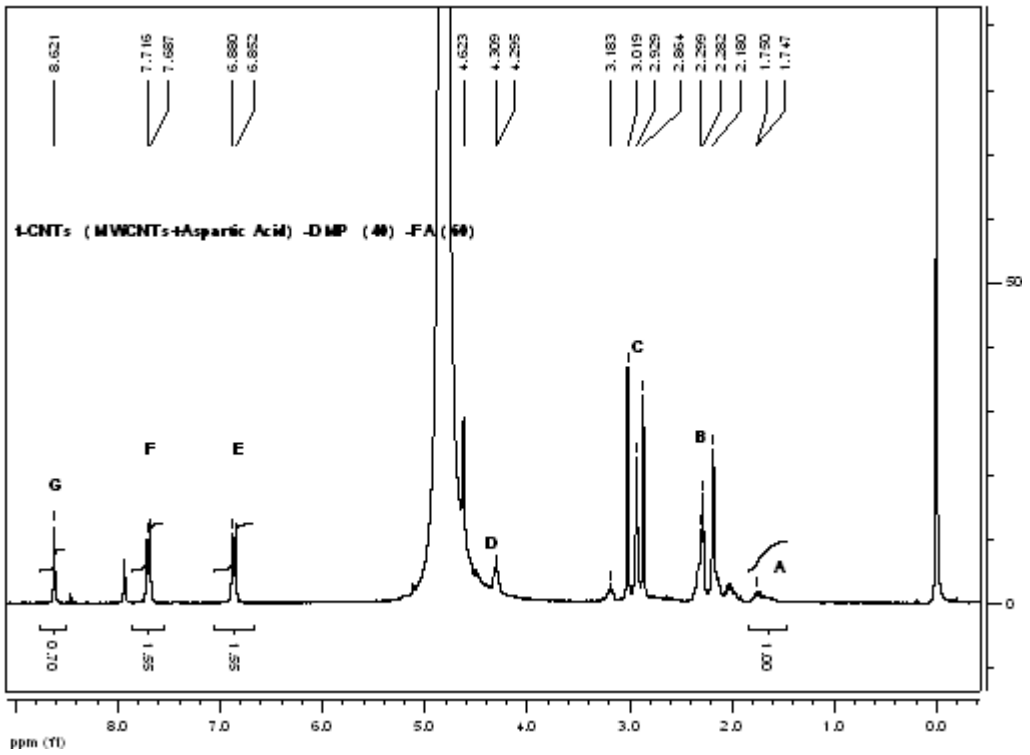

**$^{1}$H NMR SPECTRA (33): f-CNTs (MWCNTs+PSI)-DMP (40)-PDA (60)-FA Incorporation FA 105.3%**